The Kondo Screening Cloud.

Brandon Leigh Panos
Supervisor: Dr Izak Snyman

Submitted in fulfillment of the requirements for the degree of
Masters in Physics
at
the University of the Witwatersrand.

November 7th, 2016.

Declaration

I declare that this dissertation is my own unaided work except where I have explicitly indicated otherwise. It is being submitted for a Degree of Master in Physics to the University of the Witwatersrand, Johannesburg. It has not been submitted before for any degree or examination at any other university.

Signature:_ _ _ _ _ _ _ _ _ _

Abstract

The spin-1/2 Kondo model describes an antiferromagnetic exchange interaction between an impurity spin and the spin-density of a Fermi gas. Although the thermodynamics of this system have been resolved, there are still some unanswered questions regarding its spatial features. The spatial region of correlation between the impurity spin and the spin-density of the Fermi gas is referred to as the Kondo screening cloud. For the case of anisotropic couplings, the cloud consists of four distinct components. In this dissertation we use the bosonization technique to derive both an exact numeric and an approximate analytic expression for the forward scattering longitudinal cloud at the Toulouse point. The expressions are then extended to incorporate the effects of a time-independent external magnetic field. The non-magnetic case displays universal scaling behavior, while the addition of an external magnetic field only slightly spoils the scaling in the vicinity of the crossover length $\xi_K^{(B)}$, but remarkably not deep inside or outside the cloud.

Dedication

To my mother and father as well as the new family member Ava.

Acknowledgements

I would like to thank my supervisor for his continual effort in my development as a scientist, as well as his availability for consultation no matter the circumstances. Few people manage to surpass expectations and muster more respect on a daily basis. In addition to providing unwavering support and patience, I was also provided with a catalogue of unscientific ~~flowery~~ words that were prohibited from entering into my dissertation. Dr, you have instilled in me an attitude of perfection and discipline that I will carry through to all areas of my life. I would like to extend a huge amount of my gratitude to The National Institute for Theoretical Physics. Without their financial assistance and genuine concern for academic development, my masters could not have become a reality. I thank all my friends that offered their guidance and understanding when I could not join them for their weekend activities, as well as all my friends operating the coffee shops in Johannesburg, David, Emmanuel and Jessy. To Emzi and Bryan, I could not have made it through this masters without your continual support and the dota games with coffee and clouds. Lastly, I thank my parents for all the sacrifices they have made for their children, and for supporting me in my physics journey.

Contents

Chapter 1

Introduction

The system studied in this dissertation is the anisotropic spin-1/2 Kondo model. This model describes a point-like interaction between the spin degrees of freedom of a local magnetic moment and an electron gas. The Hamiltonian of this model is given by

$$\begin{aligned} H_{AKM} = &\sum_{k\sigma} \epsilon_k c^\dagger_{k\sigma} c_{k\sigma} + \frac{J_\parallel}{2}\left[\psi^\dagger_\uparrow(0)\psi_\uparrow(0) - \psi^\dagger_\downarrow(0)\psi_\downarrow(0)\right]\sigma_z \\ &+ \left[J_\perp \psi^\dagger_\uparrow(0)\psi_\downarrow(0)\sigma^- + J^*_\perp \psi^\dagger_\downarrow(0)\psi_\uparrow(0)\sigma^+\right]. \end{aligned} \tag{1.1}$$

Here, $c^\dagger_{k\sigma}$ creates an electron with wave number k and spin σ, while $\psi^\dagger_\uparrow(0)$ creates a spin up electron at position $x = 0$, where the impurity is located. The first term describes the kinetic energy of the electron gas, while the second and third terms model scattering events off the impurity.

The most famous manifestation of Kondo physics is the so-called resistance minimum in dilute magnetic alloys. The predominant contribution to the electrical resistivity of a metal at room temperature is due to phonon-electron interactions. As temperature decreases, the phonon excitations start to subside and the resistivity drops to some finite value. However, in certain magnetic alloys, a resistance minimum occurs as the temperature decreases to a few Kelvin. A further decrease in temperature leads to an increase in resistivity. This is surprising and requires a scattering mechanism that increases in strength with a decrease in temperature.

Decades after first being observed, the resistance minimum was conclusively attributed to the scattering of electrons off magnetic impurities embedded within the host metal. If the impurities in the metal are dilute, we can neglect inter-impurity effects and study the physics of a single impurity. The ingredients of such a model should include the conduction band electrons of the host metal, a single localized impurity orbital, and a Coulomb repulsion between the electrons in the impurity orbital. A reasonable description is given by the Anderson impurity model

$$H_{\text{Anderson}} = \sum_{\mathbf{k}\sigma} \epsilon_{\mathbf{k}} c^\dagger_{\mathbf{k}\sigma} c_{\mathbf{k}\sigma} + \sum_\sigma \epsilon_d d^\dagger_\sigma d_\sigma + U n_{d\uparrow} n_{d\downarrow} + \sum_{\mathbf{k}\sigma} (V_{\mathbf{k}} d^\dagger c_{\mathbf{k}\sigma} + \text{h.c.}). \tag{1.2}$$

Here, $d_\sigma^\dagger$ and d_σ are the creation and annihilation operators of the impurity orbital. The first term describes the energy contribution of the conduction band electrons, whilst the next two terms describe the energy of the magnetic impurity orbital and the Coulomb penalty in the case of double occupation. The last term gives the hybridization between the impurity orbital and the conduction band, with h.c. being the Hermitian conjugate. The relevant regime is when the impurity level lies far below the Fermi surface, and when the Coulomb repulsion U is comparatively large with respect to the other energy scales of the system, i.e., $\epsilon_d \ll \epsilon_F \ll \epsilon_d + U$. This gives rise to impurities that are mostly singly occupied and hence have magnetic moments. As we will review in the next chapter, the low energy physics of this model is equivalent to the Kondo model with isotropic couplings $J_\perp = J_\perp^* = J_\parallel$.

It was soon realized that perturbation theory in the Kondo coupling J diverges. An important breakthrough was made by Wilson [1], who introduced a nonperturbative framework known as the numerical renormalisation group. He used an iterative method based on numerical diagonalization to eliminate ultraviolet degrees of freedom in a numerically exact fashion. Wilson was able to show that the Kondo model flows to a strong coupling fixed point in which the impurity spin and the spin-polarization of the conduction electrons in the vicinity of the impurity form a spin singlet. Following Wilson's work, the Kondo model was also solved exactly by Andrei [2] and by Wiegmann [3], using the Bethe Ansatz. Both methods identify the temperature at which the resistance is minimal with the scale at which Kondo correlations set in, and furthermore show that this emergent scale is exponentially small in the inverse of the coupling between the impurity and the electron gas.

The ground state of the spin 1/2 Kondo model is often described as an impurity spin that is perfectly screened by the spin polarization of the electron gas that surrounds it. This means that there exists a cloud of conduction electrons with net spin 1/2 around the impurity. The net spin and the impurity form a spin singlet. An interesting question to ask is how the conduction electron spin-density varies in space for a given impurity spin-direction. This is what is referred to as the spatial profile of the Kondo screening cloud. Surprisingly, despite the breakthroughs of Wilson, Andrei and Wiegmann, the spatial profile of the Kondo screening cloud remained challenging to calculate for a long time. This is because most of the methods used to investigate the Kondo model focused specifically on thermodynamic information, often to the detriment of good spatial resolution. For instance, the logarithmic discretization used in Wilson's numerical renormalisation group, although key to extracting the low energy spectrum of the Kondo model, results in poor resolution in real space. Only in the last decade have reliable numerical results been obtained [4–7].

In this dissertation we study the spatial profile of the Kondo screening cloud. We approach the problem by focusing on a special value of $J_\parallel$, known as the Toulouse point. For this particular longitudinal coupling, the Kondo model can be mapped to a non-interacting Hamiltonian that is quadratic in fermion operators. A large portion of the dissertation focuses on the review of this mapping. In the process we will encounter a powerful many-body technique known as bosonization, of which we will present a self-contained derivation.

After reviewing the mapping, we calculate the spatial profile of the screening cloud at the Toulouse point. Some of the screening cloud results that we present here have already appeared in the recent literature [7]. Our contribution is to fill in the steps of the published derivations, and to highlight interesting features of the known results. Furthermore, we extend the known results by including an external magnetic field. The non-magnetic singlet is the natural ground state of the Kondo model. An external magnetic field frustrates this configuration and attempts to drive the singlet into a magnetic state with the impurity and conduction electron spin aligned to the direction of the field. Therefore, a magnetic field has a non-trivial effect on the screening cloud. Analytical expressions for cloud correlations at non-zero magnetic field at the Toulouse point have not been derived in the literature. We provide both a numeric and analytic expression for the cloud. These expressions are then used to address some interesting questions, such as, does a magnetic field introduce an emergent length at which the screening cloud's profile undergoes an exponential decay? And is there a universal scaling function such that clouds at different magnetic field strengths can be collapsed onto one another?

It turns out that we cannot quantitatively study the isotropic Kondo model if we focus on the Toulouse point. The reason for this is that at the Toulouse point, $J_{\parallel} = (2-\sqrt{2})\pi$, is of order 1. If we additionally set $J_{\perp} = J_{\parallel}$, the energy scale of Kondo correlations are comparable to ultraviolet scales such as the Fermi energy, while resolving universal features of correlations inside the cloud requires this scale to be far below ultraviolet. This however does not imply that the topic we study is of academic interest only. There are several physical realizations of the anisotropic Kondo model. Some examples include molecular transport devices at large electron-phonon coupling [8], a triple quantum dot setup with a doubly degenerate ground state [9], and the charge and spin degrees of freedom of a cooper pair box coupled to a superconducting resonator [10]. The Toulouse point is therefore experimentally relevant in its own right. Furthermore, the model at the Toulouse point eventually flows to the same strong coupling fixed point as the isotropic model. As a result, correlations in the two models have many qualitative features in common, even when they are probed at finite wavelengths.

Chapter descriptions:

- Chapter 2: We discuss a technical tool called the Schriefer Wolf transformation. This tool allows us to obtain effective low energy models by eliminating ultraviolet degrees of freedom. We review the calculation that was done by Schrieffer and Wolff [11], in which the Kondo model emerges as a low energy description of the Anderson model, after the ultraviolet fluctuations of the charge in the impurity orbital have been eliminated. We then review a simple renormalisation analysis of the Kondo Hamiltonian, due to Anderson. Anderson's poor man's scaling demonstrates that the effective degrees of freedom of the Kondo model undergo a nontrivial rearrangement as the system is probed at lower and lower energy scales, or equivalently at coarser and coarser spatial resolutions.

- Chapter 3: We introduce an equivalence between bosonic and fermionic Fock spaces, known as bosonization. We present a self-contained construction of bosonization, aimed at readers who are unfamiliar with the topic.

- Chapter 4: We apply the techniques developed in the previous chapter to map the Kondo model at the Toulouse point to a model of non-interacting fermions via an intermediate bosonic model. The chapter concludes with the introduction and mapping of the observable of interest. This observable measures the spatial profile of the screening cloud. It is a correlation function between the impurity spin, and the conduction electron spin-density a distance x away from the impurity.

- Chapter 5: We develop an exact numerical and an approximate analytical expression for the correlation function. The results are then extended to incorporate the effects of an external time-independent magnetic field. The numeric and analytic results for both cases are compared, and the asymptotic behavior of the correlators investigated. For the non-magnetic case, a length scale ξ_K emerges, which characterizes the size of the cloud. The behavior of the correlations for distances inside and outside of the cloud is very different, and the correlator is shown to be a universal scaling function of x/ξ_K. The magnetic case introduces an additional scale. However, surprisingly, at large and small x, the correlator is still a universal function of $x/\xi_K(B)$, with the same emergent scale $\xi_K(B)$ at small and large distances.

Chapter 2

The Schrieffer-Wolff transformation and low energy effective models

In this chapter, we derive an effective low energy Hamiltonian of the single impurity Anderson model. The resulting expression is the famous Kondo Hamiltonian. It will then be shown that tracing out the high energy degrees of freedom of the Kondo model results in a non-trivial renormalisation of the infrared degrees of freedom. To achieve both of these tasks, we will make use of a tool known as the Schrieffer-Wolff transformation. It is therefore necessary to begin this chapter by developing the formalism of this tool.

2.1 Formalism of the Schrieffer-Wolff transformation

Consider a vector space $\mathcal{V} = \mathcal{H} \bigoplus \mathcal{L}$, where the subspaces $\mathcal{H}$ and $\mathcal{L}$ are spanned by basis states $B_{\mathcal{H}} = \{|\mathcal{H}\alpha\rangle\}$ and $B_{\mathcal{L}} = \{|\mathcal{L}\beta\rangle\}$ respectively. The vectors belonging to $B_{\mathcal{H}}$ are eigenstates of the operator $H_{\mathcal{H}}$, with eigenvalues $E_{\mathcal{H}\alpha}$:

$$H_{\mathcal{H}} |\mathcal{H}\alpha\rangle = E_{\mathcal{H}\alpha} |\mathcal{H}\alpha\rangle\,, \tag{2.1}$$

while the vectors belonging to $B_{\mathcal{L}}$ are eigenstates of the operator $H_{\mathcal{L}}$ with eigenvalues $E_{\mathcal{L}\beta} < E_{\mathcal{H}\alpha}$ for all β and α:

$$H_{\mathcal{L}} |\mathcal{L}\beta\rangle = E_{\mathcal{L}\beta} |\mathcal{L}\beta\rangle\,. \tag{2.2}$$

Since $E_{\mathcal{L}\beta} < E_{\mathcal{H}\alpha}$, we refer to $\mathcal{H}$ as the high energy subspace and to $\mathcal{L}$ as the low energy subspace.

Now consider a zero order Hamiltonian $H_0 = H_{\mathcal{H}} + H_{\mathcal{L}}$. This operator leaves the low and high energy subspaces invariant. For example, if H_0 acts on a vector in $\mathcal{L}$, the resulting vector will also belong to $\mathcal{L}$.

$$H_0 = \sum_{s=\mathcal{H},\mathcal{L}} \sum_{\gamma} \epsilon_{s\gamma} |s\gamma\rangle \langle s\gamma|\,. \tag{2.3}$$

Then consider adding a perturbation H_1 that connects the low and high energy subspaces:

$$H_1 = \lambda \sum_{\alpha\in\mathcal{H}} \sum_{\beta\in\mathcal{L}} \Bigg(V^*_{\beta\alpha} \left|\mathcal{H}\alpha\right\rangle \left\langle\mathcal{L}\beta\right| + V_{\beta\alpha} \left|\mathcal{L}\beta\right\rangle \left\langle\mathcal{H}\alpha\right| \Bigg). \tag{2.4}$$

We would like to perform a unitary transformation on $H = H_0 + H_1$, such that the operators that couple the high and low energy subspaces are eliminated to leading order in λ. This will leave us with effective low and high energy Hamiltonians $\tilde{H}_{\mathcal{L}}$ and $\tilde{H}_{\mathcal{H}}$.

A general unitary transform can be written as $\tilde{H} = e^{\theta} H e^{-\theta}$, with $\theta^\dagger = -\theta$. We propose that

$$\theta = \lambda\left(W - W^\dagger\right), \quad \text{with} \quad W = \sum_{\alpha\in\mathcal{H}} \sum_{\beta\in\mathcal{L}} \frac{V^*_{\beta\alpha}}{E_{\mathcal{H}\alpha} - E_{\mathcal{H}\beta}} \left|\mathcal{H}\alpha\right\rangle \left\langle\mathcal{L}\beta\right|, \tag{2.5}$$

diagonalizes H to leading order in λ. To prove this, we make use of the Baker-Campbell-Hausdorff (BCH) formula

$$e^B A\, e^{-B} = \sum_{n=0}^{\infty} \frac{1}{n!}[B, A]_n = A + [B, A] + \frac{1}{2!}[B, [B, A]] + \cdots . \tag{2.6}$$

This allows us to expand $\tilde{H}$ in a power series of λ:

$$\tilde{H} = H_0 + [\theta, H_0] + \frac{1}{2}[\theta, [\theta, H_0]] + H_1 + [\theta, H_1] + O(\lambda^3) + \cdots . \tag{2.7}$$

The second term in (2.7) is calculated as follows:

$$\begin{aligned}
[\theta, H_0] &= \lambda\left[(W - W^\dagger), (H_{\mathcal{L}} + H_{\mathcal{H}})\right], \\
&= \lambda\left\{(W - W^\dagger)(H_{\mathcal{L}} + H_{\mathcal{H}}) - (H_{\mathcal{L}} + H_{\mathcal{H}})(W - W^\dagger)\right\}, \\
&= \lambda\left\{W H_{\mathcal{L}} - H_{\mathcal{H}} W + H_{\mathcal{L}} W^\dagger - W^\dagger H_{\mathcal{H}}\right\}, \\
&= \lambda\left\{(W H_{\mathcal{L}} - H_{\mathcal{H}} W) + (W H_{\mathcal{L}} - H_{\mathcal{H}} W)^\dagger\right\},
\end{aligned} \tag{2.8}$$

with

$$\begin{aligned}
W H_{\mathcal{L}} - H_{\mathcal{H}} W &= \sum_{\alpha\in\mathcal{H}} \sum_{\beta\in\mathcal{L}} \left(\frac{V^*_{\beta\alpha}}{E_{\mathcal{H}\alpha} - E_{\mathcal{L}\beta}} \left|\mathcal{H}\alpha\right\rangle \left\langle\mathcal{L}\beta\right| H_{\mathcal{L}} - H_{\mathcal{H}} \left|\mathcal{H}\alpha\right\rangle \left\langle\mathcal{L}\beta\right| \frac{V^*_{\beta\alpha}}{E_{\mathcal{H}\alpha} - E_{\mathcal{L}\beta}} \right), \\
&= \sum_{\alpha\in\mathcal{H}} \sum_{\beta\in\mathcal{L}} \left(\frac{E_{\mathcal{L}\beta} - E_{\mathcal{H}\alpha}}{E_{\mathcal{H}\alpha} - E_{\mathcal{L}\beta}} \right) V^*_{\beta\alpha} \left|\mathcal{H}\alpha\right\rangle \left\langle\mathcal{L}\beta\right| = -V^\dagger.
\end{aligned} \tag{2.9}$$

This implies that

$$[\theta, H_0] = \lambda(V^\dagger + V) = -H_1. \tag{2.10}$$

Substituting the above result back into (2.7) simplifies the expression for the effective Hamiltonian to

$$\tilde{H} = H_0 + \frac{1}{2}[\theta, H_1] + \mathcal{O}(\lambda^3)\cdots . \tag{2.11}$$

The unitary transformation changes H by an amount $\delta H = \frac{1}{2}[\theta, H_1]$, which is given by

$$\begin{aligned}
\frac{1}{2}[\theta, H_1] &= \frac{\lambda^2}{2}\left[(W - W^\dagger), (V^\dagger + V)\right], \\
&= \frac{\lambda^2}{2}\left\{(W - W^\dagger)(V^\dagger + V) - (V^\dagger + V)(W - W^\dagger)\right\}, \\
&= \frac{\lambda^2}{2}\left\{WV - W^\dagger V^\dagger - VW + V^\dagger W^\dagger\right\}, \\
&= \frac{\lambda^2}{2}\left\{-(W^\dagger V^\dagger + VW) + (V^\dagger W^\dagger + WV)\right\},
\end{aligned} \tag{2.12}$$

with terms

$$\begin{aligned}
W^\dagger V^\dagger + VW = \sum_{\alpha\gamma\in\mathcal{H}}\sum_{\beta\delta\in\mathcal{L}} \Bigg[&\frac{V_{\beta\alpha}}{E_{\mathcal{H}\alpha} - E_{\mathcal{L}\beta}} \left|\mathcal{L}\beta\right\rangle \left\langle\mathcal{H}\alpha\right|\left.\mathcal{H}\gamma\right\rangle \left\langle\mathcal{L}\delta\right| V^*_{\delta\gamma} \\
&+ V_{\beta\alpha}\left|\mathcal{L}\beta\right\rangle \left\langle\mathcal{H}\alpha\right|\left.\mathcal{H}\gamma\right\rangle \left\langle\mathcal{L}\delta\right| \frac{V^*_{\delta\gamma}}{E_{\mathcal{H}\gamma} - E_{\mathcal{L}\delta}}\Bigg], \\
=2\sum_{\alpha\in\mathcal{H}}\sum_{\beta\delta\in\mathcal{L}} &\frac{V_{\beta\alpha}V^*_{\delta\alpha}}{E_{\mathcal{H}\alpha} - E_{\mathcal{L}\beta}} \left|\mathcal{L}\beta\right\rangle \left\langle\mathcal{L}\delta\right| .
\end{aligned} \tag{2.13}$$

and

$$\begin{aligned}
V^\dagger W^\dagger + WV = \sum_{\alpha\gamma\in\mathcal{H}}\sum_{\beta\delta\in\mathcal{L}} \Bigg[&V^*_{\delta\gamma}\left|\mathcal{H}\gamma\right\rangle \left\langle\mathcal{L}\delta\right|\left.\mathcal{L}\beta\right\rangle \left\langle\mathcal{H}\alpha\right| \frac{V_{\beta\alpha}}{E_{\mathcal{H}\alpha} - E_{\mathcal{L}\beta}} \\
&+ \frac{V^*_{\delta\gamma}}{E_{\mathcal{H}\gamma} - E_{\mathcal{L}\delta}} \left|\mathcal{H}\gamma\right\rangle \left\langle\mathcal{L}\delta\right|\left.\mathcal{L}\beta\right\rangle \left\langle\mathcal{H}\alpha\right| V_{\beta\alpha}\Bigg], \\
=2\sum_{\alpha\in\mathcal{H}}\sum_{\beta\delta\in\mathcal{L}} &\frac{V^*_{\beta\gamma}V_{\beta\alpha}}{E_{\mathcal{H}\alpha} - E_{\mathcal{L}\beta}} \left|\mathcal{H}\gamma\right\rangle \left\langle\mathcal{H}\alpha\right| .
\end{aligned} \tag{2.14}$$

Substituting the above results back into (2.12) and (2.11) gives us the effective low and high energy Hamiltonians

$$\boxed{\tilde{H}_{\mathcal{L}} = H_{\mathcal{L}} - \lambda^2 \sum_{\alpha\in\mathcal{H}}\sum_{\beta\delta\in\mathcal{L}} \frac{V_{\beta\alpha}V^*_{\delta\alpha}}{E_{\mathcal{H}\alpha} - E_{\mathcal{L}\beta}} \left|\mathcal{L}\beta\right\rangle \left\langle\mathcal{L}\delta\right| ,} \tag{2.15}$$

and

$$\boxed{\tilde{H}_{\mathcal{H}} = H_{\mathcal{H}} + \lambda^2 \sum_{\alpha\gamma\in\mathcal{H}} \sum_{\beta\in\mathcal{L}} \frac{V^*_{\beta\gamma} V_{\beta\alpha}}{E_{\mathcal{H}\alpha} - E_{\mathcal{L}\beta}} \left|\mathcal{H}\gamma\right\rangle \left\langle\mathcal{H}\alpha\right| .} \tag{2.16}$$

Often the dependance of the denominator on the indices α and β is weak, and we can replace $E_{\mathcal{H}\alpha} - E_{\mathcal{L}\beta}$ with a constant Ω. Eq.(2.15) can then be written as

$$\tilde{H}_{\mathcal{L}} = H_{\mathcal{L}} - \frac{\lambda^2}{\Omega} V V^\dagger, \tag{2.17}$$

where one can verify that

$$V V^\dagger = \sum_{\beta\delta\in\mathcal{L}} V_{\beta\alpha} V^*_{\delta\alpha} \left|\mathcal{L}\beta\right\rangle \left\langle\mathcal{L}\delta\right| . \tag{2.18}$$

Eq.(2.17) can easily be generalized when the sum in (2.15) extends over several high energy subspaces associated with different denominators.

2.2 Application of the Schrieffer-Wolff transformation to the single impurity Anderson Hamiltonian

The formalism above was first applied to the Anderson impurity model in the work by Schrieffer and Wolff [11] where they successfully derived the Kondo Hamiltonian from the Anderson model. The regime of interest $\epsilon_d \ll \epsilon_F \ll \epsilon_d + U$ allows for the separation of high and low energy subspaces as follows. The high energy configurations of the system correspond to double and zero occupancy of the local d-orbital, while the low energy configuration corresponds to a single occupation of the d-orbital. The low energy subspace $\mathcal{L}$ is then the span of vectors $|\mathcal{L}\beta\rangle = |\{n_{k\sigma}\}, \sigma_{\text{imp}}\rangle$ where $\{n_{k\sigma}\}$ refers to the set of occupation numbers of the Fermi sea, and σ_{imp} refers to the spin of the single electron in the impurity orbital. On the other hand, the high energy subspace $\mathcal{H} = \mathcal{H}_0 \bigoplus \mathcal{H}_2$ is given by the span of vectors $|\mathcal{H}\alpha_q\rangle = |\{n_{k\sigma}\}, q\rangle$, where $q \in \{0, 2\}$ indicates whether the impurity orbital is unoccupied or doubly occupied. These states obey the orthogonality conditions

$$\langle\mathcal{L}\beta|\,\mathcal{H}\alpha\rangle = 0 \quad \text{and} \quad \langle\mathcal{L}\gamma|\,\mathcal{L}\gamma'\rangle = \langle\mathcal{H}\gamma|\,\mathcal{H}\gamma'\rangle = \delta_{\gamma\gamma'}. \tag{2.19}$$

In order to apply the Schrieffer-Wolff transformation, we need to write the Anderson impurity Hamiltonian in the form

$$H = \underbrace{\sum_{s=\mathcal{H},\mathcal{L}} \sum_{\gamma} \epsilon_{s\gamma} \left|s\gamma\right\rangle \left\langle s\gamma\right|}_{H_0} + \underbrace{\sum_{\alpha\in\mathcal{H}} \sum_{\beta\in\mathcal{L}} \left(V^*_{\beta\alpha} \left|\mathcal{H}\alpha\right\rangle \left\langle\mathcal{L}\beta\right| + V_{\beta\alpha} \left|\mathcal{L}\beta\right\rangle \left\langle\mathcal{H}\alpha\right| \right)}_{H_1}. \tag{2.20}$$

Here H_0 only connects states from the same subspace, which means it is composed of all the operators that leave the occupation of the d-orbital unaltered. This allows us to identify H_0 as

$$H_0 \;=\; \sum_{\mathbf{k}\sigma} \epsilon_{\mathbf{k}} c^\dagger_{\mathbf{k}\sigma} c_{\mathbf{k}\sigma} + \sum_{\sigma} \epsilon_d d^\dagger_\sigma d_\sigma + U n_{d\uparrow} n_{d\downarrow}. \tag{2.21}$$

On the other hand, H_1 must contain the operators of the model that alter the number of electrons on the d-orbital. This job is performed by the hybridization function

$$H_1 = \sum_{\mathbf{k}\sigma} (V_{\mathbf{k}} d^\dagger_\sigma c_{\mathbf{k}\sigma} + \text{h.c.}). \tag{2.22}$$

The projection operator that projects onto the low energy subspace is

$$P = (1 - n_\uparrow)n_\downarrow + (1 - n_\downarrow)n_\uparrow. \tag{2.23}$$

We can identify the high and low energy Hamiltonians, as well as V and $V^\dagger$ by applying the projection operator to H_0 and H_1. Using the fact that $I = P + (1-P)$ and that H_0 commutes with P, we obtain $H_0 = PH_0 + (1-P)H = H_{\mathcal{L}} + H_{\mathcal{H}}$. On the other-hand $H_1 = PH_1 + H_1P$, where

$$PH_1 = \underbrace{\sum_{\mathbf{k}\sigma} V_{\mathbf{k}}(1 - n_{\bar{\sigma}})d^\dagger_\sigma c_{\mathbf{k}\sigma}}_{V^{(10)}} + \underbrace{\sum_{\mathbf{k}\sigma} V^*_{\mathbf{k}} n_{\bar{\sigma}} c^\dagger_{\mathbf{k}\sigma} d_\sigma}_{V^{(12)}} = V, \tag{2.24}$$

$$H_1P = \underbrace{\sum_{\mathbf{k}\sigma} V^*_{\mathbf{k}} c^\dagger_{\mathbf{k}\sigma} d_\sigma (1 - n_{\bar{\sigma}})}_{V^{(10)\dagger}} + \underbrace{\sum_{\mathbf{k}\sigma} V_{\mathbf{k}} d^\dagger_\sigma c_{\mathbf{k}} n_{\bar{\sigma}}}_{V^{(12)\dagger}} = V^\dagger. \tag{2.25}$$

Here, $\bar{\sigma}$ is opposite in spin to σ. The meaning of the subscript notation $V^{(ij)}$ is as follows. $V^{(ij)}$ refers to an operator that takes us from a state with a d-orbital occupancy of j, into a state with a d-orbital occupancy of i, where i and j can take on the values 0, 1 or 2. For example, $V^{(12)}$ is an operator that takes us from a high doubly occupied state into a low singly occupied state. The eigenvalue equations of the operators $H_{\mathcal{L}}$ and $H_{\mathcal{H}}$ are

$$H_{\mathcal{L}} |\mathcal{L}\beta\rangle = \left(\sum_{\mathbf{k}\sigma} n_{\mathbf{k}\sigma}\epsilon_{\mathbf{k}} + \epsilon_d \right) |\mathcal{L}\beta\rangle, \tag{2.26}$$

$$H_{\mathcal{H}} |\mathcal{H}\alpha_2\rangle = \left(\sum_{\mathbf{k}\sigma} n_{\mathbf{k}\sigma}\epsilon_{\mathbf{k}} + 2\epsilon_d + U \right) |\mathcal{H}\alpha_2\rangle, \tag{2.27}$$

$$H_{\mathcal{H}} |\mathcal{H}\alpha_0\rangle = \sum_{\mathbf{k}\sigma} n_{\mathbf{k}\sigma}\epsilon_{\mathbf{k}} |\mathcal{H}\alpha_0\rangle. \tag{2.28}$$

It is now possible to calculate the effective low energy Hamiltonian from (2.15):

$$\delta H_{\mathcal{L}} = -\lambda^2 \sum_{\beta\delta\in\mathcal{L}} \sum_{\alpha_0} \frac{V^{(10)}_{\beta\alpha_0} V^{(10)*}_{\delta\alpha_0}}{E_{\mathcal{H}\alpha_0} - E_{\mathcal{L}\beta}} |\mathcal{L}\beta\rangle \langle\mathcal{L}\delta| - \lambda^2 \sum_{\beta\delta\in\mathcal{L}} \sum_{\alpha_2} \frac{V^{(12)}_{\beta\alpha_2} V^{(12)*}_{\delta\alpha_2}}{E_{\mathcal{H}\alpha_2} - E_{\mathcal{L}\beta}} |\mathcal{L}\beta\rangle \langle\mathcal{L}\delta|. \tag{2.29}$$

To make use of (2.17), the many-body energies in the denominator must be replaced with a constant. This will allow us to remove the denominators from the summation.

The denominator of a particular term in the first double summation is given by

$$E_{\mathcal{H}\alpha_0'} - E_{\mathcal{L}\beta'} = \sum_{\mathbf{k}\sigma} n_{\mathbf{k}\sigma}\epsilon_k - \left(\sum_{\mathbf{k}\sigma} n'_{\mathbf{k}\sigma}\epsilon_{\mathbf{k}} + \epsilon_d\right). \tag{2.30}$$

Since the operator $V^{(10)}_{\beta\alpha_0}$ promotes an electron from the Fermi sea to the unoccupied d-orbital, the sets $\{n_{\mathbf{k}\sigma}\}$ and $\{n'_{\mathbf{k}\sigma}\}$ must be the same except for a single occupation number, say $k_0\sigma_0$, for which $n_{\mathbf{k}_0\sigma_0} = 1$ and $n'_{\mathbf{k}_0\sigma_0} = 0$. The denominator then reads $E_{\mathcal{H}\alpha_0'} - E_{\mathcal{L}\beta'} = \epsilon_{\mathbf{k}_0} - \epsilon_d$. Assuming that matrix elements $V_{\mathbf{k}_0}$ are non-zero only for states much closer to the Fermi level than to ϵ_d, we can make the approximation $\epsilon_{\mathbf{k}_0} - \epsilon_d \simeq \epsilon_{\mathbf{k}_F} - \epsilon_d = -\epsilon_d$, where we have measured energies from the Fermi energy, i.e., set $\epsilon_{\mathbf{k}_F} = 0$. Similarly, since the $V^{(12)}$ operators only connect states between subspaces that differ by a single occupation number, we can approximate the denominators appearing in the second double summation as $E_{\mathcal{H}\alpha_2'} - E_{\mathcal{L}\beta'} = \epsilon_d + U - \epsilon_{\mathbf{k}_0} \simeq \epsilon_d + U - \epsilon_{\mathbf{k}_F} = \epsilon_d + U$. This allows us to write the effective low energy Hamiltonian as

$$\delta H_{\mathcal{L}} = \frac{\lambda^2}{\epsilon_d} \sum_{\beta\delta\in\mathcal{L}} \sum_{\alpha_0} V^{(10)}_{\beta\alpha_0} V^{(10)*}_{\delta\alpha_0} \left|\mathcal{L}\beta\right\rangle \left\langle\mathcal{L}\delta\right| - \frac{\lambda^2}{\epsilon_d + U} \sum_{\beta\delta\in\mathcal{L}} \sum_{\alpha_2} V^{(12)}_{\beta\alpha_2} V^{(12)*}_{\delta\alpha_2} \left|\mathcal{L}\beta\right\rangle \left\langle\mathcal{L}\delta\right|. \tag{2.31}$$

From (2.18), we have

$$\delta H_{\mathcal{L}} = -\lambda^2 \sum_{\mathbf{k}\mathbf{k}'} \sum_{\sigma\sigma'} V_{\mathbf{k}} V^*_{\mathbf{k}'} \left[\frac{(1-n_{\bar\sigma}) d^\dagger_{\sigma'} c_{\mathbf{k}'\sigma'} c^\dagger_{\mathbf{k}\sigma} d_\sigma (1-n_{\bar\sigma'})}{-\epsilon_d} + \frac{n_{\bar\sigma} c^\dagger_{\mathbf{k}\sigma} d_\sigma d^\dagger_{\sigma'} c_{\mathbf{k}'\sigma'} n_{\bar\sigma'}}{\epsilon_d + U}\right]. \tag{2.32}$$

Scaling the dimensionless parameter λ to one, and keeping in mind that the initial and final states are fixed to single d-orbital states, we can write the effective low energy Hamiltonian as

$$\tilde H_{\mathcal{L}} = \sum_{\mathbf{k}\sigma} \epsilon_{\mathbf{k}} c^\dagger_{\mathbf{k}\sigma} c_{\mathbf{k}\sigma} - \sum_{\mathbf{k}\mathbf{k}'} \sum_{\sigma\sigma'} V_{\mathbf{k}} V^*_{\mathbf{k}'} \left[\frac{d^\dagger_{\sigma'} c_{\mathbf{k}'\sigma'} c^\dagger_{\mathbf{k}\sigma} d_\sigma}{-\epsilon_d} + \frac{c^\dagger_{\mathbf{k}\sigma} d_\sigma d^\dagger_{\sigma'} c_{\mathbf{k}'}}{\epsilon_d + U}\right]. \tag{2.33}$$

We can express (2.33) in terms of spin matrices [12] by using the Pauli matrix identity

$$\vec\sigma_{\sigma\sigma'} \cdot \vec\sigma_{\delta\gamma} = 2\delta_{\sigma'\delta}\delta_{\sigma\gamma} - \delta_{\sigma'\sigma}\delta_{\gamma\delta}, \tag{2.34}$$

from which it follows

$$\sum_{\sigma\sigma'} d^\dagger_{\sigma'} c_{\mathbf{k}'\sigma'} c^\dagger_{\mathbf{k}\sigma} d_\sigma = -\frac{1}{2} \sum_{\sigma\sigma'} c^\dagger_{\mathbf{k}\sigma} c_{\mathbf{k}'\sigma} n_{d\sigma'} - \sum_{\sigma\sigma'} \sum_{\delta\gamma} (c^\dagger_{\mathbf{k}\sigma} \vec\sigma_{\sigma\sigma'} c_{\mathbf{k}'\sigma'}) \cdot (d^\dagger_\delta \frac{\vec\sigma_{\delta\gamma}}{2} d_\gamma), \tag{2.35}$$

while

$$\sum_{\sigma\sigma'} c^\dagger_{\mathbf{k}\sigma} d_\sigma d^\dagger_{\sigma'} c_{\mathbf{k}'} = \frac{1}{2} \sum_{\sigma\sigma'} c^\dagger_{\mathbf{k}\sigma} c_{\mathbf{k}'\sigma} n_{d\sigma'} - \sum_{\sigma\sigma'} \sum_{\delta\gamma} (c^\dagger_{\mathbf{k}\sigma} \vec\sigma_{\sigma\sigma'} c_{\mathbf{k}'\sigma'}) \cdot (d^\dagger_\delta \frac{\vec\sigma_{\delta\gamma}}{2} d_\gamma). \tag{2.36}$$

Substituting these expressions into (2.33), we find that the low energy effective Hamiltonian is given by

$$\tilde{H}_{\mathcal{L}} = \sum_{\mathbf{k}\sigma} \epsilon_{\mathbf{k}} c^{\dagger}_{\mathbf{k}\sigma} c_{\mathbf{k}\sigma} + \sum_{\mathbf{k}\mathbf{k}'} \sum_{\sigma\sigma'} J_{\mathbf{k}\mathbf{k}'} (c^{\dagger}_{\mathbf{k}\sigma} \vec{\sigma}_{\sigma\sigma'} c_{\mathbf{k}'\sigma'}) \cdot \vec{S}^{\text{imp}} - \sum_{\mathbf{k}\mathbf{k}'} \sum_{\sigma} K_{\mathbf{k}\mathbf{k}'} c^{\dagger}_{\mathbf{k}\sigma} c_{\mathbf{k}'\sigma}, \tag{2.37}$$

where $\vec{S}^{\text{imp}} = \sum_{\delta\gamma} d^{\dagger}_{\delta} \frac{\vec{\sigma}_{\delta\gamma}}{2} d_{\gamma}$ describes the impurity spin, while the coupling constants are given by

$$\begin{aligned} J_{\mathbf{k}\mathbf{k}'} =& V_{\mathbf{k}} V^{*}_{\mathbf{k}'} \left(\frac{1}{\epsilon_d + U} - \frac{1}{\epsilon_d} \right), \\ K_{\mathbf{k}\mathbf{k}'} =& \frac{V_{\mathbf{k}} V^{*}_{\mathbf{k}'}}{2} \left(\frac{1}{\epsilon_d + U} + \frac{1}{\epsilon_d} \right). \end{aligned} \tag{2.38}$$

The potential scattering term in (2.37) vanishes for the particle-hole symmetric case $\epsilon_d = -U/2$. Since Kondo physics does not hinge on this term, we can drop it without jeopardizing any of the interesting strong coupling physics. Additionally, since $J_{\mathbf{k}\mathbf{k}'}$ varies with $\mathbf{k}$ on the scale $\sim 1/a$, where a is the lattice constant, the long wavelength physics is still described accurately if we replace $J_{\mathbf{k}\mathbf{k}'}$ by a constant J, with the understanding that the $\mathbf{k}$-sums are cut off at an ultraviolet scale less than the Fermi energy. We can then write

$$\tilde{H}_{\mathcal{L}} = \sum_{\mathbf{k}\sigma} \epsilon_{\mathbf{k}} c^{\dagger}_{\mathbf{k}\sigma} c_{\mathbf{k}\sigma} + J \sum_{\mathbf{k}\mathbf{k}'} \sum_{\sigma\sigma'} \sum_{j} c^{\dagger}_{\mathbf{k}\sigma} [\sigma_j]_{\sigma\sigma'} c_{\mathbf{k}'\sigma'} S^{\text{imp}}_{j}. \tag{2.39}$$

Furthermore, since in position space $\psi^{\dagger}_{\sigma}(0) = L^{-1/2} \sum_{\mathbf{k}} c^{\dagger}_{\mathbf{k}\sigma}$, we have that

$$\tilde{H}_{\mathcal{L}} = \sum_{\mathbf{k}\sigma} \epsilon_{\mathbf{k}} c^{\dagger}_{\mathbf{k}\sigma} c_{\mathbf{k}\sigma} + J \sum_{\sigma\sigma'} \sum_{j} \psi^{\dagger}_{\sigma}(0) [\sigma_j]_{\sigma\sigma'} \psi_{\sigma'}(0) S^{\text{imp}}_{j}. \tag{2.40}$$

Additionally, one can identify the electron spin-density $\vec{S}^{\text{el}} = \sum_{\sigma\sigma'} \sum_{j} \psi^{\dagger}_{\sigma}(x) [\sigma_j]_{\sigma\sigma'} \psi_{\sigma'}(x)$ and write the Hamiltonian in the more compact form

$$\boxed{\tilde{H}_{\mathcal{L}} = \sum_{\mathbf{k}\sigma} \epsilon_{\mathbf{k}} c^{\dagger}_{\mathbf{k}\sigma} c_{\mathbf{k}\sigma} + J \vec{S}^{\text{el}}(0) \cdot \vec{S}^{\text{imp}}.} \tag{2.41}$$

This is the famous isotropic Kondo Hamiltonian. We conclude that the high energy charge fluctuations of the d-orbital induce an antiferromagnetic interaction between the electron spin-density and the impurity spin. If we expand the plane wave electron states $\mathbf{k}$ in spherical waves around $r = 0$, only electrons with angular momentum quantum numbers $l = m = 0$ couple to the impurity [13]. In this case, the magnitude of the wave vector $|\mathbf{k}|$ becomes the only relevant characterization of a state, making the Kondo problem an effective one-dimensional problem.

We will generalize the Kondo Hamiltonian by breaking the isotropy of the coupling constant to include both a longitudinal $J_{\parallel}$ and a transverse component $J_{\perp}$, where $J_{\perp}$ is real and symmetric about the z-axis. Since we are interested in the low energy dynamics of the problem, it is acceptable to linearize the spectrum, i.e., $\epsilon_k \simeq v_F k$. Combining all of these considerations and defining the spin operators

$$\sigma^+ = c^\dagger_\uparrow c_\downarrow \quad , \quad \sigma^- = c^\dagger_\downarrow c_\uparrow \quad , \quad \sigma_z = (\hat{n}_{d\uparrow} - \hat{n}_{d\downarrow}), \tag{2.42}$$

of the impurity, we obtain the anisotropic Kondo Hamiltonian in units $v_F = 1$:

$$\boxed{\begin{aligned} H_{AKM} = &\sum_{k\sigma} k \; c^\dagger_{k\sigma} c_{k\sigma} + \frac{J_\parallel}{2}\left[\psi^\dagger_\uparrow(0)\psi_\uparrow(0) - \psi^\dagger_\downarrow(0)\psi_\downarrow(0)\right]\sigma_z \\ &+ J_\perp\left[\psi^\dagger_\uparrow(0)\psi_\downarrow(0)\sigma^- + \psi^\dagger_\downarrow(0)\psi_\uparrow(0)\sigma^+\right]. \end{aligned}} \tag{2.43}$$

2.3 Application of the Schrieffer-Wolff transformation to the anisotropic Kondo Hamiltonian

The effective low energy Hamiltonian derived in (2.43) was used by Kondo [14] to calculate scattering probabilities of the conduction electrons to the second Born approximation. He found that the dynamical character of the localized spin system gave rise to a logarithmic term in the resistivity, that when combined with the lattice resistivity managed to account for the experimentally observed resistance minimum. However, this additional term has the form $\ln T$, and therefore diverges along with other physical quantities at low temperature. This is in contrast to the experimental results that indicated a finite resistance at temperature $T = 0$. Many perturbation theories, although seemingly plausible due to the small size of the coupling constant J, diverged below a certain critical temperature T_K, known as the Kondo temperature.

Wilson made an important breakthrough when he introduced a non-perturbative framework known as the numerical renormalisation group. With this framework, he was able to confirm the suspicions of a singlet ground state. Exact numeric solutions were later obtained independently by Andrei [2] and Wiegmann [3] using the Bethe ansatz. These are sophisticated techniques that are non-trivial to implement. However, the essentials are captured by Anderson's poor man's scaling, which is another application of the Schrieffer-Wolff transformation.

We will now reproduce Anderson's poor man's scaling argument [15] by applying the Schrieffer-Wolff transformation to the anisotropic Kondo Hamiltonian. Essentially, this involves the absorption of the high energy scattering processes into a renormalisation of the coupling constants. To do this, we divide the conduction band of width 2Λ into three different zones, as seen in Fig. 2.1. The first zone contains the states $0 < |\epsilon_k| < \Lambda - |\delta\Lambda|$, and will be referred to as the reduced band. The set of single particle energies in the reduced band are denoted K, while the set of single particle energies in the upper and lower band edges $|\delta\Lambda|$ are denoted by δk_+ and δk_- respectively. The low energy subspace $\mathcal{L}$ consists of many-electron states $|\mathcal{L}\beta\rangle$, for which all orbitals in δk_- are doubly occupied (i.e., no holes in the lower band edge) and all orbitals in δk_+ are empty. On the other hand, the high energy subspace $\mathcal{H} = \mathcal{H}_+ \bigoplus \mathcal{H}_-$ is spanned by the vectors

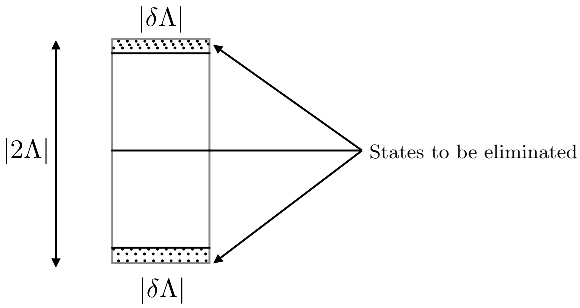

Figure 2.1: States to be eliminated after reducing the bandwidth by an amount $|\delta\Lambda|$.

$|\mathcal{H}\alpha_+\rangle$ and $|\mathcal{H}\alpha_-\rangle$, where α_+ labels the high energy states that contain at leased one occupied orbital in δk_+ and no holes in the lower band edge, while α_- labels the high energy states where no orbitals in δk_+ are occupied but there exists at leased one hole in the lower band edge. The high energy states are to be eliminate, while the low energy states will be retained.

The technical details of the procedure are as follows. The full anisotropic Kondo Hamiltonian can be compactly written as

$$H_{\mathcal{L}} = \sum_k \sum_\sigma \epsilon_k c^\dagger_{k\sigma} c_{k\sigma} + \frac{1}{2} \sum_{kq} \sum_{\sigma\sigma'} \sum_{i=1}^{3} J_i \tau^i_{\sigma\sigma'} \eta^i c^\dagger_{k\sigma} c_{q\sigma'}, \tag{2.44}$$

where τ^i and η^i are Pauli spin matrices, with $\tau^i_{\sigma\sigma'}$ being the element of the i'th Pauli matrix, and k and q run over the entire conduction band $\delta k_- \cup K \cup \delta k_+$. Here, $\{J_i\} = (J_1, J_2, J_3) \equiv (J_x, J_y, J_z)$. We will take $J_x = J_y \equiv J_\pm$ at the end of the calculation. To apply the Schrieffer-Wolff transformation, we once again have to write this Hamiltonian in the form

$$H = \underbrace{\sum_{s=\mathcal{H},\mathcal{L}} \sum_{\gamma} \epsilon_{s\gamma} |s\gamma\rangle \langle s\gamma|}_{H_0} + \underbrace{\sum_{\alpha\in\mathcal{H}} \sum_{\beta\in\mathcal{L}} \left(V^*_{\beta\alpha} |\mathcal{H}\alpha\rangle \langle \mathcal{L}\beta| + V_{\beta\alpha} |\mathcal{L}\beta\rangle \langle \mathcal{H}\alpha| \right)}_{H_1}. \tag{2.45}$$

The operator H_0 that only connects vector within the same subspace is given by

$$H_0 = \sum_{k\sigma} \epsilon_k c^\dagger_{k\sigma} c_{k\sigma} + \frac{1}{2} \sum_{\sigma\sigma'} \sum_{i=1}^{3} J_i \tau^i_{\sigma\sigma'} \eta^i \left(\sum_{kq\in\delta k_+} c^\dagger_{k\sigma} c_{q\sigma'} + \sum_{kq\in\delta k_-} c^\dagger_{k\sigma} c_{q\sigma'} + \sum_{kq\in K} c^\dagger_{k\sigma} c_{q\sigma'} \right). \tag{2.46}$$

On the other hand, the operator H_1 that connects vectors from different subspaces is given by

$$H_1 = \frac{1}{2} \sum_{\sigma\sigma'} \sum_{i=1}^{3} J_i \tau^i_{\sigma\sigma'} \eta^i \left(\sum_{\substack{k\in K \\ q\in\delta k_+}} c^\dagger_{k\sigma} c_{q\sigma'} + \sum_{\substack{k\in K \\ q\in\delta k_-}} c^\dagger_{k\sigma} c_{q\sigma'} + \sum_{\substack{k\in\delta k_+ \\ q\in\delta k_-}} c^\dagger_{k\sigma} c_{q\sigma'} \right) + \text{h.c.}, \tag{2.47}$$

where h.c. is the Hermitian conjugate of the first term. To find $H_{\mathcal{L}}$, $H_{\mathcal{H}}$, V and $V^\dagger$, we use the projection operator that projects onto the low energy subspace. This operator is given by

$$P = \prod_{\substack{p\in\delta k_- \\ \beta}} n_{p\beta} \prod_{\substack{l\in\delta k_+ \\ \alpha}} (1 - n_{l\alpha}), \tag{2.48}$$

so that if there exist any particles in the upper or holes in the lower band edges, P will return zero. Once again, $PH_0 = H_{\mathcal{L}}$ and $H_0 P = H_{\mathcal{H}}$, while $H_1 = PH_1 + H_1 P$, with

$$\begin{aligned} PH_1 =& \underbrace{\frac{1}{2}P \sum_{\substack{k\in K \\ q\in\delta k_+}} \sum_{\sigma\sigma'} \sum_{i=1}^{3} J_i \tau^i_{\sigma\sigma'} \eta^i c^\dagger_{k\sigma} c_{q\sigma'}}_{V^{(+)}} + \underbrace{\frac{1}{2}P \sum_{\substack{k\in K \\ q\in\delta k_-}} \sum_{\sigma\sigma'} \sum_{i=1}^{3} J_i \tau^i_{\sigma\sigma'} \eta^i c^\dagger_{q\sigma} c_{k\sigma'}}_{V^{(-)}} \\ &+ \underbrace{\frac{1}{2}P \sum_{\substack{k\in\delta k_+ \\ q\in\delta k_-}} \sum_{\sigma\sigma'} \sum_{i=1}^{3} J_i \tau^i_{\sigma\sigma'} \eta^i c^\dagger_{q\sigma} c_{k\sigma'}}_{V^{(2)}} + \text{h.c.}, \end{aligned} \tag{2.49}$$

and

$$\begin{aligned} H_1 P =& \underbrace{\frac{1}{2} \sum_{\substack{k\in K \\ q\in\delta k_+}} \sum_{\sigma\sigma'} \sum_{i=1}^{3} J_i \tau^i_{\sigma\sigma'} \eta^i c^\dagger_{q\sigma} c_{k\sigma'} P}_{V^{(+)\dagger}} + \underbrace{\frac{1}{2}P \sum_{\substack{k\in K \\ q\in\delta k_-}} \sum_{\sigma\sigma'} \sum_{i=1}^{3} J_i \tau^i_{\sigma\sigma'} \eta^i c^\dagger_{k\sigma} c_{q\sigma'} P}_{V^{(-)\dagger}} \\ &+ \underbrace{\frac{1}{2}P \sum_{\substack{k\in\delta k_+ \\ q\in\delta k_-}} \sum_{\sigma\sigma'} \sum_{i=1}^{3} J_i \tau^i_{\sigma\sigma'} \eta^i c^\dagger_{k\sigma} c_{q\sigma'} P}_{V^{(2)\dagger}} + \text{h.c.}. \end{aligned} \tag{2.50}$$

Here, $V^{(+)}$ connects states $|\mathcal{H}\alpha_+\rangle$ and $|\mathcal{L}\beta\rangle$ by taking electrons out of the upper band edge and putting them into the reduced band, while $V^{(-)}$ connects the vectors $|\mathcal{L}\beta\rangle$ and $|\mathcal{H}\alpha_-\rangle$ by filling the holes in the lower band edge with electrons from the reduced band. Finally, $V^{(2)}$ is the operator that connects the vectors $|\mathcal{H}\alpha_+\rangle$ and $|\mathcal{H}\alpha_-\rangle$ by filling the holes in the lower band edge with electrons from the upper band edge. The change in the low energy Hamiltonian is then given by

$$\begin{aligned} \delta H_{\mathcal{L}} =& -\lambda^2 \sum_{\beta\delta\in\mathcal{L}} \sum_{\alpha_+} \frac{V^{(+)}_{\beta\alpha_+} V^{(+)*}_{\delta\alpha_+}}{E_{\mathcal{H}\alpha_+} - E_{\mathcal{L}\beta}} |\mathcal{L}\beta\rangle \langle\mathcal{L}\delta| - \lambda^2 \sum_{\beta\delta\in\mathcal{L}} \sum_{\alpha_-} \frac{V^{(-)}_{\beta\alpha_+} V^{(-)*}_{\delta\alpha_-}}{E_{\mathcal{H}\alpha_-} - E_{\mathcal{L}\beta}} |\mathcal{L}\beta\rangle \langle\mathcal{L}\delta| \\ &- \lambda^2 \sum_{\beta\delta\in\mathcal{L}} \sum_{\alpha_2} \frac{V^{(2)}_{\beta\alpha_+} V^{(2)*}_{\delta\alpha_2}}{E_{\mathcal{H}\alpha_2} - E_{\mathcal{L}\beta}} |\mathcal{L}\beta\rangle \langle\mathcal{L}\delta|. \end{aligned} \tag{2.51}$$

Now E and $|\mathcal{L}\beta\rangle$ are complicated many-body eigenstates and energies of the Kondo model restricted to the reduced band. However, to leading order in the couplings J_i, we can replace E and $|\mathcal{L}\beta\rangle$ with free electron states and energies. Additionally, since $|\delta\Lambda| \ll \Lambda$, the energy of an electron in the region $|\delta\Lambda|$ can be approximated by Λ. Furthermore, since the couplings J_i are only sizable near the Fermi surface, the relevant scattering events involve electrons with energies approximately given by the Fermi energy, which can be taken as zero. This allows us to replace the many-body energies in the denominators of the first two terms by a constant Λ, while the last term's denominator can be replaced with 2Λ. However, the contribution of the last term to $\delta H_{\mathcal{L}}$ can be omitted. To see why, consider the following matrix element

$$\langle\mathcal{L}\beta|\, V^{(2)}V^{(2)\dagger}\, |\mathcal{L}\delta\rangle = \frac{1}{4}\sum_{\substack{kq\in\delta k_+\\ pl\in\delta k_-}}\sum_{\substack{\sigma_1\sigma_2\\ \sigma_3\sigma_4}}\sum_{i=1}^{3} J_iJ_j\tau^i_{\sigma_1\sigma_2}\tau^j_{\sigma_3\sigma_4}\,\langle\mathcal{L}\beta|\,\eta^i\eta^j c^\dagger_{p\sigma_1}c_{k\sigma_2}c^\dagger_{q\sigma_3}c_{l\sigma_4}\,|\mathcal{L}\delta\rangle\,. \tag{2.52}$$

Since $|\mathcal{L}\beta\rangle$ contains no particles in the upper band, or holes in the lower band, any electron that is removed from δk_- and added to δk_+ must be put back into the same orbital, otherwise $\langle\mathcal{L}\beta|\, V^{(2)}V^{(2)\dagger}\,|\mathcal{L}\delta\rangle = 0$. Therefore, we can replace the operators $c_{k\sigma_2}c^\dagger_{q\sigma_3}$ and $c^\dagger_{p\sigma_1}c_{l\sigma_4}$ with $\delta_{kq}\delta_{\sigma_2\sigma_3}$ and $\delta_{pl}\delta_{\sigma_1\sigma_4}$ respectively. Assuming a constant density of states ρ_0, we can write

$$\sum_{\substack{kq\in\delta k_+\\ pl\in\delta k_-}}\delta_{kq}\delta_{pl} = \rho_0^2(\delta\Lambda)^2. \tag{2.53}$$

It follows that the matrix elements of $V^{(2)}V^{(2)\dagger}$ are proportional to $(\delta\Lambda)^2$, so that they can be dropped in the limit where $\delta\Lambda$ vanishes with respect to Λ. We can therefore write

$$\delta H_{\mathcal{L}} = -\frac{\lambda^2}{\Lambda}\sum_{\beta\delta\in\mathcal{L}}\sum_{\alpha_+}V^{(+)}_{\beta\alpha_+}V^{(+)*}_{\delta\alpha_+}\,|\mathcal{L}\beta\rangle\langle\mathcal{L}\delta| - \frac{\lambda^2}{\Lambda}\sum_{\beta\delta\in\mathcal{L}}\sum_{\alpha_-}V^{(-)}_{\beta\alpha_+}V^{(-)*}_{\delta\alpha_-}\,|\mathcal{L}\beta\rangle\langle\mathcal{L}\delta|\,. \tag{2.54}$$

Using (2.18), and scaling the dimensionless parameter λ to one gives

$$\delta H_{\mathcal{L}} = -\frac{1}{\Lambda}\left(V^{(+)}V^{(+)\dagger} + V^{(-)}V^{(-)\dagger}\right). \tag{2.55}$$

The factors P can be dropped if we remember to restrict the operators to the low energy subspace. The first term inside the bracket of (2.55) is then explicitly given by

$$V^{(+)}V^{(+)\dagger} = \frac{1}{4}\sum_{\substack{kq\in K\\ pl\in\delta k_+}}\sum_{\sigma\beta\gamma\alpha}\sum_{i,j=1}^{3} J_iJ_j\tau^i_{\alpha\sigma}\tau^j_{\beta\gamma}\eta^i\eta^j c^\dagger_{k\alpha}c_{p\sigma}c^\dagger_{l\beta}c_{q\gamma}. \tag{2.56}$$

In the low energy subspace, the orbitals in δk_+ are unoccupied. For calculating matrix elements between low and high energy states, the operator $c_{p\sigma}c^\dagger_{l\beta}$ in (2.56) which adds and removes a particle in the shell δk_+, can be replaced by $\delta_{pl}\delta_{\sigma\beta}$. Once again, for a constant density of states ρ_0, we can write $\sum_{p\sigma l\beta}\delta_{pl}\delta_{\sigma\beta} = \rho_0|\delta\Lambda|$. These considerations give

$$
\begin{aligned}
V^{(+)}V^{(+)\dagger} =&\frac{\rho_0|\delta\Lambda|}{4}\sum_{kq\in K}\sum_{\beta\gamma\alpha}\sum_{i,j=1}^{3} J_iJ_j[\tau^i_{\alpha\beta}\tau^j_{\beta\gamma}][\eta^i\eta^j]c^\dagger_{k\alpha}c_{q\gamma},\\
=&\frac{\rho_0|\delta\Lambda|}{4}\sum_{kq\in K}\sum_{\gamma\alpha}\sum_{i,j,k,l=1}^{3} J_iJ_j\left(i\epsilon^{ijk}\tau^k_{\alpha\gamma}+\delta_{ij}\delta_{\alpha\gamma}\right)\left(i\epsilon^{ijl}\eta^l+\delta_{ij}\right)c^\dagger_{k\alpha}c_{q\gamma},\\
=&\frac{\rho_0|\delta\Lambda|}{4}\sum_{kq\in K}\sum_{\gamma\alpha}\sum_{i,j,k,l=1}^{3} J_iJ_j\big(-\epsilon^{ijk}\epsilon^{ijl}\tau^k_{\alpha\gamma}\eta^l+i\delta_{\alpha\gamma}\delta_{ij}\epsilon^{ijl}\eta^l\\
&+i\delta_{ij}\epsilon^{ijk}\tau^k_{\alpha\gamma}+\delta_{ij}\delta_{\alpha\gamma}\big)c^\dagger_{k\alpha}c_{q\gamma},
\end{aligned}
\tag{2.57}
$$

$$
\begin{aligned}
=&-\frac{\rho_0|\delta\Lambda|}{4}\sum_{kq\in K}\sum_{\gamma\alpha}\sum_{i,j,k=1}^{3}(1-\delta_{ij})(1-\delta_{ik})(1-\delta_{jk})J_iJ_j\tau^k_{\alpha\gamma}\eta^k c^\dagger_{k\alpha}c_{q\gamma}\\
&+\frac{\rho_0|\delta\Lambda|}{4}\sum_{kq\in K}\sum_{\alpha}\sum_{i=1}^{3}J_i^2c^\dagger_{k\alpha}c_{q\alpha}.
\end{aligned}
\tag{2.58}
$$

A similar calculation can be performed for the hole excitations:

$$
\begin{aligned}
V^{(-)}V^{(-)\dagger} =& \frac{1}{4}\sum_{\substack{kq\in K\\ pl\in\delta k_-}}\sum_{\sigma\beta\gamma\alpha}\sum_{i,j=1}^{3} J_iJ_j\tau^i_{\sigma\gamma}\tau^j_{\alpha\beta}\eta^i\eta^j c^\dagger_{p\sigma}c_{q\gamma}c^\dagger_{k\alpha}c_{\mathcal{L}\beta},\\
=&\frac{\rho_0|\delta\Lambda|}{4}\sum_{kq\in K}\sum_{\sigma\gamma\alpha}\sum_{i,j=1}^{3} J_iJ_j[\tau^j_{\alpha\sigma}\tau^i_{\sigma\gamma}][\eta^i\eta^j]c_{k\gamma}c^\dagger_{q\alpha}.
\end{aligned}
\tag{2.59}
$$

In the last expression we have commuted $\tau^j_{\alpha\sigma}$ to the left of $\tau^i_{\sigma\gamma}$. This allows us to contract the inner indices at the price of a change of sign. In the previous calculation we had $\mathrm{sgn}(\tau^i\tau^j\eta^i\eta^j)=-1$, whereas now we have $\mathrm{sgn}(\tau^j\tau^i\eta^i\eta^j)=+1$. Paying special attention to the position of the indices i and j we have

$$
\begin{aligned}
V^{(-)}V^{(-)\dagger} =& \frac{\rho_0|\delta\Lambda|}{4} \sum_{kq\in K} \sum_{\gamma\alpha} \sum_{i,j,k,l=1}^{3} J_i J_j \left(i\epsilon^{jik}\tau^k_{\alpha\gamma} + \delta_{ij}\delta_{\alpha\gamma}\right) \left(i\epsilon^{ijl}\eta^l + \delta_{ij}\right) c_{q\gamma}c^\dagger_{k\alpha}, \\
=& \frac{\rho_0|\delta\Lambda|}{4} \sum_{kq\in K} \sum_{\gamma\alpha} \sum_{i,j,k,l=1}^{3} J_i J_j \Big(- \epsilon^{jik}\epsilon^{ijl}\tau^k_{\alpha\gamma}\eta^l + i\delta_{\alpha\gamma}\delta_{ij}\epsilon^{ijl}\eta^l \\
& + i\delta_{ij}\epsilon^{jik}\tau^k_{\alpha\gamma} + \delta_{ij}\delta_{\alpha\gamma}\Big) c_{q\gamma}c^\dagger_{k\alpha}, \\
=& - \frac{\rho_0|\delta\Lambda|}{4} \sum_{kq\in K} \sum_{\gamma\alpha} \sum_{i,j,k=1}^{3} (1-\delta_{ij})(1-\delta_{ik})(1-\delta_{jk}) J_i J_j \tau^k_{\alpha\gamma}\eta^k c^\dagger_{k\alpha}c_{q\gamma} \\
& - \frac{\rho_0|\delta\Lambda|}{4} \sum_{kq\in K} \sum_{\alpha} \sum_{i=1}^{3} J_i^2 c^\dagger_{k\alpha}c_{q\alpha}.
\end{aligned} \tag{2.60}
$$

The change in $\tilde{H}_{\mathcal{L}}$ is then given by

$$
\begin{aligned}
\delta H_{\mathcal{L}} =& - \frac{1}{\Lambda} \left(V^{(+)}V^{(+)\dagger} + V^{(-)}V^{(-)\dagger}\right), \\
=& \frac{\rho_0|\delta\Lambda|}{2\Lambda} \sum_{kq\in K} \sum_{\gamma\alpha} \sum_{i,j,k=1}^{3} (1-\delta_{ij})(1-\delta_{ik})(1-\delta_{jk}) J_i J_j \tau^k_{\alpha\gamma}\eta^k c^\dagger_{k\alpha}c_{q\gamma}, \\
=& \frac{\rho_0|\delta\Lambda|}{\Lambda} \sum_{kq\in K} \sum_{\alpha\gamma} \left[J_\pm J_z \left(\tau^x_{\alpha\gamma}\eta^x + \tau^y_{\alpha\gamma}\eta^y\right) + J_\pm^2 \tau^z_{\alpha\gamma}\eta^z\right] c^\dagger_{k\alpha}c_{q\gamma}.
\end{aligned} \tag{2.61}
$$

Thus $\tilde{H}_{\mathcal{L}} = H_{\mathcal{L}} + \delta H_{\mathcal{L}}$ is structurally similar to the original Hamiltonian, except for a shift in the couplings by an amount $\delta J_\pm = 2\rho_0|\delta\Lambda|J_\pm J_z/\Lambda$ and $\delta J_z = 2\rho_0|\delta\Lambda|J_\pm^2/\Lambda$. Remembering that $\delta\Lambda$ is negative we obtain the relations

$$
\boxed{\frac{dJ_\pm}{d\ln\Lambda} = -2\rho_0 J_\pm J_z, \quad \text{and} \quad \frac{dJ_z}{d\ln\Lambda} = -2\rho_0 J_\pm^2.} \tag{2.62}
$$

These differential equations tell us how the couplings respond to a reduction of the bandwidth. We will first analyze the isotropic $J_z = J_\pm$ case, for which the differential equation is given by

$$
\frac{dg}{d\ln\Lambda} = -2g^2. \tag{2.63}
$$

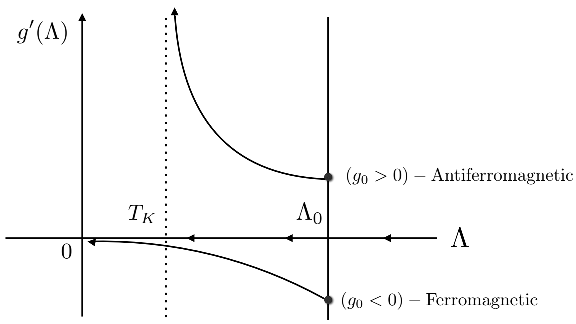

Figure 2.2: Renormalization flow for the isotropic Kondo model, depicting both ferromagnetic $g_0 < 0$ and antiferromagnetic $g_0 > 0$ trajectories.

Here, we have set $g = \rho_0 J$ as our dimensionless coupling. The scaling equation for our dimensionless coupling is obtained upon integration of (2.63):

$$-\int_{g_0}^{g'} \frac{dg}{g^2} = 2\int_{\Lambda_0}^{\Lambda'} d(\ln\Lambda), \tag{2.64}$$

which implies

$$\boxed{g(\Lambda') = \frac{g_0}{1 - 2g_0 \ln\left(\frac{\Lambda_0}{\Lambda'}\right)}.} \tag{2.65}$$

This scaling equation is depicted graphically in Fig. 2.2. The ferromagnetic $g_0 < 0$ case scales to zero, while the antiferromagnetic $g_0 > 0$ case scales to infinity at some critical value. The value of Λ at which g diverges is called the Kondo temperature T_K, and it serves as the natural energy scale of the Kondo problem. For instance, up to a prefactor of $\mathcal{O}(1)$, it equals the temperature of the resistance minimum.

Let us relate the Kondo temperature to the initial ultraviolet scale Λ_0 and the bare coupling g_0. From (2.63) we have

$$\frac{1}{g_0} - \frac{1}{g'} = 2\ln\left(\frac{\Lambda_0}{\Lambda'}\right). \tag{2.66}$$

At $\Lambda' = T_K$, $g' \to \infty$ so that

$$T_K = \Lambda_0 e^{-1/2g_0}. \tag{2.67}$$

Since we can write

$$2g(\Lambda') = \frac{1}{\ln(\frac{\Lambda'}{T_K})}, \tag{2.68}$$

the low energy physics only depends on the ultraviolet physics through T_k. Furthermore, (2.68) makes it clear that the running coupling $g(\Lambda')$ diverges at the scale $\Lambda' = T_K$, so that perturbative results are only valid for quantities that probe the system at energy scales sufficiently larger than T_K.

Returning to the anisotropic case, the scaling trajectories of the dimensionless couplings can be obtained by combining the two equations in (2.62) to give

$$\frac{dJ_z}{dJ_\pm} = \frac{J_\pm}{J_z}, \tag{2.69}$$

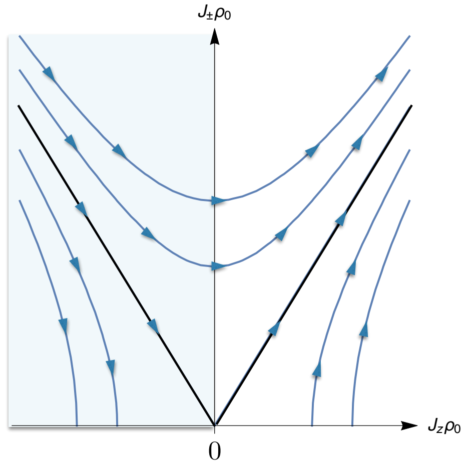

Figure 2.3: Renormalisation flow for the anisotropic Kondo model.

which implies

$$\boxed{J_z^2 - J_{\pm}^2 = \text{const.}} \tag{2.70}$$

Fig. 2.3 is the renormalisation flow diagram of the anisotropic Kondo model, with blue and white regions representing the ferromagnetic and antiferromagnetic sectors respectively, while the black line is the $J_z = J_{\pm}$ isotropic trajectory. We first notice that the trajectories flow from left to right, which is a consequence of $dJ_z/d\ln\Lambda$ always being negative. Secondly, all curves bellow the isotropic line, and in the ferromagnetic sector scale into the $J_{\pm} = 0$ axis. This is a solvable problem because it represents a static, Ising model type spin perturbing the free electron gas [16]. However, for the remainder of the parameter space $J_{\pm} > |J_z|$, all models flow to strong coupling and are beyond the regime of perturbation theory.

Although Anderson's poor man's scaling technique is not the final word on the Kondo problem, it nevertheless offers us some very important insight into the main difficulties in Kondo physics. Not only does it demonstrate the shortcomings of perturbation theory for the case of $J > 0$, but it provides an effective energy scale at which this breakdown occurs. Furthermore, we have learned that no matter how small J is in the antiferromagnetic case, one can always find a corresponding Kondo temperature T_K for which the problem flows to strong coupling. In short, perturbative techniques are always bound to fail, making the Kondo problem highly non-trivial.

Chapter 3

The bosonization technique

Bosonization is a mapping between fermionic and bosonic Hilbert spaces. This mapping was formally developed by Mattis and Lieb in their work on Luttinger liquid theory [17]. This surprising correspondence was based on the earlier observations of Tomonaga [18], who found that certain elementary excitations of interacting electrons in one-dimension displayed boson-like behavior. We will make use of this correspondence to map the anisotropic Kondo Hamiltonian onto a Hamiltonian constructed out of bosonic degrees of freedom. After a few simplifying manipulations in the bosonic space, the Hamiltonian will be cast back into the fermionic space using new fermionic degrees of freedom. Performing this mapping back to fermionic degrees of freedom at one particular (non-trivial) point in the Kondo parameter space results in a noninteracting Hamiltonian which is quadratic in new fermion operators.

In this chapter we derive the formalism of the bosonization technique, and in particular the so called bosonization identity, which relates a fermionic field to an exponential of a bosonic field. Our approach is similar to that of Haldane [19] and von Delft and Schoeller [20], in that it follows what is known as the constructive approach to bosonization. For an alternative field theoretic construction, we refer the reader to the work of Kopietz and Schönhammer [21].

3.1 Fermionic theory and bosonization prerequisites

We consider fermions confined to the interval $[-\frac{L}{2}, \frac{L}{2}]$ in one-dimension, with boundary conditions

$$\psi_\eta(x + L/2) = e^{i\pi\delta_b}\psi_\eta(x - L/2). \tag{3.1}$$

Here, η is a species (e.g. spin) index, and $\delta_b = 0$ or 1 depending on whether we want the fields to obey periodic or anti-periodic boundary conditions. In terms of the annihilation operators $c_{k\eta}$ of a particle with momentum k ($\hbar = 1$) and species η, the fermionic field is expanded as

$$\boxed{\psi_\eta(x) \equiv \frac{1}{\sqrt{L}}\sum_k e^{ikx}c_{k\eta},} \tag{3.2}$$

where k runs from $-\infty$ to ∞. We call the $c_{k\eta}$'s mode operators. The modes and fields obey the standard anticommutation relations

$$\{c_{k\eta}, c^{\dagger}_{k'\eta'}\} = \delta_{kk'}\delta_{\eta\eta'}, \qquad \{\psi_{\eta}(x), \psi^{\dagger}_{\eta'}(x')\} = \delta_{\eta\eta'}\delta(x-x'). \tag{3.3}$$

The allowed set of momentum values are:

$$k = \frac{2\pi}{L}\left(n_k - \frac{1}{2}\delta_b\right), \qquad n_k \in Z. \tag{3.4}$$

It is important for the bosonization procedure that the label n_k runs from $-\infty$ to ∞.

The above set of mode operators defines the vacuum state $|0\rangle$ as

$$c_{k\eta}|0\rangle = 0, \quad k > 0, \tag{3.5}$$

$$c^{\dagger}_{k\eta}|0\rangle = 0, \quad k \leq 0. \tag{3.6}$$

It must be mentioned that the vacuum state $|0\rangle$ refers to the Fermi sea and not the state in which there are no particles. The state $|0\rangle$ serves as our reference state relative to which all other states in Fock space are defined. Now that we have our vacuum state, it is possible to define the operation of Fermi normal ordering denoted by ": :". Given a string of fermionic operators A,B,C,...$\in$ $\{c_{k\eta}, c^{\dagger}_{k\eta}\}$, the procedure of normal ordering places all operators $c_{k\eta}$ with $k > 0$ and operators $c^{\dagger}_{k\eta}$ with $k \leq 0$ to the right of all other operators.

Wick's theorem establishes the relation

$$\begin{aligned} : ABC... :=ABC... &- \sum_{\sqcup} \underbrace{: ABC... :}_{\text{all single contractions}} - \sum_{\sqcup\sqcup} \underbrace{: ABC... :}_{\text{all double contractions}} \\ &- \sum_{\sqcup\sqcup\sqcup} \underbrace{: ABC... :}_{\text{all triple contractions}} - \quad ..., \end{aligned} \tag{3.7}$$

where a contraction is defined by

$$\underbrace{AB}_{\sqcup} \equiv \langle 0|\, AB\, |0\rangle\,. \tag{3.8}$$

Additionally, before performing a contraction, the two operators being contracted must be moved next to each other, which in the case of fermions results in a change of sign for odd permutations.

We are now in a position to define the number operator $\hat{N}_{\eta}$ which counts the number of particles of a particular species in a state relative to the Fermi sea. To do this we must subtract off the infinite contribution from the vacuum. For quadratic operators this simply amounts to normal ordering the product

$$\hat{N}_{\eta} \equiv \sum_{k} : c^{\dagger}_{k\eta} c_{k\eta} := \sum_{k} \left(c^{\dagger}_{k\eta} c_{k\eta} - \langle 0|\, c^{\dagger}_{k\eta} c_{k\eta}\, |0\rangle \right). \tag{3.9}$$

The number operators $\hat{\vec{N}} = (\hat{N}_1, \cdots, \hat{N}_M)$ partition the fermionic Fock space $\mathcal{H}_c$ into subspaces labeled by eigenvalues $\vec{N} = (N_1, N_2, ...N_M)$, where N_η is the eigenvalue of $\hat{N}_\eta$ and there are M species. Each subspace is infinite dimensional because the single particle Hilbert space is infinite dimensional. The space spanned by the set of all eigenvectors sharing the same eigenvalues form an $\vec{N}$-particle Hilbert space is denoted by $\mathcal{H}_{\vec{N}}$.

For future reference we define an effective low energy Hamiltonian for non-interacting fermions in one dimension

$$H_{0\eta} = \sum_k k : c^\dagger_{k\eta} c_{k\eta} : . \tag{3.10}$$

For the moment, $H_{0\eta}$ is just an operator whose eigenvectors provide a useful basis for $\mathcal{H}_c$. However, very often in applications where bosonization is useful, the operator $H_{0\eta}$ serves as a good approximation to the system's kinetic energy. At this point we will already start using language associated with Hamiltonian quantum mechanics, such as ground state or Fermi level. Note however that bosonization is valid whether or not the systems Hamiltonian is $H_{0\eta}$. Using our operator $H_{0\eta}$, the ground state can be defined as the lowest energy configuration of a set of $\vec{N}$-particles. Each $\vec{N}$-particle Hilbert space now has its own unique ground state which consists of the state with no particle-hole excitations. This state serves as the vacuum state for $\mathcal{H}_{\vec{N}}$. To ensure there is no sign ambiguity in our labeling, we introduce the following packing convention for the case of $\eta = (\uparrow, \downarrow)$

$$|\vec{N}\rangle \equiv (c_\downarrow)^{N_\downarrow} (c_\uparrow)^{N_\uparrow} |0\rangle, \tag{3.11}$$

where,

$$(c_\uparrow) \equiv \begin{cases} c^\dagger_{N_\uparrow \uparrow} c^\dagger_{(N_\uparrow - 1)\uparrow} \cdots c^\dagger_{1\uparrow} & \text{if } N_\uparrow > 0, \\ 1 & \text{if } N_\uparrow = 0, \\ c_{(N_\uparrow+1)\uparrow} c_{(N_\uparrow+2)\uparrow} \cdots c_{0\uparrow} & \text{if } N_\uparrow < 0. \end{cases} \tag{3.12}$$

According to (3.11), we first pack the spin up particles. The order in which we pack these particles is dictated by (3.12), where if we have particles in excess of the Fermi sea, the packing is in ascending order of N. However if the particle number is less than that of the Fermi number, then the systematic removal of modes is carried out from the Fermi level down. Finally in the case where there are no spin up particles ($N_\uparrow = 0$), we have that $(c_\uparrow)^{N_\uparrow} = 1$ and consequently the vacuum state is unaffected. We then proceed to pack the spin down particles in a similar fashion.

3.2 Creating a bosonic operator algebra

This section deals with the development of a bosonic operator algebra using fermionic operators as building blocks. We will show that up to a proportionality constant, the Fourier transform of the density operator is bosonic in nature. Furthermore, we shall prove that the bosonic Fock space $\mathcal{H}_b$, on which these bosonic operators are defined, is equivalent to the fermionic Fock space $\mathcal{H}_c$.

3.2.1 Bosonic particle-hole operators

We begin by considering the Fourier transform of the density operator

$$\rho_q = \int_{-L/2}^{L/2} dx \; e^{-iqx} \rho(x), \tag{3.13}$$

with the density operator given by $\rho(x) =: \psi^\dagger(x)\psi(x) :$. In conjunction with (3.2), it follows that

$$\begin{aligned}
\rho_q &= \frac{1}{L} \int_{-L/2}^{L/2} dx \; e^{-i(q+p-k)x} \sum_{pk} : c_p^\dagger \; c_k :, \\
&= \sum_{pk} \delta_{p+q,k} : c_p^\dagger \; c_k :, \\
&= \sum_{k} : c_{k-q}^\dagger c_k :, \\
&= \begin{cases} \sum_k c_{k-q}^\dagger c_k & , \text{if} \;\; q \neq 0, \\ \sum_k : c_k^\dagger c_k : & , \text{if} \;\; q = 0, \end{cases}
\end{aligned} \tag{3.14}$$

where for the case $q \neq 0$ we have dropped the normal ordering notation, since for $q > 0$ or $q < 0$ the operators are either both creation operator or both annihilation operators and therefore are automatically normal ordered. However for the case $q = 0$, the normal ordering notation must be maintained and simply results in the number operator. The operators ρ_q are associated with charge-density fluctuations. As we now show, there are bosonic quanta associated with these fluctuations. We start by considering the commutator $[\rho_{q\eta}, \rho_{-q\eta'}]$. This commutator is nontrivial as first demonstrated in the work of Mattis and Lieb [17]:

$$\begin{aligned}
[\rho_{q\eta}, \rho_{-q'\eta'}] &= \sum_{kk'} \left[c_{k-q\eta}^\dagger c_{k\eta}, c_{k'+q'\eta'}^\dagger c_{k'\eta'} \right], \\
&= \delta_{\eta\eta'} \sum_{kk'} \left(c_{k-q\eta}^\dagger c_{k'\eta'} \delta_{k,k'+q'} - c_{k'+q'\eta'}^\dagger c_{k\eta} \delta_{k-q,k'} \right), \\
&= \delta_{\eta\eta'} \sum_{k} \left(c_{k-q\eta}^\dagger c_{k-q'\eta} - c_{k-q+q'\eta}^\dagger c_{k\eta} \right).
\end{aligned} \tag{3.15}$$

At this point we would like to sum the two terms in (4.6) separately. In that case we could for instance shift $k \to k - q'$ in the second term, i.e.,

$$\sum_k c_{k-q+q'}^\dagger c_k = \sum_k c_{k-q}^\dagger c_{k-q'}, \tag{3.16}$$

after which it cancels with the first term. However, we can only split an infinite sum if the sum of the individual terms converge. To ensure that we work with convergent quantities, we add and subtract the vacuum expectation values:

$$
\begin{aligned}
\delta_{\eta\eta'} \sum_k \left(c^\dagger_{k-q\eta} c_{k-q'\eta} - c^\dagger_{k-q+q'\eta} c_{k\eta} \right) \\
&= \delta_{\eta\eta'} \sum_k \Big(c^\dagger_{k-q\eta} c_{k-q'\eta} - \langle 0 | \, c^\dagger_{k-q\eta} c_{k-q'\eta} \, | 0 \rangle \\
&- c^\dagger_{k-q+q'\eta} c_{k\eta} + \langle 0 | \, c^\dagger_{k-q+q'\eta} c_{k\eta} \, | 0 \rangle + \langle 0 | \, c^\dagger_{k-q\eta} c_{k-q'\eta} \, | 0 \rangle - \langle 0 | \, c^\dagger_{k-q+q'\eta} c_{k\eta} \, | 0 \rangle \Big), \\
&= \delta_{\eta\eta'} \sum_k \Big(: c^\dagger_{k-q\eta} c_{k-q'\eta} : - : c^\dagger_{k-q+q'\eta} c_{k\eta} : \\
&+ \langle 0 | \, c^\dagger_{k-q\eta} c_{k-q'\eta} \, | 0 \rangle - \langle 0 | \, c^\dagger_{k-q+q'\eta} c_{k\eta} \, | 0 \rangle \Big). \qquad (3.17)
\end{aligned}
$$

Assuming that $\sum : c^\dagger c :$ converges (which we do not prove here), we can now split the sum and shift the indices in the second normal ordered term to $k \to k - q'$. The only non-vanishing contribution is given by two terms which simply count the particle occupations of the N_η-particle ground state. We therefore have

$$
\begin{aligned}
[\rho_{q\eta}, \rho_{-q'\eta'}] &= \delta_{\eta\eta'} \sum_k \left(: c^\dagger_{k-q\eta} c_{k-q'\eta} : - : c^\dagger_{k-q\eta} c_{k-q'\eta} : + \, \delta_{qq'} \left[\theta(q-k) - \theta(-k) \right] \right) \\
&= \delta_{\eta\eta'} \delta_{qq'} \sum_k \theta(q-k) - \theta(-k), \\
&= \delta_{\eta\eta'} \delta_{qq'} n_q, \qquad (3.18)
\end{aligned}
$$

where $n_q = Lq/2\pi$. This result confirms the bosonic nature of the density operator ρ_q. If it were not for the n_q appearing on the right hand side of (3.18), the density operators ρ_q would satisfy the bosonic commutation relations exactly. We therefore introduce normalized operators

$$
\boxed{ b^\dagger_{q\eta} \equiv \frac{1}{\sqrt{n_q}} \sum_k c^\dagger_{k+q\eta} c_{k\eta}, \qquad b_{q\eta} \equiv \frac{1}{\sqrt{n_q}} \sum_k c^\dagger_{k-q\eta} c_{k\eta}, } \qquad (3.19)
$$

with $q > 0$. We refer to these operators as particle-hole operators. They obey the usual commutation relations

$$
[b_{q\eta}, b_{q'\eta'}] = [b^\dagger_{q\eta}, b^\dagger_{q'\eta'}] = 0, \quad [b_{q\eta}, b^\dagger_{q'\eta'}] = \delta_{qq'} \delta_{\eta\eta'}. \qquad (3.20)
$$

We now define the bosonic Fock space $\mathcal{H}_b$ as a subspace of $\mathcal{H}_c$ that is spanned by the vectors $|\vec{N}, \{n_{q\eta}\}_b\rangle$, where linear combinations run over all $\vec{N}$ and $\{n_{q\eta}\}$. These bosonic states are constructed by acting on each $\vec{N}$-particle ground state with particle-hole operators $b^\dagger_{q\eta}$:

$$|\vec{N}, \{n_{q\eta}\}_b\rangle = \prod_{q>0} \frac{(b^\dagger_{q\eta})^{n_{q\eta}}}{\sqrt{n_{q\eta}!}} |\vec{N}, \{0\}\rangle \,, \tag{3.21}$$

with $n_{q\eta} \geq 0$, $N_\eta \in Z$, $q = \frac{2\pi}{L} n_q > 0$ and n_q being a positive integer. The numbers N_η in (3.21) refer to the number of particles of species η in the system, while $\{n_{q\eta}\}$ refers to the set of particle-hole excitations created on top of that particular $\vec{N}$-particle ground state. The b index will always be used to represent the excitations induced by bosonic operators. We note that

$$b_{q\eta} |\vec{N}, \{0\}\rangle = 0, \quad \text{ for all } \eta \text{ and } \vec{N}. \tag{3.22}$$

Therefore, the vacuum state for the particle-hole operator is simply the state in the $\vec{N}$-particle Hilbert space with no particle-hole excitations.

We will now show that $\mathcal{H}_b$ is in fact the full space $\mathcal{H}_c$. For simplicity our analysis will be confined to a single species. The arguments can be trivially extended to deal with more than one species.

Consider the Hamiltonian operator

$$H_0 = \sum_k k : c^\dagger_k \, c_k : \,. \tag{3.23}$$

Remember that it does not have to be the actual Hamiltonian of the system. What we call the Hamiltonian here is simply an operator that is useful for the proof. The full Fock space is the span of the orthonormal basis $B_c = \{|\{n_k\}\rangle\}$, where the basis elements are the eigenstates of H_0:

$$H_0 |\{n_k\}\rangle = \sum_k k \; n_k |\{n_k\}\rangle \,. \tag{3.24}$$

We now prove that the set of bosonic Fock states defined in (3.21) are also eigenstates of H_0. Considering the commutation relation between the Hamiltonian operator and particle-hole operator $b_q^\dagger$, we find that

$$\begin{aligned}
[H_0, b_q^\dagger] &= \left[\sum_k k\ c_k^\dagger c_k, \sum_l c_{l+q}^\dagger c_l\right], \\
&= \sum_{kl} k[c_k^\dagger c_k, c_{l+q}^\dagger c_l], \\
&= \sum_{kl} k(\delta_{k,k+l} c_k^\dagger c_l - \delta_{k,l} c_{l+q}^\dagger\ c_k), \\
&= \sum_{kl} (l+q) c_k^\dagger c_{k-q} - l\ c_{k+q}^\dagger c_k, \\
&= q \sum_k c_{k+q}^\dagger c_k, \\
&= q\ b_q^\dagger,
\end{aligned} \tag{3.25}$$

so that in the subspace $\mathcal{H}_b$, the Hamiltonian operator takes the form

$$H_0 = \sum_{q>0} q\ b_q^\dagger b_q, \tag{3.26}$$

and consequentially leaves the subspace $\mathcal{H}_b$ invariant. It follows that an orthonormal basis for $\mathcal{H}_c$ exists of the form $B_c = B_b \cup B_b^\perp$, where B_b are the bosonic Fock states, or eigenvectors of (3.26), and the elements of $B_b^\perp$ are orthogonal to those of B_b, and represent the possible missing vectors of the full space. Each set of vectors define their own particular space, i.e., $\mathcal{H}_b = \text{span}(B_b)$, $\mathcal{H}_b^\perp = \text{span}(B_b^\perp)$ and $\mathcal{H}_c = \mathcal{H}_b \oplus \mathcal{H}_b^\perp$.

An elegant way to demonstrate the equivalence of $\mathcal{H}_c$ and $\mathcal{H}_b$ is to calculate the grand-canonical partition function

$$\begin{aligned}
Z_c(\beta) &= \text{Tr}_{\mathcal{H}_c}\left[e^{-\beta(H_0-\mu\hat{N})}\right], \\
&= \sum_{|\alpha\rangle\in B_c} \langle\alpha|\, e^{-\beta(H_0-\mu\hat{N})}\,|\alpha\rangle, \\
&= \underbrace{\sum_{|\alpha\rangle\in B_b} \langle\alpha|\, e^{-\beta(H_0-\mu\hat{N})}\,|\alpha\rangle}_{Z_b(\beta)} + \sum_{|\alpha\rangle\in B_b^\perp} \langle\alpha|\, e^{-\beta(H_0-\mu\hat{N})}\,|\alpha\rangle.
\end{aligned} \tag{3.27}$$

The partition function is a sum over positive quantities. Therefore, proving the equivalence of the partition functions $Z_c(\beta)$ and $Z_b(\beta)$ shows that $B_b^\perp$ is in fact the empty set. This immediately implies that the set of bosonic states B_b are the entire set of fermionic states B_c. The equivalence of $Z_c(\beta)$ and $Z_b(\beta)$ was first established by Haldane [19]. The proof requires anti-periodic boundary conditions on the fermions, i.e., $\delta_b = 1$ in (3.4). However, in the thermodynamic limit $L \to \infty$, results are independent of boundary conditions. The anti-periodic boundary conditions lead to the quantization $k = 2\pi(n_k - 1/2)/L,\ n_k \in Z$. The Hamiltonian then reads

$$H_0 = \frac{2\pi}{L}\sum_k \left(n_k - \frac{1}{2}\right) : c_k^\dagger c_k : . \tag{3.28}$$

The partition function $Z_c(\beta)$ can be expressed as the product of single fermionic mode partition functions, where we have summed over the possible occupations of that mode

$$\begin{aligned} Z_c(\beta) &= \prod_{n_k=1}^{\infty}\left(1 + e^{-\beta 2\pi/L(n_k-1/2)}e^{\beta\mu n_k}\right)\prod_{n_k=-\infty}^{-1}\left(1 + e^{-\beta 2\pi/L|n_k-1/2|}e^{\beta\mu n_k}\right), \\ &= \prod_{n=1}^{\infty}\left(1 + w^{2n-1}v^n\right)\left(1 + w^{2n-1}v^{-1}\right), \end{aligned} \tag{3.29}$$

with $w \equiv e^{-\beta\pi/L}$ and $v \equiv e^{\beta\mu}$. Our task is to show that $Z_b(\beta)$ has the same form as (3.29). As already mentioned, the bosonic states are eigenstates of both the number operator $\hat{N}$ and Hamiltonian H_0, with eigenvalues

$$\hat{N}\left|N, \{m_q\}_b\right\rangle = N\left|N, \{m_q\}_b\right\rangle, \tag{3.30}$$

$$H_0\left|N, \{m_q\}_b\right\rangle = \left(\frac{2\pi}{L}\frac{N^2}{2} + \sum_{q>0} q m_q\right)\left|N, \{m_q\}_b\right\rangle. \tag{3.31}$$

As such, the grand partition function is given by

$$\begin{aligned} Z_b(\beta) &= \sum_{N=-\infty}^{\infty}\sum_{\{m_q\}}\left\langle N; \{m_q\}_b\right| e^{-\beta(H_0-\mu\hat{N})}\left|N; \{m_q\}_b\right\rangle, \\ &= \sum_{N=-\infty}^{\infty}\sum_{\{m_q\}} e^{-\beta 2\pi/L(N^2/2+\sum_{q>0} n_q m_q)}e^{\mu\beta N}, \\ &= \left(\sum_{N=-\infty}^{\infty} w^{N^2}v^N\right)\left(\sum_{M=0}^{\infty} P(M)w^{2M}\right). \end{aligned} \tag{3.32}$$

Here $P(M)$ represents the number of states satisfying the restriction $\sum_{n_q=1}^{\infty} n_q m_q = M$ for some $\{m_q\}$, and $P(M)$ is the number of partitions of M and thus also occurs in the power series expansion of the function

$$\frac{1}{\prod_{n=1}^{\infty}(1-y^n)} = \prod_{n=1}^{\infty}\left[\sum_{m=0}^{\infty}(y^n)^m\right] = \sum_{M=0}^{\infty} P(M)y^M. \tag{3.33}$$

Substituting this into (3.32) gives

$$Z_b = \frac{\sum_{N=-\infty}^{\infty} w^{N^2}v^N}{\prod_{n=1}^{\infty}(1-w^{2n})}. \tag{3.34}$$

The proof is completed by rewriting the numerator using the Jacobi triple product identity

$$\sum_{N=-\infty}^{\infty} w^{N^2} v^N = \prod_{n=1}^{\infty} (1 + w^{2n-1} v)(1 + w^{2n-1} v^{-1})(1 - w^{2n}). \tag{3.35}$$

For a proof of this identity, see the appendix at the end of the chapter. Substituting this result into (3.34) gives us back the same form as $Z_c(\beta)$ in (3.29). Therefore, we can conclude that $B_b^\perp$ is the empty set, and that the bosonic Fock states defined in (3.21) span the entire space.

3.2.2 Klein factors

Although we have constructed operators which allow us to span each subspace $\mathcal{H}_{\vec{N}}$ separately, we still do not have the means to connect the separate $\vec{N}$-particle Hilbert spaces. This requires the construction of a ladder operator called a Klein factor. These Klein factors, denoted by $F_\eta^\dagger$ and F_η, serve a two-fold purpose. Firstly, they connect the different $\vec{N}$-particle subspaces by creating or destroying a fermion of type η. Secondly, they allow us to construct fermionic operators with the correct anti-commutation relations using as building blocks $F_\eta, F_\eta^\dagger$ and $b_{q\eta}, b_{q\eta}^\dagger$.

As already demonstrated, the states

$$|\vec{N}, \{n_{q\eta}\}_b\rangle = \prod_{q>0} \frac{(b_{q\eta}^\dagger)^{n_{q\eta}}}{\sqrt{n_{q\eta}!}} |\vec{N}, \{0\}\rangle \,, \tag{3.36}$$

form a basis for $\vec{N}$-particle Fock space. The ladder operator F_η is defined by its action on this basis as follows

$$\begin{aligned} F_\eta |\vec{N}, \{n_{q\eta}\}_b\rangle &\equiv \prod_{q>0} \frac{(b_{q\eta}^\dagger)^{n_{q\eta}}}{\sqrt{n_{q\eta}!}} c_{N_\eta} |N_1, ..., N_\eta, ...N_M, \{0\}\rangle \,, \\ &= \prod_{q>0} \frac{(b_{q\eta}^\dagger)^{n_{q\eta}}}{\sqrt{n_{q\eta}!}} \hat{T}_\eta |N_1, ..., N_\eta - 1, ...N_M, \{0\}\rangle \,, \end{aligned} \tag{3.37}$$

$$\begin{aligned} F_\eta^\dagger |\vec{N}, \{n_{q\eta}\}_b\rangle &\equiv \prod_{q>0} \frac{(b_{q\eta}^\dagger)^{n_{q\eta}}}{\sqrt{n_{q\eta}!}} c_{N_\eta+1}^\dagger |N_1, ..., N_\eta, ...N_M, \{0\}\rangle \,, \\ &= \prod_{q>0} \frac{(b_{q\eta}^\dagger)^{n_{q\eta}}}{\sqrt{n_{q\eta}!}} \hat{T}_\eta |N_1, ..., N_\eta + 1, ...N_M, \{0\}\rangle \,, \end{aligned} \tag{3.38}$$

with the $\hat{T}_\eta$ operator keeping track of the signs picked up due to the permutation of $c_{k\eta}$ to the location of its action

$$\hat{T} \equiv (-)^{\sum_{\hat{\eta}=1}^{\eta-1} \hat{N}_{\hat{\eta}}}. \tag{3.39}$$

The Klein factors commute with the particle-hole operators. For example we consider the commutation $[b_q, F]$, where for simplicity we will work with one species. From (3.37) it follows that

$$\begin{aligned}
[b_p, F]\,|N, \{n_q\}_b\rangle =& b_p \prod_{q>0} \frac{(b_q^\dagger)^{n_q}}{\sqrt{n_q!}} c_N\,|N, \{0\}\rangle - F b_p \prod_{q>0} \frac{(b_q^\dagger)^{n_q}}{\sqrt{n_q!}}\,|N, \{0\}\rangle\,, \\
=& b_p \prod_{q>0} \frac{(b_q^\dagger)^{n_q}}{\sqrt{n_q!}}\,|N-1, \{0\}\rangle - F b_p \prod_{q>0} \frac{(b_q^\dagger)^{n_q}}{\sqrt{n_q!}}\,|N, \{0\}\rangle\,, \\
=& \left[b_p, \prod_{q>0} \frac{(b_q^\dagger)^{n_q}}{\sqrt{n_q!}}\right]|N-1, \{0\}\rangle - F\left[b_p \prod_{q>0} \frac{(b_q^\dagger)^{n_q}}{\sqrt{n_q!}}\right]|N, \{0\}\rangle\,, \quad (3.40)
\end{aligned}$$

where in the last line we have substituted the commutator, since the action of any particle-hole annihilation operator on an N-particle ground state returns zero. With the help of the identity $[b_i, (b_j^\dagger)^n] = n(b_i^\dagger)^{n-1}$, we find

$$\left[b_p, \prod_{q>0} \frac{(b_q^\dagger)^{n_q}}{\sqrt{n_q!}}\right] = \prod_{q\neq p} \frac{(b_q^\dagger)^{n_q}}{\sqrt{n_q!}} \frac{(b_p^\dagger)^{n_p-1}}{\sqrt{(n_p-1)!}}. \quad (3.41)$$

It follows that

$$[b_p, F]\,|N, \{n_q\}_b\rangle = |N-1, \{n_1, ..., n_p-1, ...\}_b\rangle - F\,|N, \{n_1, ..., n_p, ...\}_b\rangle = 0. \quad (3.42)$$

Therefore $[b_{q\eta}, F_{\eta'}] = 0$, since the states we are operating on form a complete basis. Similarly we can prove the commutation relations

$$[b_{q\eta}^\dagger, F_{\eta'}^\dagger] = [b_{q\eta}^\dagger, F_{\eta'}] = [b_{q\eta}, F_{\eta'}^\dagger] = 0. \quad (3.43)$$

These relations imply that the Klein factors do not affect the particle-hole structure. Furthermore

$$\begin{aligned}
\langle M, \{m_q\}_b|\, F^\dagger F\,|N, \{n_q\}_b\rangle &= \langle M-1, \{m_q\}_b|\, N-1, \{n_q\}_b\rangle, \\
&= \delta_{MN}\delta_{\{m_q\}\{n_q\}}, \\
&= \langle M, \{m_q\}_b|\, N, \{n_q\}_b\rangle. \quad (3.44)
\end{aligned}$$

Thus F, preserves the orthonormality of the basis B_b of $\mathcal{H}_c$ and is therefore unitary. The algebra of the Klein factors can be obtained by acting with them in different combinations on an arbitrary state. Firstly we note that

$$F_\eta^\dagger F_{\eta'}^\dagger\,|\vec{N}, \{n_{q\eta}\}_b\rangle = \pm\,|N_1, ..., N_{\eta'}+1, ..., N_\eta+1, ..., \{n_{q\eta}\}_b\rangle\,, \quad (3.45)$$

whereas

$$F^\dagger_{\eta'}F^\dagger_\eta\,|\vec{N},\{n_{q\eta}\}_b\rangle = \mp\,|N_1,...,N_{\eta'}+1,...,N_\eta+1,...,\{n_{q\eta}\}_b\rangle\,. \tag{3.46}$$

The change of sign arises from the fact that in the second case, the $c^\dagger_{N_{\eta'}+1}$ operator in (3.38) has to commute past either one more or one less fermion. This change in sign must also occur for the F_η and $F_{\eta'}$ operators and leads to the following anticomutation relations

$$\{F^\dagger_\eta, F^\dagger_{\eta'}\} = \{F_\eta, F_{\eta'}\} = 0, \quad \text{for} \quad \eta \neq \eta'. \tag{3.47}$$

However, if $\eta = \eta'$, then since F_η is unitary

$$F^\dagger_\eta F_\eta = F_\eta F^\dagger_\eta = 1 \to \{F^\dagger_\eta, F_{\eta'}\} = 2\delta_{\eta\eta'}. \tag{3.48}$$

The ladder properties of the Klein factors can be seen when considering their action on an arbitrary state in combination with the number operator $\hat{N}$. For brevity the bosonic Fock states will be defined as $|N_\eta, N_{\eta'}\rangle$, since neither the Klein factor, nor the number operator affect the particle-hole excitations. We then have that

$$\begin{aligned}[\hat{N}_\eta, F^\dagger_\eta]\,|N_\eta, N_{\eta'}\rangle =&(N_\eta+1)F^\dagger_\eta\,|N_\eta, N_{\eta'}\rangle - N_\eta F^\dagger_\eta\,|N_\eta, N_{\eta'}\rangle\,,\\ =&F^\dagger_\eta\,|N_\eta, N_{\eta'}\rangle\,,\end{aligned} \tag{3.49}$$

$$\begin{aligned}[\hat{N}_\eta, F^\dagger_{\eta'}]\,|N_\eta, N_{\eta'}\rangle =&(N_\eta+1)F^\dagger_{\eta'}\,|N_\eta, N_{\eta'}\rangle - N_\eta F^\dagger_{\eta'}\,|N_\eta, N_{\eta'}\rangle\,,\\ =&F^\dagger_{\eta'}\,|N_\eta, N_{\eta'}\rangle\,,\\ =&[\hat{N}_\eta, F_{\eta'}]\,|N_\eta, N_{\eta'}\rangle = 0,\end{aligned} \tag{3.50}$$

$$\begin{aligned}[\hat{N}_\eta, F_\eta]\,|N_\eta, N_{\eta'}\rangle =&(N_\eta-1)F_\eta\,|N_\eta, N_{\eta'}\rangle - N_\eta F_\eta\,|N_\eta, N_{\eta'}\rangle\,,\\ =&-F_\eta\,|N_\eta, N_{\eta'}\rangle\,.\end{aligned} \tag{3.51}$$

In conclusion

$$[\hat{N}_\eta, F^\dagger_{\eta'}] = \delta_{\eta\eta'}F^\dagger_\eta, \qquad [\hat{N}_\eta, F_{\eta'}] = -\delta_{\eta\eta'}F_\eta. \tag{3.52}$$

Now that we have formulated all the fundamental operators of the bosonization procedure, it is instructive to analyze their action graphically.

We first analyze the effect of the particle-hole operator $b^\dagger_2$ on the vacuum state. Fig. 3.1 shows how $b^\dagger_2$ searches for particles that can be shifted two levels above their current position. If a particle already exists at that level, nothing happens. However, if the level is empty, the particle is promoted to it. The behavior of the operator remains the same when the state being acted on already has particle-hole excitations. Take for example the state $c^\dagger_1 c_{-1}\,|0\rangle$ in Fig. 3.2. In general, $b^\dagger_q$ consists of all possible ways to

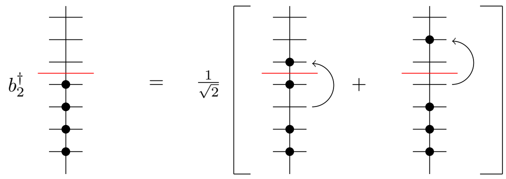

Figure 3.1: Action of the particle-hole operator $b_2^\dagger$ on the $N = 0$ ground state.

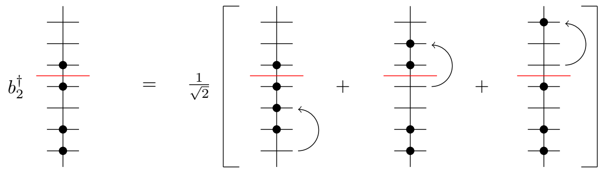

Figure 3.2: Action of the particle-hole operator $b_2^\dagger$ on the state $c_1^\dagger c_{-1} |0\rangle$.

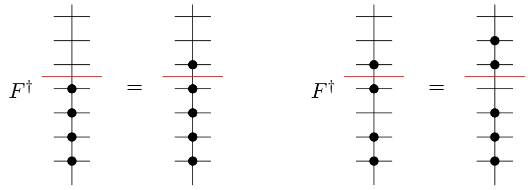

Figure 3.3: Action of the Klein factor $F^\dagger$ on the $N = 0$ ground state (left), and the $c_1^\dagger c_{-1} |0\rangle$ excited state (right).

create particle-hole excitations that increase the total energy by q. Similarly, b_q consists of linear combinations of all possible ways to annihilate particle-hole excitations with energy q. Turning our attention to the Klein factors, the first panel of Fig. 3.3 shows how $F^\dagger$ acting on the Fermi sea $|0\rangle$ simply adds a particle to the first unoccupied level. If there are already particle-hole excitations, their structure is left unaltered and each particle is simply promoted by one level. For instance consider $F^\dagger(c_1^\dagger c_{-1} |0\rangle)$ in Fig. 3.3.

3.2.3 Boson fields

Bosonic modes b_q carry momentum indices. It is useful to introduce bosonic fields labeled by positions x, namely

$$\boxed{\varphi_\eta(x) \equiv -\sum_{q>0} \frac{i}{\sqrt{n_q}} e^{iqx} b_{q\eta} e^{-aq/2}, \qquad \varphi_\eta^\dagger(x) \equiv \sum_{q>0} \frac{i}{\sqrt{n_q}} e^{-iqx} b_{q\eta}^\dagger e^{-aq/2},} \tag{3.53}$$

and

$$\boxed{\phi_\eta(x) = \varphi_\eta^\dagger(x) + \varphi_\eta(x) = \sum_{q>0} \frac{i}{\sqrt{n_q}} \left(e^{-iqx} b_{q\eta}^\dagger - e^{iqx} b_{q\eta}\right) e^{-aq/2}.} \tag{3.54}$$

Here, a is a positive infinitesimal regularization parameter which is of the order of the lattice spacing. It can be thought of as the maximum momentum transfer of the system, where $1/a$ plays the role of an effective band width. It has been manually inserted into the definition of the bosonic fields in order to govern ultraviolet $q \to \infty$ divergent momentum sums. The Hermitian field $\phi_\eta(x)$ has been introduced for notational brevity. The boson fields commute as follows

$$[\varphi^\dagger_\eta(x), \varphi^\dagger_{\eta'}(x')] = [\varphi_\eta(x), \varphi_{\eta'}(x')] = 0, \tag{3.55}$$

$$\begin{aligned} [\varphi_\eta(x), \partial_{x'}\varphi^\dagger_{\eta'}(x')] &= \delta_{\eta\eta'} 2\pi i \left[\frac{a/\pi}{(x-x')^2 + a^2} - \frac{1}{L}\right], \\ &= 2\pi i \left[\delta(x-x') - \frac{1}{L}\right]. \end{aligned} \tag{3.56}$$

$$\begin{aligned} [\varphi_\eta(x), \varphi^\dagger_{\eta'}(x')] &= \delta_{\eta\eta'} \sum_{q>0} \frac{1}{n_q} e^{-iq(x-x'-ia)}, \\ &= -\delta_{\eta\eta'} \ln\left[1 - e^{-i2\pi/L(x-x'-ia)}\right], \\ &= -\delta_{\eta\eta'} \ln\left[i\frac{2\pi}{L}(x-x'-ia)\right]. \end{aligned} \tag{3.57}$$

To arrive at (3.56) we have first taken the limit $L \to \infty$ and then the limit $a \to 0^+$. The last commutation will be very important in what follows. Eq.(3.57) was obtained by expanding the exponential and retaining terms up to order $1/L$. Note in particular that it requires both an infrared and ultraviolet regulator. The utility of $\phi_\eta(x)$ becomes immediately obvious as it manages to capture the normal ordered electron density in a very compact way:

$$\begin{aligned} \rho_\eta(x) &= :\psi^\dagger_\eta(x)\psi_\eta(x):, \\ &= \frac{1}{L}\sum_{k'k} e^{-i(k'-k)x} :c^\dagger_{k'\eta}c_{k\eta}:, \\ &= \frac{1}{L}\sum_q e^{-iqx} \sum_k :c^\dagger_{k+q\eta}c_{k\eta}:, \\ &= \frac{1}{L}\sum_{q>0}\left[e^{-iqx}\sum_k :c^\dagger_{k+q\eta}c_{k\eta}: + e^{iqx}\sum_k :c^\dagger_{k-q\eta}c_{k\eta}:\right] + \frac{1}{L}\sum_k :c^\dagger_{k\eta}c_{k\eta}:, \\ &= \frac{1}{L}\sum_{q>0}\sqrt{n_q}\left(e^{-iqx}b^\dagger_{q\eta} + e^{iqx}b_{q\eta}\right) + \frac{1}{L}\hat{N}_\eta. \end{aligned} \tag{3.58}$$

Here, we have implemented a shift of indices $q \to k' - k$, singled out the $q = 0$ component and used the definitions of the particle-hole operators (3.19). On the other hand, considering the x-derivative of $\phi_\eta(x)$, we find

$$\begin{aligned}\partial_x\phi_\eta(x) &= \partial_x\left[\sum_{q>0}\frac{i}{\sqrt{n_q}}\left(e^{-iqx}b^\dagger_{q\eta}-e^{iqx}b_{q\eta}\right)e^{-aq/2}\right], \\ &= \sum_{q>0}\frac{q}{\sqrt{n_q}}\left(e^{-iqx}b^\dagger_{q\eta}+e^{iqx}b_{q\eta}\right)e^{-aq/2}. \end{aligned} \quad (3.59)$$

Therefore, in the limit $a\to 0^+$ the electron density can be expressed simply as the position derivative of the bosonic field $\phi_\eta(x)$ and the number operator:

$$\boxed{\rho_\eta(x) =: \psi^\dagger_\eta(x)\psi_\eta(x) := \frac{1}{2\pi}\partial_x\phi_\eta(x)+\frac{1}{L}\hat{N}_\eta.} \quad (3.60)$$

Not only does the definition of $\phi_\eta(x)$ provide a compact description of a very important quantity, but already in this early stage we get a feeling for the simplifying nature of the bosonization technique. Where the electron density was formerly quadratic in fermionic fields, it now becomes linear in a bosonic field.

3.2.4 Bosonization identity

We now derive an expression which is the inverse of (3.19). The expression obtained is called the bosonization identity and tells us how to write fermions in terms of bosons.

As a first step, we develop some technology on the boson side, known as coherent states. For simplicity we consider a single bosonic mode. Later we generalize to an arbitrary number of modes. Coherent states are defined as the eigenvectors of the boson annihilation operator:

$$b\left|\alpha\right\rangle = \alpha\left|\alpha\right\rangle. \quad (3.61)$$

An arbitrary state can be written as a power series in $b^\dagger$ acting on the vacuum state. We can therefore write

$$\left|\alpha\right\rangle = \sum_{n=0}^{\infty} a_n\frac{(b^\dagger)^n}{n!}\left|0\right\rangle. \quad (3.62)$$

The eigenvalue condition of (3.61) places a restriction on the coefficients a_n. By considering the left and right hand sides of (3.61) separately, we find

$$b\left|\alpha\right\rangle = \sum_{n=0}^{\infty} a_n n\frac{(b^\dagger)^{n-1}}{n!}\left|0\right\rangle,$$

$$= \sum_{n=0}^{\infty}\frac{a_{n+1}}{n!}(b^\dagger)^n\left|0\right\rangle, \quad (3.63)$$

whereas

$$\alpha\left|\alpha\right\rangle = \alpha\sum_{n=0}^{\infty}\frac{a_n(b^\dagger)^n}{n!}\left|0\right\rangle. \quad (3.64)$$

This implies the recursion relation $a_{n+1} = \alpha a_n$ and hence $a_n = \alpha^n a_0$. If the vacuum is unique, $b\,|\alpha\rangle = \alpha\,|\alpha\rangle$ defines $|\alpha\rangle$ up to a normalization constant. It further implies that a solution exists for every $\alpha \in \mathbb{C}$. It is worth keeping in mind that later we will be working with many vacua. We can set the coefficient of the vacuum equal to one, and write $|\alpha\rangle$ in coherent state form

$$|\alpha\rangle = \sum_{n=0}^{\infty} \frac{\left(\alpha b^{\dagger}\right)^n}{n!}\,|0\rangle = e^{\alpha b^{\dagger}}\,|0\rangle\,. \tag{3.65}$$

The generalization to many bosonic modes is trivial.

Now we construct coherent states using the bosonic particle-hole operators of (3.19). We need to include a label $\vec{N}$ to specify the vacuum state $|\vec{N},\{0\}\rangle$ on top of which the coherent state is built. Thus we define

$$|\vec{N},\{\alpha_q\}\rangle_{\text{coherent}} = c\; e^{\sum_q \alpha_q b_q^{\dagger}}\,|\vec{N},\{0\}\rangle\,, \tag{3.66}$$

where c is some complex number. We now show that $\psi_\eta(x)\,|\vec{N},\{0\}\rangle$ is a coherent state of $b_{q\eta}$. In other words we prove that

$$b_q\psi_\eta(x)\,|\vec{N},\{0\}\rangle = \alpha_q(x)\psi_\eta(x)\,|\vec{N},\{0\}\rangle\,, \tag{3.67}$$

and determine $\alpha_q(x)$. To this end, it is necessary to first calculate the following two commutators using the definitions given in (3.2) and (3.19):

$$\begin{aligned}
[b_{q\eta'},\psi_\eta(x)] =& \frac{1}{\sqrt{n_q}}\frac{1}{\sqrt{L}}\sum_{kk'}\left[c^{\dagger}_{k-q\eta'}c_{k\eta'},c_{k'\eta}\right]e^{ik'x},\\
=& \frac{1}{\sqrt{n_q}}\frac{1}{\sqrt{L}}\sum_{kk'}\left(-c_{k\eta'}\delta_{\eta\eta'}\delta_{k-q,k'}\right)e^{ik'x},\\
=& -\delta_{\eta\eta'}\left(\frac{1}{\sqrt{n_q}}e^{-iqx}\right)\frac{1}{\sqrt{L}}\sum_k e^{ikx}c_{k\eta},\\
=& \delta_{\eta\eta'}\alpha_q(x)\psi_\eta(x),
\end{aligned} \tag{3.68}$$

where we have shifted indices $k' \to k-q$ and defined $\alpha_q(x) \equiv (-1/\sqrt{n_q})e^{-iqx}$. Similarly,

$$\begin{aligned}
[\psi_{\eta'}(x), b^\dagger_{q\eta}] =& \frac{1}{\sqrt{n_q}}\frac{1}{\sqrt{L}}\sum_{kk'}\left[c_{k'\eta'}, c^\dagger_{k+q\eta}, c_{k\eta}\right]e^{ik'x}, \\
=& \frac{1}{\sqrt{n_q}}\frac{1}{\sqrt{L}}\sum_{kk'}\left(\delta_{\eta\eta'}\delta_{k',k+q}c_{k\eta}\right)e^{ik'x}, \\
=& \delta_{\eta\eta'}\left(\frac{1}{\sqrt{n_q}}e^{iqx}\right)\frac{1}{\sqrt{L}}\sum_{k}e^{ikx}c_{k\eta}, \\
=& -\delta_{\eta\eta'}\alpha^*_q(x)\psi_\eta(x).
\end{aligned} \tag{3.69}$$

It follows that

$$\begin{aligned}
b_{q\eta'}\psi_\eta(x)\,|\vec{N},\{0\}\rangle - \underbrace{\psi_\eta(x)b_{q\eta'}\,|\vec{N},\{0\}\rangle}_{=0} =& [b_{q\eta'}, \psi_\eta(x)]\,|\vec{N},\{0\}\rangle\,, \\
=& \delta_{\eta\eta'}\alpha_q(x)\psi_\eta(x)\,|\vec{N},\{0\}\rangle\,,
\end{aligned} \tag{3.70}$$

$$b_{q\eta'}\psi_\eta(x)\,|\vec{N},\{0\}\rangle = \delta_{\eta\eta'}\alpha_q(x)\psi_\eta(x)\,|\vec{N},\{0\}\rangle\,. \tag{3.71}$$

We identify $\psi_\eta(x)\,|\vec{N},\{0\}\rangle$ as a coherent state of $b_{q\eta}$. This means it can be written as

$$\begin{aligned}
\psi_\eta(x)\,|\vec{N},\{0\}\rangle &= \lambda_N(x)\,\exp\left[\sum_{q>0}\alpha_q(x)b^\dagger_{q\eta}\right]F_\eta\,|\vec{N},\{0\}\rangle\,, \\
&= \lambda_N(x)\,\exp\left[-\sum_{q>0}\frac{1}{\sqrt{n_q}}e^{-iqx}b^\dagger_{q\eta}\right]F_\eta\,|\vec{N},\{0\}\rangle\,, \\
&= \lambda_N(x)e^{i\varphi^\dagger_\eta(x)}F_\eta\,|\vec{N},\{0\}\rangle\,,
\end{aligned} \tag{3.72}$$

where $\lambda_N(x)$ is a complex number. In the last step we used definition (3.53) of $\varphi^\dagger_\eta(x)$. The inclusion of the Klein factor F_η is necessary as the fermion field $\psi_\eta(x)$ destroys an electron of type η. We still need to fix the complex number $\lambda_N(x)$. This can be done by evaluating the expectation value of $F^\dagger_\eta\psi_\eta(x)$ in the $\vec{N}$-particle ground-state $|\vec{N},\{0\}\rangle$ as follows

$$\begin{aligned}
\langle\vec{N},\{0\}|\,F^\dagger_\eta\psi_\eta(x)\,|\vec{N},\{0\}\rangle &= \lambda_N(x)\,\langle\vec{N},\{0\}|\,F^\dagger_\eta e^{i\varphi^\dagger_\eta(x)}F_\eta\,|\vec{N},\{0\}\rangle\,, \\
&= \lambda_N(x)\,\langle\vec{N},\{0\}|\,e^{i\varphi^\dagger_\eta(x)}F_\eta F^\dagger_\eta\,|\vec{N},\{0\}\rangle\,, \\
&= \lambda_N(x)\,\langle\vec{N},\{0\}|\,\vec{N},\{0\}\rangle, \\
&= \lambda_N(x).
\end{aligned} \tag{3.73}$$

To obtain the second line we have used the fact that bosonic operators such as $\varphi_\eta^\dagger(x)$ commute with the Klein factors. The third line is obtained by invoking the unitarity of the Klein factors, and the fact that $\varphi_\eta^\dagger(x)$ is a linear combination of creation operators, while $|\vec{N},\{0\}\rangle$ is a bosonic vacuum. Performing the same calculation in the fermionic representation we find

$$\begin{aligned}\langle\vec{N},\{0\}|\, F_\eta^\dagger\psi_\eta(x)\,|\vec{N},\{0\}\rangle &= \frac{1}{\sqrt{L}}\sum_k e^{ikx}\,\langle\vec{N},\{0\}|\, c^\dagger_{N\eta}c_{n_k\eta}\,|\vec{N},\{0\}\rangle\,, \\ &= \frac{1}{\sqrt{L}}e^{i\frac{2\pi}{L}(N_\eta-\frac{1}{2}\delta_b)x}. \end{aligned} \tag{3.74}$$

Comparing the two results gives

$$\boxed{\hat{\lambda}_N(x) = \frac{1}{\sqrt{L}}e^{i\frac{2\pi}{L}(\hat{N}_\eta-\frac{1}{2}\delta_b)x}.} \tag{3.75}$$

Having established that $\psi_\eta(x)\,|\vec{N},\{0\}\rangle$ is a coherent state, we now consider the action of $\psi_\eta(x)$ on basis elements of $\mathcal{H}_c$ in the bosonic representation. The quantity under investigation is

$$\psi_\eta(x)\prod_{q>0}\frac{(b^\dagger_{q\eta'})^{n_{q\eta'}}}{\sqrt{n_{q\eta'}!}}\,|\vec{N},\{0\}\rangle\,. \tag{3.76}$$

The aim is to commute $\psi_\eta(x)$ past $\prod_{q>0}\frac{(b^\dagger_{q\eta})^{n_{q\eta}}}{\sqrt{n_{q\eta}!}}$ in order to make use of (3.72). To this end we develop two useful results. The first result is a consequence of the BCH formula

$$e^{-B}A\,e^{B} = \sum_{n=0}^{\infty}\frac{1}{n!}[A,B]_n = A + [A,B] + \frac{1}{2!}[[A,B],B] + ... \tag{3.77}$$

Setting operators $A = b^\dagger_{q\eta'}$ and $B = -i\varphi_\eta(x)$, we find that

$$[b^\dagger_{q\eta'}, -i\varphi_\eta(x)] = -\frac{1}{\sqrt{n_q}}\sum_{q>0}[b^\dagger_{q\eta'}, b_{q\eta}]e^{iqx} = \frac{\delta_{\eta\eta'}}{\sqrt{n_q}}e^{iqx} = -\delta_{\eta\eta'}\alpha_q^*(x), \tag{3.78}$$

and consequently

$$e^{i\varphi_\eta(x)}b^\dagger_{q\eta'}e^{-i\varphi_\eta(x)} = b^\dagger_{q\eta'} - \delta_{\eta\eta'}\alpha_q^*(x). \tag{3.79}$$

The second useful result follows from the commutator calculated in (3.69), and gives

$$[\psi_\eta(x), b^\dagger_{q\eta'}] = -\delta_{\eta\eta'}\alpha_q^*(x) \to \psi_\eta(x)b^\dagger_{q\eta'} = (b^\dagger_{q\eta'} - \delta_{\eta\eta'}\alpha_q^*(x))\psi_\eta(x). \tag{3.80}$$

Together these two results give

$$\psi_\eta(x)b^\dagger_{q\eta'} = e^{i\varphi_\eta(x)}b^\dagger_{q\eta'}e^{-i\varphi_\eta(x)}\psi_\eta(x). \tag{3.81}$$

This allows us to make use of the fact that $\psi_\eta(x)\,|\vec{N},\{0\}\rangle$ is a coherent state:

$$\begin{aligned}\psi_\eta(x)\prod_{q>0}\frac{(b^\dagger_{q\eta'})^{n_{q\eta'}}}{\sqrt{n_{q\eta'}!}}\,|\vec{N},\{0\}\rangle =& e^{i\varphi_\eta(x)}\prod_{q>0}\frac{(b^\dagger_{q\eta'})^{n_{q\eta'}}}{\sqrt{n_{q\eta'}!}}e^{-i\varphi_\eta(x)}\psi_\eta(x)\,|\vec{N},\{0\}\rangle\,,\\ =&\lambda_N(x)F_\eta e^{i\varphi_\eta(x)}\prod_{q>0}\frac{(b^\dagger_{q\eta'})^{n_{q\eta'}}}{\sqrt{n_{q\eta'}!}}e^{-i\varphi_\eta(x)}e^{i\varphi^\dagger_\eta(x)}\,|\vec{N},\{0\}\rangle\,.\end{aligned} \tag{3.82}$$

At this point it would be nice to commute $e^{i\varphi^\dagger_\eta(x)}$ past $e^{-i\varphi_\eta(x)}$ since as already mentioned, $\varphi_\eta(x)$ consists of linear combinations of the bosonic annihilation operator, meaning that when it is exponentiated, the only term in the expansion that does not return zero when acting on the vacuums is unity. Furthermore, we can avoid picking up an extra factor from the commutation so long as we also commute $e^{i\varphi^\dagger_\eta(x)}$ past $e^{i\varphi_\eta(x)}$. To demonstrate that this statement is true, we develop a commutation rule for exponential operators.

Setting $A \to e^A$ in the BCH formula gives

$$e^{-B}e^Ae^B = \sum_{n=0}^{\infty}\frac{1}{n!}[e^A,B]_n = e^A + \frac{1}{2!}[e^A,B] + \frac{1}{3!}[[e^A,B],B] + \cdots\,. \tag{3.83}$$

Note that

$$[e^A,B] = \sum_{n=0}^{\infty}\frac{1}{n!}[A^n,B] = \sum_{n=1}^{\infty}\frac{n}{n!}A^{n-1}[A,B] = e^A[A,B]. \tag{3.84}$$

The second last step in (3.84) is only true if the operators satisfy the restriction $[[A,B],B] = [[A,B],B] = 0$. Substituting the result found for $[e^A,B]$ into (3.83) and acting on the left of both sides of the equation with e^B, gives us the identity

$$e^Ae^B = e^Be^Ae^{[A,B]}. \tag{3.85}$$

We now recall the commutation relation $[\varphi_\eta(x),\varphi^\dagger_{\eta'}(x')]$ which was calculated in (3.57). Setting $x = x'$, we find that

$$[-i\varphi_\eta(x), i\varphi^\dagger_\eta(x)] = [\varphi_\eta(x),\varphi^\dagger_\eta(x)] = -\ln\left(\frac{2\pi a}{L}\right), \tag{3.86}$$

and

$$[i\varphi_\eta(x), i\varphi^\dagger_\eta(x)] = -[\varphi_\eta(x),\varphi^\dagger_\eta(x)] = \ln\left(\frac{2\pi a}{L}\right). \tag{3.87}$$

Both commutations come to a number, therefore it is safe to make use of the identity $e^Ae^B = e^Be^Ae^{[A,B]}$. Commuting $e^{i\varphi^\dagger_\eta(x)}$ past $e^{-i\varphi_\eta(x)}$ results in

$$\begin{aligned}e^{-i\varphi_\eta(x)}e^{i\varphi^\dagger_\eta(x)} &= e^{i\varphi^\dagger_\eta(x)}e^{-i\varphi_\eta(x)}e^{-\ln\left(\frac{2\pi a}{L}\right)},\\ &= \left(\frac{L}{2\pi a}\right)e^{i\varphi^\dagger_\eta(x)}e^{-i\varphi_\eta(x)},\end{aligned} \tag{3.88}$$

while a reciprocal factor is generated when commuting $e^{i\varphi_\eta^\dagger(x)}$ past $e^{i\varphi_\eta(x)}$:

$$\begin{aligned} e^{i\varphi_\eta(x)}e^{i\varphi_\eta^\dagger(x)} &= e^{i\varphi_\eta^\dagger(x)}e^{i\varphi_\eta(x)}e^{\ln\left(\frac{2\pi a}{L}\right)}, \\ &= \left(\frac{2\pi a}{L}\right)e^{i\varphi_\eta^\dagger(x)}e^{i\varphi_\eta(x)}. \end{aligned} \tag{3.89}$$

Returning to the main line of the calculation, we can now write

$$\begin{aligned} \psi_\eta(x)\,|\vec{N},\{n_{q\eta'}\}_b\rangle &= \lambda_N(x)F_\eta e^{i\varphi_\eta^\dagger(x)}e^{i\varphi_\eta(x)}\prod_{q>0}\frac{(b_{q\eta'}^\dagger)^{n_{q\eta'}}}{\sqrt{n_{q\eta'}!}}\,|\vec{N},\{0\}\rangle\,, \\ &= \lambda_N(x)F_\eta e^{i\varphi_\eta^\dagger(x)}e^{i\varphi_\eta(x)}\,|\vec{N},\{n_{q\eta}\}_b\rangle\,, \\ &= L^{-\frac{1}{2}}e^{i\frac{2\pi}{L}(N_\eta-\frac{1}{2}\delta_b)x}F_\eta e^{i\varphi_\eta^\dagger(x)}e^{i\varphi_\eta(x)}\,|\vec{N},\{n_{q\eta}\}_b\rangle\,. \end{aligned} \tag{3.90}$$

This expression can be written as an operator identity, since $|\vec{N},\{n_{q\eta}\}_b\rangle$ is a basis for $\mathcal{H}_c$:

$$\boxed{\psi_\eta(x) = F_\eta L^{-\frac{1}{2}}e^{i\frac{2\pi}{L}(\hat{N}_\eta-\frac{1}{2}\delta_b)x}e^{i\varphi_\eta^\dagger(x)}e^{i\varphi_\eta(x)}.} \tag{3.91}$$

Note that in going from (3.90) to (3.91) we have replaced N_η with the number operator $\hat{N}_\eta$. In order to bring the bosonization identity into the compact form used in this dissertation, we make use of one more identity from the BCH formula. When $[A,B]$ commutes to a $\mathbb{C}$ number, then $e^Ae^B = e^{A+B}e^{[A,B]/2}$. Using this identity and the commutator calculated in (3.86), we get

$$e^{i\varphi_\eta^\dagger(x)}e^{i\varphi_\eta(x)} = \left(\frac{L}{2\pi a}\right)^{1/2}e^{i\phi_\eta(x)}. \tag{3.92}$$

Finally, substituting the above result into (3.91) and taking the limit $L\to\infty$, which allows us to drop the $\hat{N}_\eta x/L$ factor, we obtain

$$\boxed{\lim_{L\to\infty}\psi_\eta(x) = \frac{F_\eta}{\sqrt{2\pi a}}e^{i\phi_\eta(x)}.} \tag{3.93}$$

Eq.(3.91) allows us to express the Klein factors in terms of fermions

$$\boxed{F_\eta = L^{\frac{1}{2}}\psi_\eta(x)e^{-i\varphi_\eta(x)}e^{-i\varphi_\eta^\dagger(x)}e^{-i\frac{2\pi}{L}(\hat{N}_\eta-\frac{1}{2}\delta_b)x}.} \tag{3.94}$$

There is something peculiar about this relation. The left hand side is independent of x, while it is not obvious that the right hand side is x-independent. Let us prove it:

Denote the right hand side of the above equation by $\tilde{F}_\eta(x)$. We will first show that $\tilde{F}_\eta(x)$ commutes with the bosons. Since the fields $\varphi_\eta(x)$ and $\varphi^\dagger_\eta(x)$ satisfy

$$[b^\dagger_{q\eta'}, \varphi_\eta(x)] = -i\delta_{\eta\eta'}\alpha^*_q(x), \tag{3.95}$$

$$[b^\dagger_{q\eta'}, \psi_\eta(x)] = -\delta_{\eta\eta'}\alpha^*_q(x). \tag{3.96}$$

Using the result $[A, e^B] = [A, B]e^B$ found in (3.84), we see that the factor picked up by commuting $b^\dagger_{q\eta'}$ to the right of $\psi_\eta(x)$ is exactly canceled by the factor picked up by commuting $b^\dagger_{q\eta}$ to the right of $e^{-i\varphi_\eta(x)}$:

$$[b^\dagger_{q\eta'}, \tilde{F}_\eta(x)] = L^{\frac{1}{2}}\psi_\eta(x)e^{-i\varphi_\eta(x)}\left[-\delta_{\eta\eta'}\alpha^*_q(x) + \delta_{\eta\eta'}\alpha^*_q(x)\right]e^{-i\varphi^\dagger_\eta(x)}e^{-i\frac{2\pi}{L}(\hat{N}_\eta-\delta_b)x} = 0. \tag{3.97}$$

Similar calculations can be used to prove $[b^\dagger_{q\eta'}, \tilde{F}^\dagger_\eta(x)] = 0$. Now we consider the matrix elements of $\tilde{F}(x)$ between arbitrary basis elements. Working with a single species for simplicity, we have

$$\langle M, \{m_q\}_b| \tilde{F}(x) |N, \{n_q\}_b\rangle = \langle M, \{0\}| \prod_{q>0} \frac{(b_q)^{m_q}}{\sqrt{m_q!}} \tilde{F}(x) \prod_{q>0} \frac{(b^\dagger_q)^{n_q}}{\sqrt{n_q!}} |N, \{0\}\rangle . \tag{3.98}$$

It has already been shown that $\tilde{F}(x)$ commutes with the bosons, so that if any $m_{q'} > n_{q'}$ then

$$\prod_{\substack{q>0\\q\neq q'}} \frac{(b_q)^{m_q}}{\sqrt{m_q!}} \tilde{F}(x) \prod_{\substack{q>0\\q\neq q'}} \frac{(b^\dagger_q)^{n_q}}{\sqrt{n_q!}} \left[\frac{(b_{q'})^{m_{q'}}}{\sqrt{m_{q'}!}} \frac{(b^\dagger_{q'})^{n_{q'}}}{\sqrt{n_{q'}!}}\right] |N, \{0\}\rangle = 0, \tag{3.99}$$

while if any $m_{q'} < n_{q'}$

$$\langle M, \{0\}| \left[\frac{(b_{q'})^{m_{q'}}}{\sqrt{m_{q'}!}} \frac{(b^\dagger_{q'})^{n_{q'}}}{\sqrt{n_{q'}!}}\right] \prod_{\substack{q>0\\q\neq q'}} \frac{(b_q)^{m_q}}{\sqrt{m_q!}} \tilde{F}(x) \prod_{\substack{q>0\\q\neq q'}} \frac{(b^\dagger_q)^{n_q}}{\sqrt{n_q!}} = 0. \tag{3.100}$$

This implies that the only non-vanishing matrix elements of $\tilde{F}(x)$ are between states with $\{m_q\} = \{n_q\}$, i.e.,

$$\langle M, \{n_q\}_b| \tilde{F}(x) |N, \{n_q\}_b\rangle = \langle M, \{0\}| \tilde{F}(x) |N, \{0\}\rangle . \tag{3.101}$$

Now we have to show that the last expression is independent of x. Let us consider the explicit form of the expectation values of $\tilde{F}^\dagger(x)$:

$$\langle M, \{0\}| \tilde{F}^\dagger(x) |N, \{0\}\rangle = \langle M, \{0\}| L^{\frac{1}{2}} e^{i\frac{2\pi}{L}(\hat{N}-\frac{1}{2}\delta_b)x} e^{i\varphi(x)} e^{i\varphi^\dagger(x)} \psi^\dagger(x) |N, \{0\}\rangle . \tag{3.102}$$

We would like to commute the exponential field $e^{i\varphi^\dagger(x)}$ to the left, and $e^{i\varphi(x)}$ to the right, so that they can act on the vacuum states $\langle M, \{0\}|$ and $|N, \{0\}\rangle$ respectively. To avoid computing unnecessary commutation relations, we simply make use of the fact that $\tilde{F}^\dagger(x)$ commutes with the bosons. It follows that

$$\tilde{F}^\dagger(x) = e^{-i\varphi(x)}\tilde{F}^\dagger(x)e^{i\varphi(x)}, \tag{3.103}$$

and the calculation proceeds simply:

$$\begin{aligned}\langle M,\{0\}|\,\tilde{F}^\dagger(x)\,|N,\{0\}\rangle &= \langle M,\{0\}|\,e^{i\varphi^\dagger(x)}L^{\frac{1}{2}}e^{i\frac{2\pi}{L}(\hat{N}-\frac{1}{2}\delta_b)x}\psi^\dagger(x)e^{i\varphi(x)}\,|N,\{0\}\rangle \\ &= \langle M,\{0\}|\,L^{\frac{1}{2}}e^{i\frac{2\pi}{L}(\hat{N}-\frac{1}{2}\delta_b)x}\psi^\dagger(x)\,|N,\{0\}\rangle\,, \\ &= \langle M,\{0\}|\,L^{\frac{1}{2}}e^{i\frac{2\pi}{L}(\hat{N}-\frac{1}{2}\delta_b)x}\left(L^{-\frac{1}{2}}\sum_k e^{-ikx}c_k^\dagger\right)|N,\{0\}\rangle\,, \\ &= \delta_{M,N+1}\,\langle N+1,\{0\}|\,e^{i\frac{2\pi}{L}(\hat{N}-\frac{1}{2}\delta_b)x}e^{-ik_{N+1}x}c_{k_{N+1}}^\dagger\,|N,\{0\}\rangle\,.\end{aligned} \tag{3.104}$$

In the last line, the exponential operator $e^{i\frac{2\pi}{L}(\hat{N}-\frac{1}{2}\delta_b)x}$ disappears since both $\langle N+1,\{0\}|$ and $|N,\{0\}\rangle$ contain no particle-hole excitations. As such, the overlap is only non-vanishing if $c_k^\dagger$ adds this particle to the lowest available empty state of $|N,\{0\}\rangle$. This fixes the momentum at $k = 2\pi/L(N+1-\frac{1}{2}\delta_b)$ and leads to the cancelation of $e^{i\frac{2\pi}{L}(\hat{N}-\frac{1}{2}\delta_b)x}$. Thus we have explicitly verified that the right hand side of (3.94) is independent of x, and we can freely set $x = 0$:

$$\boxed{F_\eta = L^{\frac{1}{2}}\psi_\eta(0)e^{-i\varphi_\eta(0)}e^{-i\varphi_\eta^\dagger(0)}.} \tag{3.105}$$

3.3 Appendix: The Jacobi triple product

We offer a simple algebraic proof of the Jacobi triple product identity that we used in Section 3.2.1 [22].

Define the following function

$$F(v) \equiv \prod_{n=1}^{\infty}(1+w^{2n-1}v)(1+w^{2n-1}v^{-1}),$$

$$=(1+wv)(1+wv^{-1})(1+w^3v)(1+w^3v^{-1})$$

$$\times (1+w^5v)(1+w^5v^{-1})(1+w^7v)(1+w^7w^{-1})\cdots, \tag{3.106}$$

for complex numbers w and v, with $|w|<1$ and $v \neq 0$. Now consider this function with the argument (w^2v):

$$F(w^2v) \equiv \prod_{n=1}^{\infty}(1+w^{2n+1}v)(1+w^{2n-3}v^{-1}),$$

$$=(1+w^3v)\left(1+\frac{1}{wv}\right)(1+w^5v)(1+wv^{-1})(1+w^7v)(1+w^3v^{-1})\cdots. \tag{3.107}$$

If we divide (3.107) by (3.106) we find

$$\frac{F(w^2v)}{F(v)} = \left(1+\frac{1}{wv}\right)\left(\frac{1}{1+wv}\right) = \frac{1}{wv}. \tag{3.108}$$

This implies the relation

$$wvF(w^2v) = F(v). \tag{3.109}$$

In the same spirit we define two more functions

$$G(v) \equiv F(v)\prod_{n=1}^{\infty}(1-w^{2n}), \tag{3.110}$$

and

$$G(w^2v) \equiv F(w^2v)\prod_{n=1}^{\infty}(1-w^{2n}). \tag{3.111}$$

By way of (3.109), (3.111) reads

$$G(w^2v) = \frac{F(v)}{wv}\prod_{n=1}^{\infty}(1-w^{2n}) = \frac{G(v)}{wv}, \tag{3.112}$$

and we establish the relation

$$wvG(w^2v) = G(v). \tag{3.113}$$

The Laurent series of $G(v)$ is given by

$$G(v) = \sum_{m=-\infty}^{\infty} a_m v^m. \tag{3.114}$$

The Jacobi triple product identity's beauty is due to the seemingly unlikely equivalence between a sum of sparse squared terms and a triple infinite product. We already have a sum from (3.114). All that remains is to figure out the coefficients a_m. We can use (3.113) to generate a recursion relation for the set of coefficients a_m:

$$G(v) = \sum_{m=-\infty}^{\infty} a_m v^m = wv \sum_{m=-\infty}^{\infty} a_m (w^2v)^m = \sum_{m=-\infty}^{\infty} a_m w^{2m+1} v^{m+1}. \tag{3.115}$$

We can shift $m' = m - 1$ on the left hand side of (3.115) since the sum is unbound from above and below. We therefore find

$$\sum_{n=-\infty}^{\infty} a_m v^m = \sum_{m=-\infty}^{\infty} a_{m-1} w^{2m-1} v^m, \tag{3.116}$$

which implies the recursion relation

$$a_m = a_{m-1} w^{2m-1}. \tag{3.117}$$

Let us see how the coefficients evolve:

$$\begin{aligned} a_1 &= a_0 w, \\ a_2 &= a_1 w^3 = a_0 w^4 = a_0 w^{2^2}, \\ a_3 &= a_2 w^5 = a_1 w^8 = a_0 w^9 = a_0 w^{3^2}. \\ &\vdots \end{aligned} \tag{3.118}$$

So we can write every coefficient in terms of a_0 as

$$a_m = a_0 w^{m^2}. \tag{3.119}$$

With this discovery, (3.114) can be written as

$$G(v) = a_0 \sum_{m=-\infty}^{\infty} w^{m^2} v^m. \tag{3.120}$$

To find the value of a_0 we simply compare the above equation to that of (3.110) at $v = 1$:

$$\begin{aligned} G(1) &= a_0 \sum_{m=-\infty}^{\infty} w^{m^2}, \\ &= \cdots + a_0 w^4 + a_0 w + a_0 + a_0 w + a_0 w^4 + \cdots \,, \end{aligned} \tag{3.121}$$

while on the other-hand

$$\begin{aligned} G(1) &= F(1) \prod_{n=1}^{\infty} (1 - w^{2n}) = \prod_{n=1}^{\infty} (1 + w^{2n-1})^2 (1 - w^{2n}), \\ &= \prod_{n=1}^{\infty} (1 - w^{6n-2} - 2w^{4n-1} + w^{4n-2} - w^{2n} + 2w^{2n-1}). \end{aligned} \tag{3.122}$$

Clearly $a_0 = 1$, since these are the only two terms which dont contain a power of w. Substituting this result into (3.120) gives us the Jacobi triple product identity:

$$\boxed{\sum_{m=-\infty}^{\infty} w^{m^2} v^m = \prod_{n=1}^{\infty} (1 + w^{2n-1} v)(1 + w^{2n-1} v^{-1})(1 - w^{2n}).} \tag{3.123}$$

Chapter 4

Bosonization of the anisotropic Kondo model

The aim of this chapter is to show that there is a point in parameter space where the anisotropic Kondo model maps onto a non-interacting resonant level model. This model consists of a single orbital situated at the Fermi energy, hybridized to a sea of fermions. To do this, we will bosonize the anisotropic Kondo Hamiltonian using the identities derived in the previous chapter. We will then perform some simplifications in the bosonic sector before refermionizing the theory at the Toulouse point. We will conclude this chapter by introducing the observable studied in the final chapter of this dissertation, namely the longitudinal forward scattering component of the spin-spin correlation function between the impurity spin and the conduction electron spin-density. This correlation function is then mapped into the resonant level setting.

Our starting point is the Kondo Hamiltonian (2.41), with anisotropic couplings and modes far from the Fermi energy integrated out so that the dispersion relation is approximately linear:

$$\begin{aligned}
H_0 =& \sum_{k\sigma} k : c^\dagger_{k\sigma} c_{k\sigma} :, \\
H_\parallel =& \frac{J_\parallel}{2} \Big(: \psi^\dagger_\uparrow(0)\psi_\uparrow(0) : - \psi^\dagger_\downarrow(0)\psi_\downarrow(0) : \Big) \sigma_z, \\
H_\perp =& J_\perp \Big(\psi^\dagger_\uparrow(0)\psi_\downarrow(0)\sigma^- + \psi^\dagger_\downarrow(0)\psi_\uparrow(0)\sigma^+ \Big).
\end{aligned} \tag{4.1}$$

Here, we have defined the slow modes

$$\begin{aligned}
c_{k\sigma} =& \frac{1}{\sqrt{2}} (\tilde{c}_{k_F+k,\sigma} + \tilde{c}_{-k_F-k,\sigma}), \\
\psi^\dagger_\sigma(x) =& \frac{1}{\sqrt{2}} \sum_k e^{-ikx} e^{-a|k|/2} c^\dagger_{k\sigma},
\end{aligned} \tag{4.2}$$

where $\tilde{c}_{k\sigma}$ annihilates an electron with wave number k and spin σ, while $c^{\dagger}_{k\sigma}$ creates a particle in the state $\sqrt{2/L}\cos[(k_F+k)x]$. Here, $1/a$ is the ultraviolet cut-off energy, and the factor $e^{-a|k|/2}$ suppresses modes that have been integrated out. To understand what $\psi^{\dagger}_{\sigma}(x)$ does, consider the action of $\psi^{\dagger}_{\sigma}(x)$ on the vacuum in the position representation:

$$\begin{aligned} \langle y|\,\psi^{\dagger}_{\sigma}(x)\,|0\rangle =& \frac{1}{\sqrt{2L}}\sum_k e^{-ikx}e^{-a|k|/2}\left[e^{i(k_F+k)y}+e^{-i(k_F+k)y}\right], \\ =& \frac{1}{\sqrt{2L}}\sum_k \left[e^{ik_Fx}e^{-i(x-y)k}+e^{-ik_Fx}e^{-i(x+y)k}\right]e^{-a|k|/2}. \end{aligned} \tag{4.3}$$

If we take the limit $L\to\infty$, we can replace momentum sums $2\pi/L\sum_k$ with integrals $\int_{-\infty}^{\infty}dk$, so that

$$\begin{aligned} \langle y|\,\psi^{\dagger}_{\sigma}(x)\,|0\rangle =& \frac{\sqrt{L}}{2\pi\sqrt{2}}\int_{-\infty}^{\infty}dk\,\left[e^{ik_Fx}e^{-i(x-y)k}+e^{-ik_Fx}e^{-i(x+y)k}\right]e^{-a|k|/2}, \\ =& \sqrt{\frac{L}{2}}\frac{1}{\pi}\left[\frac{e^{ik_Fy}}{(x-y)^2+a^2}+\frac{e^{-ik_Fy}}{(x+y)^2+a^2}\right]. \end{aligned} \tag{4.4}$$

Therefore, $\psi^{\dagger}_{\sigma}(x)$ creates an electron in an even-parity state consisting of wave packets localized at x and $-x$. For $x<0$, the wave packets propagate in opposite directions towards the impurity, while for $x>0$, the wave packets propagate in opposite directions away from the impurity.

Our first job is to bosonize (4.1). We already know from the previous chapter that the kinetic term can be written in terms of bosons as $\sum_{q>0}\sum_{\sigma}qb^{\dagger}_{q\sigma}b_{q\sigma}$. The longitudinal $\parallel$ and transverse $\perp$ components of (4.1) can be bosonized using the identities : $\psi^{\dagger}_{\sigma}(x)\psi_{\sigma}(x):=\partial_x\phi_{\sigma}(x)/2\pi$ and $\psi^{\dagger}_{\sigma}(x)=F^{\dagger}_{\sigma}\exp(-i\phi_{\sigma}(x))/\sqrt{2\pi a}$ respectively, where $\phi_{\sigma}(x)$ is defined in (3.54). This gives

$$\begin{aligned} H_0 =& \sum_{q>0}\sum_{\sigma}qb^{\dagger}_{q\sigma}b_{q\sigma}, \\ H_{\parallel} =& \frac{J_{\parallel}}{4\pi}\partial_x\left(\phi_{\uparrow}(x)-\phi_{\downarrow}(x)\right)\sigma_z\Big|_{x=0}, \\ H_{\perp} =& \frac{J_{\perp}}{2\pi a}\left(F^{\dagger}_{\uparrow}F_{\downarrow}\sigma^{-}e^{-i\phi_{\uparrow}(0)}e^{i\phi_{\downarrow}(0)}+\text{h.c.}\right). \end{aligned} \tag{4.5}$$

The kinetic and transverse terms can be written as

$$\begin{aligned} H_0 =& \sum_{q>0}\left[\frac{q}{2}(b^{\dagger}_{q\uparrow}+b^{\dagger}_{q\downarrow})(b_{q\uparrow}+b_{q\downarrow})+\frac{q}{2}(b^{\dagger}_{q\uparrow}-b^{\dagger}_{q\downarrow})(b_{q\uparrow}-b_{q\downarrow})\right], \\ H_{\perp} =& \frac{J_{\perp}}{2\pi a}\left(F^{\dagger}_{\uparrow}F_{\downarrow}\sigma^{-}e^{-(i\phi_{\uparrow}(0)-\phi_{\downarrow}(0))}+\text{h.c.}\right), \end{aligned} \tag{4.6}$$

which suggests the introduction of new charge and spin degrees of freedom

$$
\begin{aligned}
b_{qs} &= \frac{1}{\sqrt{2}}(b_{q\uparrow} - b_{q\downarrow}), \quad \phi_s(x) = \frac{1}{\sqrt{2}}(\phi_\uparrow(x) - \phi_\downarrow(x)), \\
b_{qc} &= \frac{1}{\sqrt{2}}(b_{q\uparrow} + b_{q\downarrow}), \quad \phi_c(x) = \frac{1}{\sqrt{2}}(\phi_\uparrow(x) + \phi_\downarrow(x)).
\end{aligned}
\tag{4.7}
$$

With these definitions, (4.6) along with the longitudinal component reads

$$
\begin{aligned}
H_0 &= \sum_{q>0} b^\dagger_{qs} b_{qs} + \sum_{q>0} b^\dagger_{qc} b_{qc}, \\
H_\parallel &= \frac{J_\parallel}{2\pi\sqrt{2}} \partial_x \phi_s(x) \sigma_z \Big|_{x=0}, \\
H_\perp &= \frac{J_\perp}{2\pi a}\left(F^\dagger_\uparrow F_\downarrow \sigma^- e^{-i\sqrt{2}\phi_s(0)} + \text{h.c.}\right).
\end{aligned}
\tag{4.8}
$$

Note that the charge and spin degrees of freedom separate. This is a hallmark of one-dimensional Fermi systems. Furthermore, the charge sector completely decouples from the impurity, and only contributes to the kinetic energy in a trivial way as a collection of uncoupled harmonic oscillators. Since this term does not affect any of our future calculations,we will drop it from this point on.

The quantity

$$
\rho_s(0) = \frac{\partial_x \phi_s(x)}{2\pi\sqrt{2}}\Big|_{x=0}, \tag{4.9}
$$

appearing in the longitudinal component of (4.8) represents the spin polarization of the electron gas at the position of the impurity. We will call $\rho_s(x)$ the magnetization.

4.1 Mappings

In this section we apply a unitary transformation that simplifies (4.8). In general, a unitary transformation is given by $A' = e^{-\theta} A e^{\theta}$, with $\theta^\dagger = -\theta$. It will be shown that for $\theta = iJ_\parallel \phi_s(0)\sigma_z/2\pi\sqrt{2}$, the longitudinal component of (4.8) is absorbed into the transverse component. However, for the moment we will set $\theta = i\gamma\phi_s(0)\sigma_z$ and leave γ as an adjustable parameter. This will allow us to explore other interesting maps.

In order to perform the unitary transformation we will once again make use of the BCH formula

$$
e^{-\theta} A e^{\theta} = \sum_{n=0}^{\infty} \frac{1}{n!}[A,\theta]_n = A + [A,\theta] + \frac{1}{2}[[A,\theta],\theta] + \cdots . \tag{4.10}
$$

The only operators in (4.8) that do not commute to zero under this transformation are the particle-hole operators $b^\dagger_{qs}$ and b_{qs}, as well as the impurity spin-flip operators σ^+ and σ^-. Applying the BCH formula to the particle-hole operators gives

$$e^{-\theta}b_{qs}e^{\theta} = b_{qs} + [b_{qs}, \phi_s(0)](i\gamma\sigma_z) + \frac{1}{2!}[[b_{qs}, \phi_s(0)], \phi_s(0)](i\gamma\sigma_z)^2 + \cdots . \tag{4.11}$$

Since the commutation relation $[b_{qs}, \phi_s(0)]$ is given by

$$\begin{aligned}[b_{qs}, \phi_s(0)] =& -\gamma \sum_{q>0} \frac{1}{\sqrt{n_q}} e^{-aq/2} \sigma_z [b_{qs}, b^\dagger_{qs} - b_{qs}], \\ =& -\gamma \frac{1}{\sqrt{n_q}} e^{-aq/2}\sigma_z,\end{aligned} \tag{4.12}$$

it follows that the expansion in (4.11) terminates after the second term. Therefore the particle-hole operators transform as

$$b_{qs} \rightarrow b_{qs} - \gamma \frac{1}{\sqrt{n_q}} e^{-aq/2}\sigma_z, \tag{4.13}$$

and

$$b^\dagger_{qs} \rightarrow b_{qs} - \gamma \frac{1}{\sqrt{n_q}} e^{-aq/2}\sigma_z. \tag{4.14}$$

Unlike the particle-hole operators, the expansions for the spin-flip operators σ^- and σ^+ do not terminate after the second term, but results in a Taylor series. Using the commutation relations $[\sigma^-, \sigma_z] = 2\sigma^-$ and $[\sigma^+, \sigma_z] = -2\sigma^+$, it follows that

$$\begin{aligned}e^{-\theta}\sigma^+ e^{\theta} =& \sigma^+ + [\sigma^+, \sigma_z][i\gamma\phi_s(0)] + \frac{1}{2!}[[\sigma^+, \sigma_z], \sigma_z][i\gamma\phi_s(0)]^2 + \cdots , \\ =& \sigma^+ + [-2i\gamma\phi_s(0)]\sigma^+ + \frac{1}{2!}[-2i\gamma\phi_s(0)]^2 + \cdots ,\end{aligned} \tag{4.15}$$

so that the spin-flip operators transform as

$$\sigma^+ \rightarrow e^{-2i\gamma\phi_s(0)}\sigma^+, \tag{4.16}$$

and

$$\sigma^- \rightarrow e^{2i\gamma\phi_s(0)}\sigma^-. \tag{4.17}$$

It is also useful to calculate the action of the unitary transformation on the magnetization $\rho_s(x)$. The BCH formula gives

$$\begin{aligned}e^{-\theta}\partial_x\phi_s(x)e^{\theta} =& \partial_x\phi_s(x) + [\partial_x\phi_s(x), \phi_s(0)](i\gamma\sigma_z) \\ &+ \frac{1}{2!}[[\partial_x\phi_s(x), \phi_s(0)], \phi_s(0)](i\gamma\sigma_z)^2 + \cdots ,\end{aligned} \tag{4.18}$$

where

$$[\partial_x\phi_s(x),\phi_s(0)] = i\sum_{q>0}\sum_{q'>0}\frac{q}{\sqrt{n_q n_{q'}}}\left(e^{iqx}[b_{qs},b^\dagger_{sq'}] - e^{-iqx}[b^\dagger_{qs},b_{sq'}]\right)e^{-a(q+q')/2},$$

$$= i\delta_{qq'}\sum_{q>0}\frac{2\pi}{L}\left(e^{-iqx(x-ia)} + e^{iq(x+ia)}\right). \tag{4.19}$$

Taking the limit $L\to\infty$ allows us to replace momentum sums $2\pi/L\sum_{q>0}$ with integrals $\int_0^\infty dq$, giving

$$[\partial_x\phi_s(x),\phi_s(0)] = i\int_0^\infty dq\left(e^{-iqx(x-ia)} + e^{iq(x+ia)}\right),$$

$$= \frac{2ia}{x^2+a^2} = 2\pi i\delta_a(x), \tag{4.20}$$

where the broadened Dirac delta function $\delta_a(x-x')$ is defined as

$$\delta_a(x-x') = \frac{1}{\pi}\frac{a}{(x-x')^2+a^2}. \tag{4.21}$$

The magnetization $\rho_s(x)$ therefore maps onto

$$\rho_s(x)\to\rho_s(x) - \gamma\frac{\sigma_z}{\sqrt{2}}\delta_a(x). \tag{4.22}$$

We are now in a position to transform (4.8). Starting with the kinetic term we have

$$e^{-\theta}H_0e^{\theta} = \sum_{q>0}(e^{-\theta}b^\dagger_{qs}e^{\theta})(e^{-\theta}b_{qs}e^{\theta}),$$

$$= \sum_{q>0} q\left(b^\dagger_{qs} - \frac{\gamma}{\sqrt{n_q}}e^{-aq/2}\sigma_z\right)\left(b_{qs} - \frac{\gamma}{\sqrt{n_q}}e^{-aq/2}\sigma_z\right),$$

$$= \sum_{q>0} qb^\dagger_{qs}b_{qs} - \gamma\sum_{q>0} q\frac{1}{\sqrt{n_q}}(b^\dagger_{qs}+b_{qs})e^{-aq/2}\sigma_z + \gamma^2\sum_{q>0}\frac{q}{n_q}e^{-aq},$$

$$= \sum_{q>0} qb^\dagger_{qs}b_{qs} - \gamma\partial_x\phi_s(x)\sigma_z\Big|_{x=0} + \frac{\gamma^2}{a}. \tag{4.23}$$

On the other hand, the unitary transformation simply shifts the longitudinal component of (4.8) by a real number as follows

$$e^{-\theta}H_{\parallel}e^{\theta} = \frac{J_{\parallel}}{2\pi\sqrt{2}}\left[e^{-\theta}\partial_x\phi_s(x)\Big|_{x=0}e^{\theta}\right]\sigma_z,$$

$$= \frac{J_{\parallel}}{2\pi\sqrt{2}}\left[\sum_{q>0}\frac{q}{\sqrt{n_q}}(b^{\dagger}_{qs}+b_{qs})e^{-aq/2}\right]\sigma_z - \frac{J_{\parallel}\gamma}{\sqrt{2}\pi}\sum_{q>0}\frac{2\pi}{L}e^{-aq},$$

$$= \frac{J_{\parallel}}{2\pi\sqrt{2}}\partial_x\phi_s(x)\sigma_z\Big|_{x=0} - \frac{J_{\parallel}\gamma}{\sqrt{2}\pi a}. \tag{4.24}$$

Lastly, the transverse component transforms as

$$e^{-\theta}H_{\perp}e^{\theta} = \frac{J_{\perp}}{2\pi a}\left(F^{\dagger}_{\uparrow}F_{\downarrow}[e^{-\theta}\sigma^{-}e^{\theta}]e^{-i\sqrt{2}\phi_s(0)} + \text{h.c.}\right),$$

$$= \frac{J_{\perp}}{2\pi a}\left(F^{\dagger}_{\uparrow}F_{\downarrow}\sigma^{-}e^{-i(\sqrt{2}-2\gamma)\phi_s(0)} + \text{h.c.}\right). \tag{4.25}$$

After dropping the constant terms, the transformed Hamiltonian reads

$$H'_B = \sum_{q>0} q b^{\dagger}_{qs}b_{qs} + \left(\frac{J_{\parallel}}{2\pi\sqrt{2}} - \gamma\right)\partial_x\phi_s(x)\sigma_z\Big|_{x=0} + \frac{J_{\perp}}{2\pi a}\left(F^{\dagger}_{\uparrow}F_{\downarrow}\sigma^{-}e^{-i(\sqrt{2}-2\gamma)\phi_s(0)} + \text{h.c.}\right). \tag{4.26}$$

The notation H'_B indicates a bosonized Hamiltonian that has undergone a single unitary transformation. Later on we will encounter a Hamiltonian H''_B that has undergone an additional unitary transformation as well as a Hamiltonian H_F that has been written in terms of new fermions. As advertised, setting $\gamma = J_{\parallel}/2\pi\sqrt{2}$ absorbs the longitudinal term into the transverse component. However, before we do this, we take a short detour and explore an alternative map.

4.1.1 Mapping to a spin-boson model

If we set $\gamma = 1/\sqrt{2}$, we obtain

$$\begin{aligned} H_{SB} &= \sum_{q>0} q b^{\dagger}_{qs}b_{qs} + \left(\frac{J_{\parallel}}{2\pi\sqrt{2}} - \frac{1}{\sqrt{2}}\right)\partial_x\phi(0)\sigma_z + \frac{J_{\perp}}{2\pi a}\left(F^{\dagger}_{\uparrow}F_{\downarrow}\sigma^{-} + F^{\dagger}_{\downarrow}F_{\uparrow}\sigma^{+}\right), \\ &= \sum_{q>0} q b^{\dagger}_{qs}b_{qs} - \left(1 - \frac{J_{\parallel}}{2\pi}\right)\sum_{q>0}\sqrt{\frac{\pi q}{L}}\left(b^{\dagger}_{qs}+b_{qs}\right)e^{-aq/2}\sigma_z + \frac{J_{\perp}}{2\pi a}\sigma_x, \\ &= \sum_{q>0} q b^{\dagger}_{qs}b_{qs} - \sum_{q>0}\frac{g_q}{2}\left(b^{\dagger}_{qs}+b_{qs}\right)\sigma_z + \frac{\Delta}{2}\sigma_x. \end{aligned} \tag{4.27}$$

where

$$g_q \equiv 2\sqrt{\frac{\alpha\pi q}{L}}e^{-aq/2} \quad , \quad \alpha \equiv \left(1 - \frac{J_{\parallel}}{2\pi}\right)^2 \quad , \quad \Delta \equiv \frac{J_{\perp}}{\pi a}. \tag{4.28}$$

The Hamiltonian (4.27) is referred to as the ohmic spin-boson model and describes a two-state spin system coupled to a dissipative environment. The environment is represented by an infinite set of harmonic oscillators. Each oscillator couples to the coordinate σ_z with strength g_q. The effect of the environment on the two-state system is encapsulated by the the spectral function $J(\omega)$, which for the case of ohmic dissipation has the form $J(\omega) \sim \alpha\omega$. The spectral function along with the bare tunneling matrix element Δ between the states $|\uparrow\rangle$ and $|\downarrow\rangle$, completely defines the system. In this circumstance, it can be shown that α plays the role of a classical friction coefficient [23].

The spin-boson system is known to undergo a dissipation driven quantum phase transition at the point $\alpha = 1$ [24]. For a dissipation strength of $\alpha > 1$, a spin that is initialized in one of the σ_z eigenstates $|\uparrow\rangle$ or $|\downarrow\rangle$, never tunnels into the other state, despite the presence of the tunneling term. On the other hand, for $0 < \alpha < 1$, the spin eventually reaches a state in which the probability to find $|\uparrow\rangle$ and $|\downarrow\rangle$ are both 0.5. This is referred to as the localization-delocalization transition. Our knowledge of the behavior of the Kondo model, that is equivalent to the spin boson model, allows us to form a simple picture of this transition. The point $\alpha = 1$ at which this quantum phase transition occurs, corresponds precisely to the critical point $J_\parallel = 0$ in the Kondo model. This point marks the boundary between the ferromagnetic and antiferromagnetic regions of the Kondo model. Additionally, the localized region of the spin-boson parameter space $\alpha > 1$ corresponds to the ferromagnetic region with longitudinal coupling $J_\parallel < 0$. We know that in this region, the transverse coupling $J_\perp$ responsible for the systems spin-flip dynamics scales to zero. The correspondence in (4.28) equates this behavior to the vanishing of the effective tunneling amplitude Δ. Furthermore, the delocalized region $0 < \alpha < 1$ corresponds to the antiferromagnetic $J_\parallel > 0$ sector of the Kondo model, for which the coupling $J_\perp$ increases indefinitely, resulting in a unique singlet ground state. For a comprehensive overview of dissipative two-state systems, see [13].

4.1.2 The non-interacting resonant level model

We now return to the main line of argument which is the mapping of the anisotropic Kondo model onto a non-interacting resonant level model. Setting $\gamma = J_\parallel/2\pi\sqrt{2}$ eliminates the second term in (4.26) to give

$$H'_B = \sum_{q>0} q b^\dagger_{qs} b_{qs} + \frac{J_\perp}{2\pi a}\left(F^\dagger_\uparrow F_\downarrow \sigma^- e^{-i(\sqrt{2}-J_\parallel/\sqrt{2}\pi)\phi_s(0)} + \text{h.c.}\right). \tag{4.29}$$

It is not immediately clear that this is a simplification. However, at the point $J_\parallel = (2-\sqrt{2})\pi$ we get

$$H'_B = \sum_{q>0} q b^\dagger_{qs} b_{qs} + \frac{J_\perp}{2\pi a}\left(F^\dagger_\uparrow F_\downarrow \sigma^- e^{-i\phi_s(0)} + \text{h.c.}\right), \tag{4.30}$$

which allows us to identify a new fermionic degree of freedom

$$\bar{\psi}^\dagger(x) = \frac{F_s^\dagger}{\sqrt{2\pi a}} e^{-i\phi_s(x)},$$

$$= \frac{1}{\sqrt{L}} \sum_k e^{-ikx} e^{-a|k|/2} \bar{c}_k^\dagger, \tag{4.31}$$

with new Klein factors $F_s^\dagger \equiv F_\uparrow^\dagger F_\downarrow$ which obey the usual anticommutation relation $\{F_s^\dagger, F_s\} = 2$. Instead of altering the number of fermions by one, the new Klein factors alter the spin polarity of the electron gas in integer steps. The operator that preserves the commutation relations $[\hat{N}, F_s^\dagger] = F_s^\dagger$ and $[\hat{N}, F_s] = -F_s$ is given by

$$\hat{N}_- = \frac{1}{2}(\hat{N}_\uparrow - \hat{N}_\downarrow), \tag{4.32}$$

which measures the z-component of the total spin of the electron gas. In this setting, one can think of the impurity spin-flip operators σ^+ and σ^- as pseudo fermion creation and annihilation operators. We can construct fermionic representations of these operators and ensure that they obey the proper anticommutation relations by performing one last unitary transformation with $\theta = i\pi\sigma_z\hat{N}_-$. This transformation acts on the Klein factors and spin-flip operators to give

$$e^{-\theta} F_s^\dagger e^\theta = F_s^\dagger + [F_s^\dagger, \hat{N}_-](i\pi\sigma_z) + \frac{1}{2!}[[F_s^\dagger, \hat{N}_-], \hat{N}_-](i\pi\sigma_z)^2 + \cdots,$$

$$= F_s^\dagger - i\pi\sigma_z F_s^\dagger - \frac{1}{2!}(\pi\sigma_z)^2 F_s^\dagger - \cdots,$$

$$= e^{-i\pi\sigma_z} F_s^\dagger \tag{4.33}$$

and

$$e^{-\theta}\sigma^- e^\theta = \sigma^- + [\sigma^-, \sigma_z](i\pi\hat{N}_-) + \frac{1}{2!}[[\sigma^-, \sigma_z], \sigma_z](i\pi\hat{N}_-)^2 + \cdots,$$

$$= \sigma^- + 2i\pi\hat{N}_-\sigma^- + \frac{1}{2!}(2\pi i\hat{N}_-)^2\sigma^- + \cdots,$$

$$= e^{2\pi i\hat{N}_-}\sigma^-. \tag{4.34}$$

Under this transformation, (4.30) becomes

$$H_B'' = \sum_{q>0} q b_{qs}^\dagger b_{qs} + \frac{J_\perp}{2\pi a}\left(F_s^\dagger e^{-i\phi_s(0)} e^{-i(\sigma_z - 2\hat{N}_-)\pi}\sigma^- + \text{h.c.}\right), \tag{4.35}$$

allowing us to identify additional fermionic degrees of freedom

$$d^\dagger = \sigma^+ e^{i(\sigma_z - 2\hat{N}_-)\pi}, \quad d = e^{-i(\sigma_z - 2\hat{N}_-)\pi}\sigma^-. \tag{4.36}$$

The new fermionic degrees of freedom obey the standard commutation relations

$$\{\bar{c}_k, \bar{c}^\dagger_{k'}\} = \delta_{kk'}, \quad \{d, d^\dagger\} = 1,$$

$$\{d, \bar{c}^\dagger_k\} = \{d, \bar{c}_k\} = 0, \tag{4.37}$$

$$[d, \hat{N}_-] = d,$$

and imply a simple representation of the impurity spin operator

$$S_z = d^\dagger d - \frac{1}{2} I. \tag{4.38}$$

Expressing (4.35) in terms of the new fermionic degrees of freedom gives

$$\boxed{H_F = \sum_k k : \bar{c}^\dagger_k \bar{c}_k : + \sum_k V_k \left(\bar{c}^\dagger_k d + d^\dagger \bar{c}_k \right),} \tag{4.39}$$

where

$$V_k \equiv \frac{J_\perp}{\sqrt{2\pi a}} e^{-a|k|/2}. \tag{4.40}$$

This is the non-interacting resonant level model with a single d-orbital situated at the Fermi energy $\epsilon_{k_F} = 0$, hybridized to a gas of new fermions through the hybridization elements V_k. The non-interacting resonant level model has a magnetization

$$\rho_s(x) \to \rho_s(x) - \left(1 - \frac{1}{\sqrt{2}}\right) \frac{\sigma_z}{2} \delta_a(x). \tag{4.41}$$

4.2 The Kondo screening cloud

We will study the spin alignment between the impurity spin and the spin of conduction electrons located a distance x away from the impurity. For the isotropic case, it does not matter which direction we choose to measure. However, for the anisotropic model with cylindrical symmetry about z, the choice of direction becomes important. We could either measure the correlation between the z-components of the impurity and conduction electron spins, or the qualitatively similar but not identical transverse components lying in the xy-plane. We will focus on the z-component for which we were able to find an analytical solution. We were not able to do the same for the transverse correlator.

The correlation function between the z-components of the impurity and the conduction electron spin-density is given by

$$X^{\parallel}(x) = 4 \left\langle S_z^{\text{imp}} S_z^{\text{el}}(x) \right\rangle_K,$$

$$= 2 \left\langle S_z \left[\tilde{\psi}^\dagger_\uparrow(x) \tilde{\psi}_\uparrow(x) - \tilde{\psi}^\dagger_\downarrow(x) \tilde{\psi}_\downarrow(x) \right] \right\rangle_K, \tag{4.42}$$

and will be referred to as the longitudinal cloud. The subscript K indicates that the expectation value is taken with respect to the Kondo ground state. The impurity spin is characterized by $\sigma_z/2$, where σ_z is a Pauli spin matrix. Here, $\tilde{\psi}_\sigma(x)$ is an annihilation operator for a particle in a standing wave packet around x. This operator is defined as

$$\tilde{\psi}_\sigma(x) = \frac{1}{\sqrt{L}} \sum_k e^{ikx} e^{-a||k|-k_F|/2} \tilde{c}_{k\sigma}, \tag{4.43}$$

with $1/a \ll k_F$. Since the ground state is an eigenstate of the parity operator, we can write (4.42) as

$$\begin{aligned} X^{\|}(x) = &\left\langle S_z \left[\tilde{\psi}^\dagger_\uparrow(x)\tilde{\psi}_\uparrow(x) + \tilde{\psi}^\dagger_\uparrow(-x)\tilde{\psi}_\uparrow(-x)\right]\right\rangle_K \\ &- \left\langle S_z \left[\tilde{\psi}^\dagger_\downarrow(x)\tilde{\psi}_\downarrow(x) + \tilde{\psi}^\dagger_\downarrow(-x)\tilde{\psi}_\downarrow(-x)\right]\right\rangle_K . \end{aligned} \tag{4.44}$$

This expression can be manipulated into

$$\begin{aligned} X^{\|}(x) = &\left\langle S_z \left[\tilde{\psi}^\dagger_\uparrow(x) + \tilde{\psi}^\dagger_\uparrow(-x)\right] \left[\tilde{\psi}_\uparrow(x) + \tilde{\psi}_\uparrow(-x)\right]\right\rangle_K \\ &+ \underbrace{\left\langle S_z \left[\tilde{\psi}^\dagger_\uparrow(x) - \tilde{\psi}^\dagger_\uparrow(-x)\right] \left[\tilde{\psi}_\uparrow(x) - \tilde{\psi}_\uparrow(-x)\right]\right\rangle_K}_{=0} \\ &- \left\langle S_z \left[\tilde{\psi}^\dagger_\downarrow(x) + \tilde{\psi}^\dagger_\downarrow(-x)\right] \left[\tilde{\psi}_\downarrow(x) + \tilde{\psi}_\downarrow(-x)\right]\right\rangle_K \\ &- \underbrace{\left\langle S_z \left[\tilde{\psi}^\dagger_\downarrow(x) - \tilde{\psi}^\dagger_\downarrow(-x)\right] \left[\tilde{\psi}_\downarrow(x) - \tilde{\psi}_\downarrow(-x)\right]\right\rangle_K}_{=0} . \end{aligned} \tag{4.45}$$

The under-braced terms are zero because $\tilde{\psi}^\dagger_\sigma(x) - \tilde{\psi}^\dagger_\sigma(-x)$ and $\tilde{\psi}_\sigma(x) - \tilde{\psi}_\sigma(-x)$ create an electron or hole in an odd-parity single particle orbital which does not couple to the impurity. As a consequence, S_z becomes uncorrelated and the expectation value factorizes

$$\begin{aligned} \left\langle S_z \left[\tilde{\psi}^\dagger_\sigma(x) - \tilde{\psi}^\dagger_\sigma(-x)\right] \left[\tilde{\psi}_\sigma(x) - \tilde{\psi}_\sigma(-x)\right]\right\rangle_K = \langle S_z\rangle \Big\langle &\left[\tilde{\psi}^\dagger_\sigma(x) - \tilde{\psi}^\dagger_\sigma(-x)\right] \\ &\left[\tilde{\psi}_\sigma(x) - \tilde{\psi}_\sigma(-x)\right] \Big\rangle_K . \end{aligned} \tag{4.46}$$

Since the antiferromagnetic Kondo ground state is a singlet, it follows that $\langle S_z\rangle = 0$.

Thus

$$X^{\parallel}(x) = \left\langle S_z \left[\tilde{\psi}^\dagger_\uparrow(x) + \tilde{\psi}^\dagger_\uparrow(-x)\right] \left[\tilde{\psi}_\uparrow(x) + \tilde{\psi}_\uparrow(-x)\right] \right\rangle_K$$

$$- \left\langle S_z \left[\tilde{\psi}^\dagger_\downarrow(x) + \tilde{\psi}^\dagger_\downarrow(-x)\right] \left[\tilde{\psi}_\downarrow(x) + \tilde{\psi}_\downarrow(-x)\right] \right\rangle_K, \tag{4.47}$$

$$= \sum_\sigma \mathrm{sgn}(\sigma) \left\langle S_z \left[\tilde{\psi}^\dagger_\sigma(x) + \tilde{\psi}^\dagger_\sigma(-x)\right] \left[\tilde{\psi}_\sigma(x) + \tilde{\psi}_\sigma(-x)\right] \right\rangle_K. \tag{4.48}$$

We have introduced the $\mathrm{sgn}(\sigma)$ function for the sake of compactness, with $\mathrm{sgn}(\uparrow) = +$ and $\mathrm{sgn}(\downarrow) = -$. We can derive an identity which allows us to express the correlation function in terms of the slow modes defined in (4.2). From the definition of $\tilde{\psi}_\sigma(x)$, it follows that

$$\frac{1}{\sqrt{2}} \left[\tilde{\psi}_\sigma(x) + \tilde{\psi}_\sigma(-x)\right] = \frac{1}{\sqrt{2L}} \sum_{|q|<\Lambda} \left[e^{i(k_F+q)x} \tilde{c}_{k_F+q,\sigma} + e^{-i(k_F+q)x} \tilde{c}_{-k_F-q,\sigma}\right] e^{-a|q|/2}$$

$$+ \frac{1}{\sqrt{2L}} \sum_{|q|<\Lambda} \left[e^{-i(k_F+q)x} \tilde{c}_{k_F+q,\sigma} + e^{i(k_F+q)x} \tilde{c}_{-k_F-q,\sigma}\right] e^{-a|q|/2},$$

$$= \frac{1}{\sqrt{2L}} e^{ik_Fx} \sum_{|q|<\Lambda} e^{iqx} \left(\tilde{c}_{k_F+q,\sigma} + \tilde{c}_{-k_F-q,\sigma}\right) e^{-a|q|/2}$$

$$+ \frac{1}{\sqrt{2L}} e^{-ik_Fx} \sum_{|q|<\Lambda} e^{-iqx} \left(\tilde{c}_{-k_F-q,\sigma} + \tilde{c}_{k_F+q,\sigma}\right) e^{-a|q|/2}. \tag{4.49}$$

The momentum sums are restricted by the cut-off $\Lambda \gg 1/a$. However, the cut-off can be taken to infinity since the $\exp(-a|k|/2)$ regularization prevents the c_q, $q > 0$ unphysical modes from participating in the physics. It follows that

$$\frac{1}{\sqrt{2}} \left[\tilde{\psi}_\sigma(x) + \tilde{\psi}_\sigma(-x)\right] = \frac{1}{\sqrt{L}} e^{ik_Fx} \sum_q e^{iqx} e^{-a|q|/2} c_{q\sigma}$$
$$+ \frac{1}{\sqrt{L}} e^{-ik_Fx} \sum_q e^{-iqx} e^{-a|q|/2} c_{q\sigma}. \tag{4.50}$$

Using the definition of the slow modes in (4.2), we find the useful relationship

$$\frac{1}{\sqrt{2}} \left[\tilde{\psi}_\sigma(x) + \tilde{\psi}_\sigma(-x)\right] = e^{ik_Fx} \psi_\sigma(x) + e^{-ik_Fx} \psi_\sigma(-x). \tag{4.51}$$

Substituting (4.51) into (4.47) gives

$$X^{\|}(x) = \frac{1}{2}\sum_{\sigma}\mathrm{sgn}(\sigma)\left\langle\sigma_z\left[\psi^{\dagger}_{\sigma}(x)\psi_{\sigma}(x)+\psi^{\dagger}_{\sigma}(-x)\psi_{\sigma}(-x)\right]\right\rangle$$
$$+\frac{1}{2}\sum_{\sigma}\mathrm{sgn}(\sigma)\left\langle\sigma_z\left[e^{-i2k_Fx}\psi_{\sigma}(x)\psi_{\sigma}(-x)+e^{i2k_Fx}\psi^{\dagger}_{\sigma}(-x)\psi_{\sigma}(x)\right]\right\rangle_K. \tag{4.52}$$

Note that (4.52) is divided into terms whose exponential arguments are 0 and $2k_F$. The first represents forward scattering in which the momentum change is much less that k_F, whilst the latter represents backscattering processes in which the change in momentum is of the order $2k_F$. This allows us to define the forward scattering longitudinal cloud as

$$\boxed{X^{\|}_0(x) = \frac{1}{2}\sum_{\sigma}\mathrm{sgn}(\sigma)\left\langle\sigma_z\left[\psi^{\dagger}_{\sigma}(x)\psi_{\sigma}(x)+\psi^{\dagger}_{\sigma}(-x)\psi_{\sigma}(-x)\right]\right\rangle_K.} \tag{4.53}$$

4.3 Resonant level representation of the forward scattering longitudinal cloud

Now that we have an expression for the forward scattering longitudinal cloud in terms of slow modes, our next task is to perform the same mapping procedure used to map the anisotropic Kondo model onto the non-interacting resonate level model. This entails bosonizing (4.53), applying the unitary transformation with $\theta = iJ_{\|}\phi_s(0)\sigma_z/2\pi\sqrt{2}$, taking the thermodynamic limit $L\to\infty$, and finally refermionizing the expression at the Toulouse point $J = (2-\sqrt{2})\pi$ in term of the new fermionic degrees of freedom defined in (4.31) and (4.36).

The forward scattering longitudinal cloud can be written in terms of bosonic degrees of freedom as

$$X^{\|}_0(x) = \frac{\partial_x}{2\pi}\left\langle S_z\left[\phi_s(x)-\phi_s(-x)\right]\right\rangle_K,$$
$$= \frac{\partial_x}{2\pi}\left\langle S_z\left[\varrho^{\dagger}(x)+\varrho(x)\right]\right\rangle_K, \tag{4.54}$$

where for simplicity we have regrouped the terms and defined the bosonic fields

$$\varrho^{\dagger}(x) = 2\sum_{q>0}\sqrt{\frac{\pi}{Lq}}e^{-aq/2}\sin(qx)b^{\dagger}_{qs}. \tag{4.55}$$

Of the two unitary transformations used on the anisotropic model, only the one with $\theta = iJ_{\|}\phi_s(0)\sigma_z/2\pi\sqrt{2}$ has an effect on the longitudinal component:

$$X^{\|}_0(x) = \frac{\partial_x}{2\pi}\left\langle S_z\left[\varrho^{\dagger}(x)+\varrho(x)\right]\right\rangle + i\frac{J_{\|}}{\pi}\sum_{q>0}\frac{2\pi}{L}e^{-aq}\cos(qx). \tag{4.56}$$

Taking the thermodynamic limit gives

$$X_0^{\parallel}(x) = \frac{\partial_x}{2\pi}\left\langle S_z\left[\varrho^\dagger(x)+\varrho(x)\right]\right\rangle + i\frac{J_\parallel}{2\pi}\int_0^\infty dq\ \left(e^{-iq(x-ia)}+e^{iq(x+ia)}\right),$$

$$= \frac{\partial_x}{2\pi}\left\langle S_z\left[\varrho^\dagger(x)+\varrho(x)\right]\right\rangle - J_\parallel\frac{a}{\pi(x^2+a^2)}. \qquad (4.57)$$

Finally, setting $J_\parallel = (2-\sqrt{2})\pi$ and using the identity $\partial_x\phi_s(x)/2\pi\sqrt{2} = \bar{\psi}^\dagger(x)\bar{\psi}(x)$, we find that the longitudinal forward scattering cloud in the resonant level representation is given by

$$\boxed{X_0^{\parallel}(x) = \sqrt{2}\left\langle\left(d^\dagger d-\frac{1}{2}\right)\left[\bar{\psi}^\dagger(x)\bar{\psi}(x)+\bar{\psi}^\dagger(-x)\bar{\psi}(-x)\right]\right\rangle - (2-\sqrt{2})\frac{a}{x^2+a^2}.} \qquad (4.58)$$

Chapter 5

Calculation of the forward scattering longitudinal cloud

In the previous chapter we introduced the correlation function between the z-components of the impurity spin and the electron spin-density $4\langle S_z^{\mathrm{imp}} S_z^{\mathrm{el}}(x)\rangle$. We saw that this correlation function consists of a back scattering component that oscillates with a wave vector $2k_F$ and a forward scattering component that varies slowly on the scale of the Fermi wavelength. Expressed in terms of the degrees of freedom of the noninteracting resonant level model, the forward scattering longitudinal cloud reads

$$X_0^{\parallel}(x) = \sqrt{2}\left\langle \left(d^\dagger d - \frac{1}{2}\right)\left[\bar{\psi}^\dagger(x)\bar{\psi}(x) + \bar{\psi}^\dagger(-x)\bar{\psi}(-x)\right]\right\rangle - (2-\sqrt{2})\frac{a}{x^2+a^2}, \quad (5.1)$$

where the expectation value is taken with respect to the ground state of the noninteracting resonant level model at half-filling. In this final chapter we will derive both an exact numerical expression and an approximate analytical expression for the forward scattering longitudinal cloud with and without the presence of an external magnetic field. The expressions for the non-magnetic case appear in the literature [4]. The magnetic case however has not been addressed in the literature and is unique to this dissertation.

5.1 Wick's theorem and Green's functions

Because the noninteracting resonant level model is quadratic in fermion creation and annihilation operators, Wick's theorem allows us to reduce the expectation value in (5.1) to a sum of expectation values of pairs of fermion operators:

$$\begin{aligned} X_0^{\parallel}(x) =& 2\sqrt{2}\left\langle \left(d^\dagger d - \frac{1}{2}\right)\right\rangle \left\langle \bar{\psi}^\dagger(x)\bar{\psi}(x)\right\rangle \\ &+ 2\sqrt{2}\left\langle d^\dagger \bar{\psi}(x)\right\rangle \left\langle d\; \bar{\psi}^\dagger(x)\right\rangle - (2-\sqrt{2})\frac{a}{x^2+a^2}. \end{aligned} \quad (5.2)$$

Since the Kondo ground state is a singlet, and S_z maps to $d^\dagger d - 1/2$, the probability of the resonant level being occupied is one half. The first term in (5.2) therefore vanishes and the forward scattering longitudinal cloud reduces to

$$\boxed{X_0^{\parallel}(x) = -2\sqrt{2}\left|\left\langle d^\dagger \bar{\psi}(x)\right\rangle\right|^2 - (2-\sqrt{2})\frac{a}{x^2+a^2}.} \tag{5.3}$$

The expectation value in (5.3) can be evaluated by exploiting some analytical properties of single particle Green's functions. We will be working with the retarded and advanced Green's functions given by

$$R_{BA^\dagger}(t) = -i\theta(t)\left\langle\{B(t), A^\dagger\}\right\rangle, \tag{5.4}$$

and

$$A_{BA^\dagger}(t) = i\theta(-t)\left\langle\{B(t), A^\dagger\}\right\rangle. \tag{5.5}$$

Here, the expectation value is taken with respect to the resonant level ground state, and $B, A \in \{\bar{c}_k, d\}$. We will now develop a simple relationship between the above Green's functions and the expectation values of two fermionic operators in the noninteracting resonant level model.

By definition, the retarded Green's function reads

$$R_{BA^\dagger}(t) = -i\theta(t)\left[\left\langle B(t)A^\dagger\right\rangle + \left\langle A^\dagger B(t)\right\rangle\right]. \tag{5.6}$$

Since the resonant level Hamiltonian H_F is time-independent, the time evolution operator in natural units $\hbar = 1$ is given by $U(t) = e^{-iH_F t}$. The explicit time dependance of the retarded Green's function is then

$$\begin{aligned} R_{BA^\dagger}(t) = &- i\theta(t)\sum_n \left[\langle 0| e^{iH_F t} B e^{-iH_F t} |n\rangle \langle n| A^\dagger |0\rangle + \langle 0| A^\dagger |n\rangle \langle n| e^{iH_F t} B e^{-iH_F t} |0\rangle\right], \\ &= -i\theta(t)\sum_n \left[e^{-i(E_n - E_0)t} \langle 0| B |n\rangle \langle n| A^\dagger |0\rangle + e^{i(E_n - E_0)t} \langle 0| A^\dagger |n\rangle \langle n| B |0\rangle\right], \end{aligned} \tag{5.7}$$

where E_n and $|n\rangle$ are the many-body energies and eigenstates of the noninteracting resonant level model. This expression can be transformed into the frequency domain using the Fourier transform

$$R(\omega^+) = \int_{-\infty}^{\infty} dt\; e^{i\omega^+ t} R(t), \tag{5.8}$$

where $\omega^+ = \omega + i\eta$. The inclusion of the infinitesimal positive imaginary $i\eta$ is to ensure that the Fourier transform converges. Eq.(5.7) then reads

$$R_{BA^\dagger}(\omega^+) = -\,i \sum_n \int_0^\infty dt e^{i\omega^+ t} e^{-i(E_n - E_0)t} \langle 0| B |n\rangle \langle n| A^\dagger |0\rangle$$

$$-\,i \sum_n \int_0^\infty dt e^{i\omega^+ t} e^{i(E_n - E_0)t} \langle 0| A^\dagger |n\rangle \langle n| B |0\rangle \,,$$

$$= \sum_n \left[\frac{\langle 0| B |n\rangle \langle n| A^\dagger |0\rangle}{\omega + i\eta - (E_n - E_0)} + \frac{\langle 0| A^\dagger |n\rangle \langle n| B |0\rangle}{\omega + i\eta + (E_n - E_0)} \right]. \tag{5.9}$$

Similarly, the advanced Green's function in (5.5) evaluates to

$$A_{BA^\dagger}(\omega^-) = \sum_n \left[\frac{\langle 0| B |n\rangle \langle n| A^\dagger |0\rangle}{\omega - i\eta - (E_n - E_0)} + \frac{\langle 0| A^\dagger |n\rangle \langle n| B |0\rangle}{\omega - i\eta + (E_n - E_0)} \right], \tag{5.10}$$

with the Fourier transform given by

$$A(\omega^-) = \int_{-\infty}^{\infty} dt\; e^{i\omega^- t} G(t), \tag{5.11}$$

where $\omega^- = \omega - i\eta$. We will integrate (5.9) and (5.10) with respect to ω over the interval $(-\infty, 0]$. If we did this without including the factor $i\eta$ in the denominator, at some point we would be dividing by zero in the second terms of (5.9) and (5.10) since $E_n - E_0 > 0$. The integrals of interest have the following general form

$$f(\omega) = \int_{-\infty}^{0} \frac{d\omega}{\omega + (\omega' \pm i\eta)}, \tag{5.12}$$

where the distribution can be split into a real and imaginary part as follows

$$\frac{1}{\omega + (\omega' \pm i\eta)} = \frac{\omega + \omega'}{(\omega + \omega')^2 + \eta^2} \mp \frac{i\eta}{(\omega + \omega')^2 + \eta^2},$$

$$= P\left(\frac{1}{\omega + \omega'}\right) \mp i\pi\delta(\omega + \omega'). \tag{5.13}$$

The first term is referred to as the principle part of the integral [25], denoted by P, and is an instruction to delete an infinitesimal segment of the ω integral lying symmetrically about the singular point $\omega = -\omega'$. Integrating (5.9) and (5.10) with respect to ω gives

$$\int_{-\infty}^{0} d\omega\; R_{BA^\dagger}(\omega^+) = \sum_n \int_{-\infty}^{0} d\omega \Big[\frac{\langle 0| B |n\rangle \langle n| A^\dagger |0\rangle}{\omega - (E_n - E_0)}$$

$$+\, P\left(\frac{1}{w + (E_n - E_0)}\right) \langle 0| A^\dagger |n\rangle \langle n| B |0\rangle \Big] - i\pi \left\langle A^\dagger B \right\rangle, \tag{5.14}$$

and

$$\int_{-\infty}^{0} d\omega\ A_{BA^\dagger}(\omega^+) = \sum_n \int_{-\infty}^{0} d\omega \Big[\frac{\langle 0| B |n\rangle \langle n| A^\dagger |0\rangle}{\omega - (E_n - E_0)}$$

$$+ P\left(\frac{1}{w + (E_n - E_0)}\right) \langle 0| A^\dagger |n\rangle \langle n| B |0\rangle \Big] + i\pi \left\langle A^\dagger B\right\rangle. \quad (5.15)$$

Subtracting the advanced Green's function from the retarded, and multiplying by $i/2\pi$ returns $\left\langle A^\dagger B\right\rangle$. We conclude that

$$\left\langle A^\dagger B\right\rangle = \frac{i}{2\pi} \int_{-\infty}^{0} dw\ \left[R_{BA^\dagger}(\omega^+) - A_{BA^\dagger}(\omega^-)\right]. \quad (5.16)$$

Furthermore, since $A_{BA^\dagger}(\omega^-) = R_{BA^\dagger}(\omega^+)^*$, we can write the expectation value completely in terms of the retarded Green's function:

$$\boxed{\left\langle A^\dagger B\right\rangle = \frac{i}{2\pi} \int_{-\infty}^{0} dw\ \left[R_{BA^\dagger}(\omega^+) - R_{BA^\dagger}(\omega^+)^*\right].} \quad (5.17)$$

5.2 Calculating the Green's functions

To calculate the retarded Green's functions of the resonant level model, we will make use of the equations of motion method [26–29]. This method relates the time derivatives of the Green's functions to the Heisenberg equations of motion of our creation/annihilation operators, and results in a set of solvable coupled differential equations.

The time derivatives of the retarded Green's functions are given by

$$\frac{dR_{ii'}}{dt} = -\delta_{ii'}\delta(t) + \theta(t) \left\langle \{[H_F, \bar{c}_i], \bar{c}^\dagger_{i'}\}\right\rangle, \quad (5.18)$$

where

$$H_F = \sum_k k : \bar{c}^\dagger_k c_k : + \sum_k V_k \left[d^\dagger \bar{c}_k + \bar{c}^\dagger_k d\right], \quad (5.19)$$

and $i, i' \in \{\bar{c}^\dagger_k, \bar{c}_k, d^\dagger, d\}$. It follows that

$$[H_F, \bar{c}_k] = -\, k\bar{c}_k - V_k d, \quad (5.20)$$

and

$$[H_F, d] = -\sum_k V_k \bar{c}_k. \quad (5.21)$$

It is now a simple matter to calculate all the time derivatives of the relevant retarded Green's functions:

$$\begin{aligned}
\frac{dR_{kk'}(t)}{dt} =& \frac{d}{dt}\left[-i\theta(t)\left\langle\{\bar{c}_k(t),\bar{c}^\dagger_{k'}\}\right\rangle\right], \\
=& -i\delta_{kk'}\delta(t)+\theta(t)\left\langle\{[H_F,\bar{c}_k],\bar{c}^\dagger_{k'}\}\right\rangle, \\
=& -i\delta_{kk'}\delta(t)-k\theta(t)\left\langle\{\bar{c}_k,\bar{c}^\dagger_{k'}\}\right\rangle-V_k\theta(t)\left\langle\{d,\bar{c}^\dagger_{k'}\}\right\rangle, \\
=& -i\delta_{kk'}\delta(t)-ikR_{kk'}(t)-iV_kR_{dk'}(t),
\end{aligned} \tag{5.22}$$

$$\begin{aligned}
\frac{dR_{kd}(t)}{dt} =& \frac{d}{dt}\left[-i\theta(t)\left\langle\{\bar{c}_k(t),d^\dagger\}\right\rangle\right], \\
=& \theta(t)\left\langle\{[H_F,\bar{c}_k],d^\dagger\}\right\rangle, \\
=& -k\theta(t)\left\langle\{\bar{c}_k,d^\dagger\}\right\rangle-V_k\theta(t)\left\langle\{d,d^\dagger\}\right\rangle, \\
=& -ikR_{kd}(t)-iV_kR_{dd}(t),
\end{aligned} \tag{5.23}$$

$$\begin{aligned}
\frac{dR_{dk}(t)}{dt} =& \frac{d}{dt}\left[-i\theta(t)\left\langle\{d(t),\bar{c}^\dagger_{k'}\}\right\rangle\right], \\
=& \theta(t)\left\langle\{[H_F,d],\bar{c}^\dagger_{k'}\}\right\rangle, \\
=& -\sum_k\theta(t)V_k\left\langle\{\bar{c}_k,\bar{c}^\dagger_{k'}\}\right\rangle, \\
=& -i\sum_{k'}V_{k'}R_{k'k}(t),
\end{aligned} \tag{5.24}$$

$$
\begin{aligned}
\frac{dR_{dd}(t)}{dt} =& \frac{d}{dt}\left[-i\theta(t)\left\langle\{d(t), d^\dagger\}\right\rangle\right],\\
=& -i\delta(t) + \theta(t)\left\langle\{[H_F, d], d^\dagger\}\right\rangle,\\
=& -i\delta(t) - \sum_k V_k\theta(t)\left\langle\{\bar{c}_k, d^\dagger\}\right\rangle,\\
=& -i\delta(t) - i\sum_k V_k R_{kd}(t).
\end{aligned} \tag{5.25}
$$

To summarize, we have generated the following set of coupled differential equations:

$$
\boxed{
\begin{aligned}
\frac{dR_{kk'}(t)}{dt} &= -i\delta_{kk'}\delta(t) - ikR_{kk'}(t) - iV_kR_{dk'}(t),\\
\frac{dR_{kd}(t)}{dt} &= -ikR_{kd}(t) - iV_kR_{dd}(t),\\
\frac{dR_{dk}(t)}{dt} &= -i\sum_{k'} V_{k'}R_{k'k}(t),\\
\frac{dR_{dd}(t)}{dt} &= -i\delta(t) - i\sum_k V_kR_{kd}(t).
\end{aligned}} \tag{5.26}
$$

This set of differential equations simplifies to a set of algebraic equations in the frequency domain

$$R_{kk'}(\omega^+) = \delta_{kk'}R_k^0(\omega^+) + V_kR_k^0R_{dk'}(\omega^+), \tag{5.27}$$

$$R_{kd}(\omega^+) = V_kR_k^0R_{dd}(\omega^+), \tag{5.28}$$

$$R_{dk}(\omega^+) = \frac{1}{\omega^+}\sum_{k'} V_{k'}R_{k'k}(\omega^+), \tag{5.29}$$

$$R_{dd}(\omega^+) = \frac{1}{\omega^+} + \frac{1}{\omega^+}\sum_k V_kR_{kd}(\omega^+). \tag{5.30}$$

Here, we have defined the unperturbed Green's functions associated with the free electrons as

$$R_k^0(\omega^+) \equiv \frac{1}{\omega^+ - k}. \tag{5.31}$$

This system of equations can easily be solved by substituting (5.29) into (5.27) with a change of primes. Similarly, one can solve the remaining Green's functions by substituting (5.28) into (5.30). Defining the resonant level self-energy

$$\sum(\omega^+) = \sum_k \frac{V_k^2}{\omega^+ - k}, \tag{5.32}$$

it follows that

$$\boxed{\begin{aligned} R_{dd}(\omega^+) &= \frac{1}{\omega^+ - \sum(\omega^+)}, && (5.33)\\ R_{kk'}(\omega^+) &= \delta_{kk'} R_k^0(\omega^+) + V_k R_k^0(\omega^+) R_{dd}(\omega^+) V_{k'} R_{k'}^0(\omega^+), && (5.34)\\ R_{kd}(\omega^+) &= V_k R_k^0(\omega^+) R_{dd}(\omega^+), && (5.35)\\ R_{dk}(\omega^+) &= V_k R_k^0(\omega^+) R_{dd}(\omega^+). && (5.36) \end{aligned}}$$

5.3 Numerical expression of the forward scattering longitudinal cloud

Using (5.17), and the expression for the single particle Green's function $R_{kd}(\omega^+)$ in (5.35), we have that

$$\begin{aligned} \langle d^\dagger \bar{c}_k \rangle =& \frac{i}{2\pi} \int_{-\infty}^{0} d\omega \left[R_{kd}(\omega^+) - R_{kd}(\omega^+)^* \right], \\ =& \frac{i}{2\pi} \int_{-\infty}^{0} d\omega \left[\frac{V_k}{(\omega^+ - k)} \frac{1}{[\omega^+ - \sum(\omega)]} - \text{c.c} \right], \end{aligned} \tag{5.37}$$

where c.c stands for the complex conjugate of the first term. Fourier transforming to $\bar{\psi}(x)$ gives

$$\langle d^\dagger \bar{\psi}(x) \rangle = \frac{i}{2\pi} \int_{-\infty}^{0} d\omega \; \frac{J_\perp}{\sqrt{2\pi a}} \frac{1}{2\pi} \left[\int_{-\infty}^{\infty} dk \; \frac{e^{ikx} e^{-a|k|/2}}{\omega^+ - k} \frac{1}{\omega^+ - \sum(\omega^+)} - \text{c.c} \right]. \tag{5.38}$$

We will now write this expression in terms of the incomplete Gamma functions of order zero, defined as

$$\Gamma(0, z) = \int_z^\infty dt \frac{e^{-t}}{t}. \tag{5.39}$$

The integration contour in the definition starts from a complex number z and terminates at an endpoint with a real part that goes to infinity, without intersecting the non-positive real line [30]. The Gamma function $\Gamma(0, z)$ has a branch-cut along $(-\infty, 0]$. The behavior of $\Gamma(0, z)$ about the branch-cut is characterized by $\Gamma(0, -(x+i\eta)) - \Gamma(0, -(x-i\eta)) = 2\pi i$ for $x > 0$.

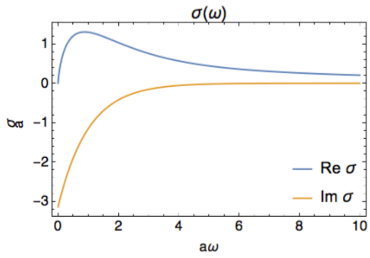

Figure 5.1: The real and imaginary parts of $\sigma(\omega)$.

Starting with the full self-energy in the denominator, we have

$$\sum(\omega) = \sum_k \frac{V_k^2}{\omega^+ - k},$$

$$\overset{L\to\infty}{=} \frac{J_\perp^2}{4\pi^2 a}\int_{-\infty}^{\infty} dk\ \frac{e^{-a|k|}}{\omega^+ - k},$$

$$= \frac{J_\perp^2}{4\pi^2 a}\int_{0}^{\infty} dk\ e^{-ak}\left[\frac{1}{\omega^+ - k} + \frac{1}{\omega^+ + k}\right]. \tag{5.40}$$

Setting $t = ak \pm a\omega^+$ and using definition (5.39) gives

$$\int_0^\infty dk \frac{e^{-ak}}{\omega^+ \pm k} = \pm \int_{\pm a\omega^+}^{\infty} dt \frac{e^{-(t\mp a\omega^+)}}{t},$$

$$= \pm\, e^{\pm a\omega^+}\int_{\pm a\omega^+}^{\infty} dt \frac{e^{-t}}{t},$$

$$= \pm\, e^{\pm a\omega^+}\Gamma(0, \pm a\omega^+), \tag{5.41}$$

so that in terms of the incomplete Gamma functions, the self-energy in (5.40) reads

$$\boxed{\sum(\omega) = \frac{J_\perp^2}{4\pi^2 a}\sigma(\omega) = \frac{J_\perp^2}{4\pi^2 a}\left[e^{a\omega}\Gamma(0, a\omega^+) - e^{-a\omega}\Gamma(0, -a\omega^+)\right].} \tag{5.42}$$

The behavior of the real and imaginary parts of $\sigma(\omega)$ in (5.42) can be seen in Fig. 5.1, where $\sigma(\omega)$ has been plotted in units of $a = 1$. Substituting (5.42) back into (5.38) gives

$$\langle d^\dagger \bar{\psi}(x)\rangle = \frac{i}{2\pi}\int_{-\infty}^{0} d\omega\ \frac{J_\perp}{\sqrt{2\pi a}}\frac{1}{2\pi}\left[\int_{-\infty}^{\infty} dk\ \frac{e^{ikx}e^{-a|k|/2}}{\omega^+ - k}\frac{1}{\omega^+ - \sum \frac{J_\perp^2}{4\pi^2 a}\sigma(\omega)} - \text{c.c}\right]. \tag{5.43}$$

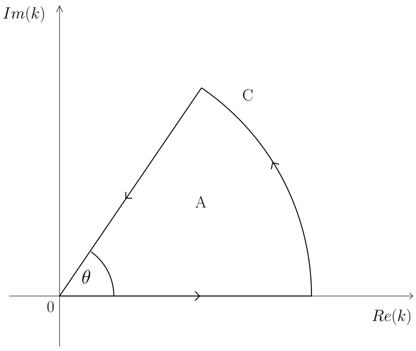

Figure 5.2: Contour used to resolve integral (5.44).

We must now evaluate the integral

$$I = \int_{-\infty}^{\infty} dk \, \frac{e^{ikx} e^{-a|k|}}{\omega^{+} - k},$$

$$= \int_{0}^{\infty} dk \, \frac{e^{-(a-ix)k}}{\omega^{+} - k} + \int_{0}^{\infty} dk \, \frac{e^{-(a+ix)k}}{\omega^{+} + k}. \tag{5.44}$$

These two integrals can be resolved by promoting k to a complex number and integrating around the pie-shaped contour shown in Fig. 5.2, where $z = a \pm ix = \rho e^{-i\theta}$. Since $z = a \pm ix$, and a is strictly positive, the pie-shaped contour is restricted to lie in the first and fourth quadrant. The first integral

$$\int_{0}^{\infty} dk \frac{e^{-zk}}{\omega^{+} - k}, \tag{5.45}$$

with $z = a - ix$, has a pole situated in the second quadrant at $k = \omega^{+} = \omega + i\eta$. Regardless of whether x is positive or negative, the contour will not enclose the pole. It follows from Cauchy's formula that

$$\int_{0}^{\infty} dk \frac{e^{-zk}}{\omega^{+} - k} + i\rho \int_{0}^{\theta'} d\theta \; e^{i\theta} \frac{e^{-r\rho e^{i(\phi+\theta)}}}{\omega^{+} - \rho e^{i\theta}} - e^{i\theta} \int_{0}^{\infty} d\rho \frac{e^{-r\rho e^{i(\phi+\theta)}}}{\omega^{+} - \rho e^{i\theta}} = 0. \tag{5.46}$$

Furthermore, since $\theta = -\arg(z)$, the exponential argument $-r\rho e^{(\phi+\theta)}$ simplifies to a negative real number $-|z|\rho$, and we get

$$\int_{0}^{\infty} dk \frac{e^{-zk}}{\omega^{+} - k} + i\rho \int_{0}^{\theta'} d\theta \; e^{i\theta} \frac{e^{-|z|\rho}}{\omega^{+} - \rho e^{i\theta}} - e^{i\theta} \int_{0}^{\infty} d\rho \frac{e^{-|z|\rho}}{\omega^{+} - \rho e^{i\theta}} = 0. \tag{5.47}$$

The integral along the arc goes to zero for $\rho \to \infty$, so that (5.51) reads

$$\int_{0}^{\infty} dk \frac{e^{-zk}}{\omega^{+} - k} = e^{i\theta} \int_{0}^{\infty} d\rho \frac{e^{-|z|\rho}}{\omega^{+} - \rho e^{i\theta}} = \int_{0}^{\infty} d\rho \frac{e^{-|z|\rho}}{\omega^{+} e^{-i\theta} - \rho}. \tag{5.48}$$

Finally, setting $t = |z|(\rho - \omega^+ e^{-i\theta})$ in (5.48), we find that

$$\int_0^\infty dk \frac{e^{-zk}}{\omega^+ - k} = -\, e^{-z\omega^+}\Gamma(0, -z\omega^+),$$

$$= -\, e^{-a\omega} e^{i\omega x}\Gamma(0, \omega(ix - a)). \tag{5.49}$$

The second integral in (5.41)

$$\int_0^\infty dk\ \frac{e^{-(a+ix)k}}{\omega^+ + k}, \tag{5.50}$$

can also be expressed in terms of the incomplete Gamma functions. However, if $x > 0$ the contour will enclose a simple pole in the forth quadrant located at $k = -\omega^+ = -\omega - i\eta$. In this case, the pie-shaped contour appears in the fourth quadrant with the contour integral running clockwise instead of anti-clockwise. By way of the residue theorem

$$\int_0^\infty dk \frac{e^{-zk}}{\omega^+ + k} = e^{i\theta} \int_0^\infty d\rho \frac{e^{-|z|\rho}}{\omega^+ + \rho e^{i\theta}} - i\rho \int_0^{\theta'} d\theta\ e^{i\theta} \frac{e^{-|z|\rho}}{\omega^+ + \rho e^{i\theta}}$$

$$+ 2\pi i\theta(x)\mathrm{Res}\left[\frac{e^{-zk}}{\omega^+ + k}, -\omega^+\right]. \tag{5.51}$$

Evaluating the θ integral along an arc at infinity, and setting $t = |z|(\rho + z\omega^+)$, we find

$$\int_0^\infty dk \frac{e^{-zk}}{\omega^+ + k} = \int_0^\infty d\rho \frac{e^{-|z|\rho}}{\omega^+ e^{-i\theta} + \rho} - 2\pi i\theta(x) e^{z\omega},$$

$$= e^{z\omega}\left[\Gamma(0, \omega(ix + a)) - 2\pi i\theta(x)\right],$$

$$= e^{a\omega} e^{i\omega x}\left[\Gamma(0, \omega(ix + a)) - 2\pi i\theta(x)\right]. \tag{5.52}$$

Finally, substituting (5.49) and (5.52) into (5.44) gives the integral I as

$$\int_{-\infty}^\infty dk\ \frac{e^{ikx}e^{-a|k|}}{\omega^+ - k} = \left[-2\pi i\theta(x)e^{a\omega} + e^{a\omega}\Gamma(0, \omega(ix + a)) - e^{-a\omega}\Gamma(0, \omega(ix - a))\right] e^{i\omega x}. \tag{5.53}$$

Substituting this result into (5.43) gives

$$\left\langle d^\dagger \bar{\psi}(x)\right\rangle = \frac{J_\perp}{\sqrt{2\pi a}} \int_{-\infty}^0 \frac{d\omega}{2\pi}\ e^{i\omega x}\left[\frac{\Theta_R(x)}{\omega - \sum(\omega)} - \frac{\Theta_R(-x)}{\omega - \sum(\omega)^*}\right], \tag{5.54}$$

where $\Theta_R(x)$ is defined as

$$\Theta_R(x) = e^{\omega a}\left[\theta(x) + \frac{i\Gamma(0, \omega(ix + a))}{2\pi}\right] - e^{-\omega a}\frac{i\Gamma(0, \omega(ix - a))}{2\pi}, \tag{5.55}$$

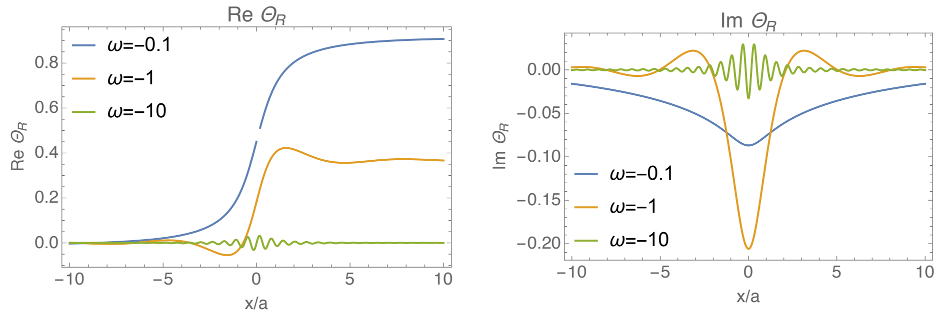

Figure 5.3: The real and imaginary part of the regularized step function $\Theta_R(x)$ evaluated for three values of ω.

and becomes a step function for $-\frac{1}{a} \ll \omega \leqslant 0$. For this reason we will refer to $\Theta_R(x)$ as a regularized step function. We have plotted the behavior of both the real and imaginary parts of $\Theta_R(x)$ in Fig. 5.3 as a function of ω in units of $a = 1$. An exact numerical expression for the forward scattering longitudinal cloud is obtained after substituting (5.54) into (5.3):

$$\boxed{X_0^{\parallel}(x) = -2\sqrt{2}\left|\frac{J_\perp}{\sqrt{2\pi a}}\int_{-\infty}^{0}\frac{d\omega}{2\pi}\,e^{i\omega x}\left[\frac{\Theta_R(x)}{\omega - \sum(\omega)} - \frac{\Theta_R(-x)}{\omega - \sum(\omega)^*}\right]\right|^2 - (2-\sqrt{2})\frac{a}{x^2+a^2}.} \tag{5.56}$$

We will delay the analysis of this result until all our calculations are complete.

Eq.(5.56) is as far as we can go without making any approximations. In the next section we will develop a closed analytical expression for $X_0^{\parallel}(x)$ valid in the regime $x \gg a$.

5.4 Analytical expression of the forward scattering longitudinal cloud

For small x, the ultraviolet regulator is important. However, in the regime of physical significance, $x \gg a$, we can drop the regulator and replace the regularized step function with a sharp step function. In this regime, the self-energy (5.42) can also be evaluated at its $\omega = 0$ value. To see why, consider Figs. 5.1, 5.3 and 5.4.

In the limit $x \gg a$, the regularized step function $\Theta_R(x)$ is indistinguishable from the normal step function so long as $-\omega < 1/a$. It is acceptable to cut off the ω integral in (5.54) at this value, since the regularized step function is suppressed as $e^{\omega a}$, which results in a strong suppression of (5.54) for $-\omega \gtrsim 1/a$. The integral is further cut off at $\omega \sim 1/x \ll 1/a$ by the highly oscillating factor $e^{i\omega x}$. However, since the self-energy only varies on the scale of $1/a$, we can safely evaluate it at $\omega = 0$.

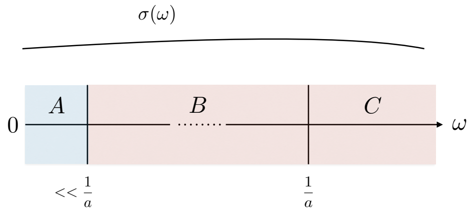

Figure 5.4: Schematic to help visualize the argument for taking $\sum(\omega^+ \to 0)$ in the regime $x \gg a$. The red region represents the values of ω for which the integral is suppressed, with region C being due to the regularized step function and region B due to the highly oscillating factor. Region A (blue), represents that part of the ω domain that gives a sizable contribution, while $\sigma(\omega)$ is represented as a slowly varying function on the scale of $1/a$.

The self-energy is explicitly given by

$$\sum(\omega^+) = \frac{J_\perp^2}{2\pi a}\sum_k \frac{e^{-a|k|}}{\omega^+ - k}, \tag{5.57}$$

which in the thermodynamic limit $L \to \infty$, reads

$$\begin{aligned}\sum(\omega^+) =& \frac{J_\perp^2}{4\pi^2 a}\int_{-\infty}^{\infty} dk\ \frac{e^{-a|k|}}{\omega^+ - k},\\ =& \frac{J_\perp^2}{4\pi^2 a}\int_{-\infty}^{\infty} dk\ \left[e^{-a|k|}P\left(\frac{1}{\omega - k}\right) - e^{a|k|}i\pi\delta(\omega - k)\right],\\ =& \frac{J_\perp^2}{4\pi^2 a}\int_{-\infty}^{\infty} dk\ e^{-a|k|}P\left(\frac{1}{\omega - k}\right) - i\frac{J_\perp^2}{4\pi a}e^{-a|\omega|}.\end{aligned} \tag{5.58}$$

Substituting $\omega = 0$ gives the self-energy as

$$\boxed{\sum(0) = -i\frac{J_\perp^2}{4\pi a}.} \tag{5.59}$$

If we now take (5.59) as the self-energy and drop the ultraviolet regulator, (5.38) becomes

$$\left\langle d^\dagger\bar{\psi}(x)\right\rangle \simeq i\frac{J_\perp}{4\pi^2\sqrt{2\pi a}}\int_{-\infty}^{0} d\omega\ \left[\int_{-\infty}^{\infty} dk\ \frac{e^{ikx}}{(\omega^+ - k)}\frac{1}{(\omega^+ + i\Delta)} - \frac{e^{ikx}}{(\omega^{+*} - k)}\frac{1}{(\omega^* - i\Delta)}\right], \tag{5.60}$$

where $\Delta \equiv J_\perp^2/4\pi a$. We will calculate (5.60) one integral at a time and then put everything together at the end.

The first integral to evaluated is

$$\int_{-\infty}^{\infty} dk \, \frac{e^{ikx}}{\omega^{+} - k}. \tag{5.61}$$

Once again we can resolve this integral by promoting k to a complex number and integrating along a closed contour. For $x > 0$, we will choose the contour to be a semi-circle in the upper half of the plane, so that the additional arc goes to zero in the limit $|k| \to \infty$. This contour encloses a pole at $k = \omega^{+} = \omega + i\eta$, allowing us to use the residue theorem. However, for $x < 0$ we must close the contour in the lower half plane. Since there are no poles with negative imaginary parts, Cauchy's formula gives zero and we have

$$\begin{aligned}
\int_{-\infty}^{\infty} dk \frac{e^{ikx}}{\omega^{+} - k} =& 2\pi i \mathrm{Res}\left[\frac{e^{ikx}}{\omega^{+} - k}, \omega^{+}\right] \theta(x), \\
=& 2\pi i \lim_{k \to \omega^{+}} \left[(k - \omega^{+}) \frac{e^{ikx}}{\omega^{+} - k}\right] \theta(x), \\
=& -2\pi i e^{i\omega x} \theta(x).
\end{aligned} \tag{5.62}$$

The integral

$$\int_{-\infty}^{\infty} dk \, \frac{e^{ikx}}{\omega^{+*} - k}, \tag{5.63}$$

is evaluated in the same way, except since the simple pole is situated in the lower half of the plane at $k = \omega^{+*} = \omega - i\eta$, the only non-zero contribution is when $x < 0$. This coupled with a change in sense gives

$$\begin{aligned}
\int_{-\infty}^{\infty} dk \, \frac{e^{ikx}}{\omega^{+*} - k} =& -2\pi i \mathrm{Res}\left[\frac{e^{ikx}}{\omega^{+*} - k}, \omega^{+*}\right] \theta(-x), \\
=& -2\pi i \lim_{k \to \omega^{+*}} \left[(k - \omega^{+*}) \frac{e^{ikx}}{\omega^{+*} - k}\right] \theta(-x), \\
=& 2\pi i e^{i\omega x} \theta(-x).
\end{aligned} \tag{5.64}$$

Substituting these two results into (5.60) we find

$$\left\langle d^{\dagger} \bar{\psi}(x) \right\rangle \simeq \frac{J_{\perp}}{2\pi\sqrt{2\pi a}} \int_{-\infty}^{0} d\omega \; e^{i\omega x} \left[\frac{\theta(x)}{\omega + i\Delta} + \frac{\theta(-x)}{\omega - i\Delta}\right]. \tag{5.65}$$

Comparing this equation with (5.54), we see that neglecting the ultraviolet regulator $e^{-a|k|}$ has resulted in the replacement of the regularized step function $\Theta_R(x)$ with a sharp step function $\theta(x)$. This result is not surprising since taking the limit $a \to 0$ in

(5.55) immediately returns an ordinary step function.

We now turn our attention to the remaining two ω integrals in (5.65), starting with

$$\int_{-\infty}^{0} d\omega \, \frac{e^{i\omega x}}{\omega + i\Delta}\theta(x). \tag{5.66}$$

This integral is resolved by performing a Wick rotation, where the path of integration along the negative arm of the real axis is replaced with an equivalent integration along the positive imaginary axis. The rotation is performed by substituting $\omega = ik$ into (5.66) which gives

$$\int_{-\infty}^{0} d\omega \, \frac{e^{i\omega x}}{\omega + i\Delta}\theta(x) = -\int_{0}^{\infty} dk \, \frac{e^{-kx}}{k + \Delta}\theta(x). \tag{5.67}$$

This integral has the same form as those in (5.41), and can therefore be written in terms of the incomplete Gamma functions as

$$\int_{-\infty}^{0} d\omega \, \frac{e^{i\omega x}}{\omega + i\Delta}\theta(x) = -e^{\Delta x}\Gamma(0, \Delta x)\theta(x). \tag{5.68}$$

Similarly

$$\int_{-\infty}^{0} d\omega \, \frac{e^{i\omega x}}{\omega - i\Delta}\theta(-x) = -e^{-\Delta x}\Gamma(0, -\Delta x)\theta(-x). \tag{5.69}$$

Substituting (5.68) and (5.69) into (5.65) gives

$$\begin{aligned} \left\langle d^\dagger \bar{\psi}(x) \right\rangle &= -\frac{J_\perp}{2\pi\sqrt{2\pi a}} \left[e^{\Delta x}\Gamma(0, \Delta x)\theta(x) + e^{-\Delta x}\Gamma(0, -\Delta x)\theta(-x) \right], \\ &= -\frac{J_\perp}{2\pi\sqrt{2\pi a}} e^{\Delta |x|}\Gamma\left(0, \Delta |x|\right). \end{aligned} \tag{5.70}$$

Defining the function $F(z) = e^{-z}\Gamma(0, -z)$ and remembering that $\Delta = J_\perp^2/4\pi a$, the expectation value reads

$$\left\langle d^\dagger \bar{\psi}(x) \right\rangle = -\frac{J_\perp}{2\pi\sqrt{2\pi a}} F\left(-\frac{J_\perp^2}{4\pi a}|x| \right). \tag{5.71}$$

We obtain an analytical expression for the forward scattering longitudinal cloud correlator in the regime $x \gg a$ after substituting this result back into (5.3) and dropping the broadened Dirac delta function:

$$\boxed{\tilde{X}_0^{\parallel}(x) = -\frac{\sqrt{2}}{\pi^2}\frac{J_\perp^2}{4\pi a} F\left(-\frac{J_\perp^2 |x|}{4\pi a} \right)^2.} \tag{5.72}$$

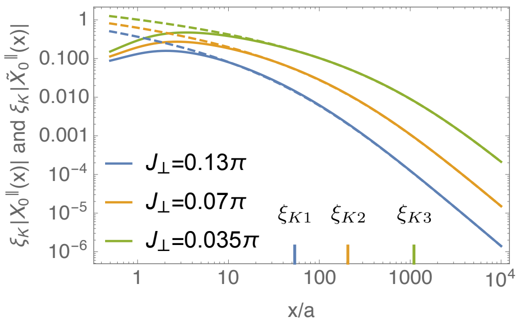

Figure 5.5: Comparison of the numeric $X_0^{\parallel}(x)$ and analytical $\tilde{X}_0^{\parallel}(x)$ forward scattering longitudinal clouds. The vertical axis is plotted in units of $1/\xi_K$, where $\xi_K = 4\pi a/J_\perp^2$, while the horizontal axis is in units of a. The Kondo lengths ξ_K of all three curves are marked on the horizontal axis.

In Fig. 5.5, we have compared the numeric $X_0^{\parallel}(x)$ and analytic $\tilde{X}_0^{\parallel}(x)$ forward scattering longitudinal clouds for three different perpendicular couplings $J_\perp$. The clouds associated with the numerical expression (5.56) are represented by solid lines, while those associated with the analytical expression (5.72) are represented by broken lines. It is clear form Fig. 5.5 that the approximate analytic solution describes the cloud almost perfectly for distances sufficiently larger than the ultraviolet length a.

A surprising feature of the cloud can be deduced from (5.72). Despite having inserted a single ultraviolet length a into the problem, an additional length scale $\xi_K = 4\pi a/J_\perp^2 = 1/\Delta$ emerges, called the Kondo length. This length describes the size of the cloud, and is infrared for small perpendicular couplings $J_\perp$. The Kondo length for each of the three clouds is shown in Fig. 5.5. Notice that smaller perpendicular couplings correspond to larger clouds.

Any cloud can be divided into three regions. The first region $x < a$ is the non-universal sector. The cloud in this region depends strongly on the details of the ultraviolet regularization. These details are system specific and our choice of regularization does not quantitatively model any particular ”real” system. The majority of the correlations occur inside of the cloud in the universal region $a < x < \xi_K$, while correlations outside of the cloud for $x > \xi_K$ experience a strong decay. To understand the specifics of this decay, as well as the significance of the Kondo length, we will analyze the asymptotic behavior of the cloud for small and large x. This behavior can be deduced through the following two expressions

$$\Gamma(0,x) = -\gamma - \ln|x| - \sum_{n=1}^{\infty} \frac{(-x)^n}{n(n!)}, \tag{5.73}$$

and

$$\Gamma(0,x) = \frac{e^{-x}}{x}\left[1 - \frac{1}{x} + \frac{2}{x^2} - \cdots\right], \tag{5.74}$$

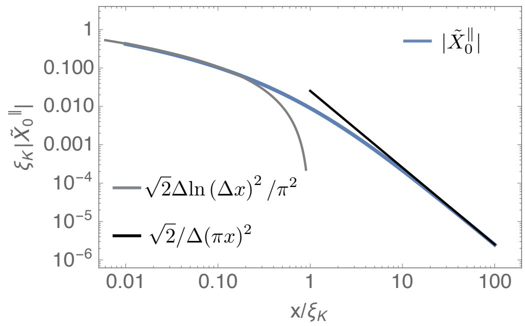

Figure 5.6: Universal scaling curve for $\tilde{X}_0^{\parallel}(x)$ in units $1/\xi_K$ on the vertical axis and ξ_K on the horizontal axis. The exact logarithmic behavior for small x is depicted by the grey curve, while the power law behavior for large x is plotted in black.

where γ is Euler's constant and is approximately 0.577 [30]. The first expression for $\Gamma(0,x)$ gives

$$\begin{aligned}\tilde{X}_0^{\parallel}(x) &= -\frac{\sqrt{2}\Delta}{\pi^2}\left|e^{\Delta|x|}\Gamma(0,\Delta|x|)\right|^2, \\ &= -\frac{\sqrt{2}\Delta}{\pi^2}e^{2|\Delta x|}\left|\gamma+\ln|\Delta x|+\sum_{n=1}^{\infty}\frac{(-\Delta x)^n}{n(n!)}\right|^2. \end{aligned}\tag{5.75}$$

For small x, the leading divergence is logarithmic and we have $\tilde{X}_0^{\parallel}(x) = -\sqrt{2}\Delta\ln(\Delta x)^2/\pi^2$. On the other hand, using (5.74) we find that

$$\begin{aligned}\tilde{X}_0^{\parallel}(x) &= -\frac{\sqrt{2}\Delta}{\pi^2}\left|e^{\Delta|x|}\Gamma(0,\Delta|x|)\right|^2, \\ &= -\frac{\sqrt{2}\Delta}{\pi^2}\left|\frac{e^{\Delta x}e^{-\Delta x}}{|\Delta x|}\left(1-\frac{1}{|\Delta x|}+\frac{2}{(\Delta x)^2}-\cdots\right)\right|^2, \end{aligned}\tag{5.76}$$

so that for large x the correlator is given by $\tilde{X}_0^{\parallel}(x) = -\sqrt{2}/\Delta(\pi x)^2$. As x approaches the Kondo length, the sub-leading terms in (5.75) become important, and the cloud crosses over to a $1/x^2$ decay.

One of the interesting things about the Toulouse point is the scaling behaviour of the clouds. The correlator in (5.72) depends on $J_\perp$ only through $J_\perp^2/4\pi a \equiv \Delta$. Therefore, curves at different $J_\perp$ can be collapsed onto each other by rescaling the x- and y-axes. Fig. 5.6 shows the universal scaling curve for the longitudinal forward scattering cloud, as well as the exact asymptotic behavior for small and large x. This scaling behavior suggests that curves at the Toulouse point $J_\parallel = (2-\sqrt{2})\pi$ but at different $J_\perp$ lie on the same renormalisation trajectory. In other words, the renormalisation trajectory at $J_\parallel = (2-\sqrt{2})\pi$ and small $J_\perp$ runs parallel to the $J_\perp$-axis.

5.5 Magnetic cloud

So far we have derived both an analytic and an exact numeric expression for the forward scattering longitudinal cloud. In this final section,we will extend formulas (5.56) and (5.72) to include the effects of an external time-independent magnetic field on the cloud.

The non-magnetic singlet ground state minimizes the interaction energy between the impurity and electron gas of the Kondo system. However, an external magnetic field frustrates the system and attempts to drive it into a magnetic state with the spin of the impurity and conduction electrons aligned to the direction of the field. It is interesting to see what compromises the system makes to accommodate the magnetic field. Analytical expressions for cloud correlations for $B \neq 0$ at the Toulouse point have not yet been derived in the literature.

It is known that for finite temperatures an additional length scale ξ_T emerges, called the thermal length scale [6]. For distances in excess of this scale, the correlations are cut off exponentially, and only short range correlations persist [7, 31]. However, the question as to whether a magnetic field induces similar exponential decay is yet to be answered. It would also be interesting to see whether the magnetic field spoils the scaling behavior of the clouds.

In the presence of a time-independent magnetic field fixed along the z-axis, the Kondo model at the Toulouse point maps onto

$$H_{FB} = \sum_k k : \bar{c}_k^\dagger \bar{c}_k : + \sum_k V_k \left(\bar{c}_k^\dagger d + d^\dagger \bar{c}_k \right) - \mu B \left(d^\dagger d - \frac{1}{2} \right). \tag{5.77}$$

The additional term $\mu B \left(d^\dagger d - \frac{1}{2} \right)$ changes the Green's functions $R_{dd}(\omega^+)$, $R_{dk}(\omega^+)$ and $R_{kk'}(\omega^+)$ to

$$R_{dd}(\omega^+) = \frac{1}{(\omega^+ - \mu B) - \sum(\omega^+)}, \tag{5.78}$$

$$R_{dk}(\omega^+) = \frac{V_k}{(\omega^+ - k)[(\omega^+ - \mu B) - \sum(\omega^+)]}, \tag{5.79}$$

and

$$R_{kk'} = \frac{\delta_{kk'}}{\omega^+ - k} + \frac{V_k V_{k'}}{(\omega^+ - k)[(\omega^+ - \mu B) - \sum(\omega^+)](\omega^+ - k')}. \tag{5.80}$$

Despite the above alteration to the Green's functions, the cloud correlator defined as

$$X_{0B}^{\parallel}(x) = 2\sqrt{2} \langle S_z \bar{\psi}^\dagger(x) \bar{\psi}(x) \rangle - 2\sqrt{2} \langle S_z \rangle \langle \bar{\psi}^\dagger(x) \bar{\psi}(x) \rangle, \tag{5.81}$$

still reduces to

$$X_{0B}^{\parallel}(x) = -2\sqrt{2} \left| \langle d^\dagger \bar{\psi}(x) \rangle \right|^2 - (2 - \sqrt{2}) \frac{a}{x^2 + a^2}. \tag{5.82}$$

Once again the quantities $\langle S_z \rangle$ and $\langle \bar{\psi}^\dagger(x)\bar{\psi}(x)\rangle$ do not appear in the expression for $X^{\parallel}_{0B}(x)$. Nevertheless these are now interesting quantities to calculate.

In terms of the new Green's function $R_{dd}(\omega^+)$, the impurity spin expectation value is given by

$$\left\langle d^\dagger d - \frac{1}{2}\right\rangle = \frac{i}{2\pi}\int_{-\infty}^{0} dw \ \left[R_{dd}(\omega^+) - R_{dd}(\omega^+)^*\right] - \frac{1}{2},$$

$$= \frac{i}{2\pi}\int_{-\infty}^{0} d\omega \left[\frac{1}{(\omega-\mu B)-\sum(\omega)} - \frac{1}{(\omega-\mu B)-\sum(\omega)^*}\right] - \frac{1}{2}. \quad (5.83)$$

A simple closed formula emerges if we take the $\omega = 0$ value of the self-energy:

$$\langle S_z \rangle = -\frac{1}{\pi}\tan^{-1}\left(\frac{4\pi a\mu B}{J_\perp^2}\right). \quad (5.84)$$

The magnetic field therefore breaks the singlet and drives the expectation value into either a spin up or a spin down state.

The calculation of the spin-density expectation value $\langle \bar{\psi}^\dagger(x)\bar{\psi}(x)\rangle$ is more subtle. In order to avoid divergences we must calculate the normal ordered expectation value by subtracting off the expectation of the spin-density with respect to the clean Fermi sea with no impurity. In the regime $x \gg a$ we can once again drop the ultraviolet regulator $e^{-a|k|/2}$ and take the $\omega = 0$ value of the self-energy. In this case the normal ordered spin-density reads

$$\langle : \bar{\psi}^\dagger(x)\bar{\psi}(x) : \rangle \simeq \frac{iJ_\perp^2}{4\pi^2 a}\int_{-\infty}^{0}\frac{d\omega}{2\pi}\left[\int_{-\infty}^{\infty} dk \frac{e^{-ikx}}{(\omega^+ - k)}\int_{-\infty}^{\infty} dk' \frac{e^{ik'x}}{(\omega^+ - k')}\frac{1}{(\omega^+ - \mu B) + i\Delta}\right.$$

$$\left. - \int_{-\infty}^{\infty} dk \frac{e^{-ikx}}{(\omega^{+*} - k)}\int_{-\infty}^{\infty} dk' \frac{e^{ik'x}}{(\omega^{+*} - k')}\frac{1}{(\omega^{+*} - \mu B) - i\Delta}\right], \quad (5.85)$$

where $\Delta \equiv J_\perp^2/4\pi a$. From (5.62) and (5.64) it follows that

$$\langle : \bar{\psi}^\dagger(x)\bar{\psi}(x) : \rangle \simeq -iJ_\perp^2\int_{-\infty}^{0}\frac{d\omega}{2\pi a}\left[\frac{\theta(x)\theta(-x)}{(\omega^+ - \mu B) + i\Delta} - \frac{\theta(-x)\theta(x)}{(\omega^{+*} - \mu B) - i\Delta}\right] = 0. \quad (5.86)$$

For distances $x \gg a$, the normal ordered spin-density is therefore equal to zero, meaning that for $x \gg a$, the average spin-density (which is non-zero) is unaffected by the impurity. However, a full numeric treatment of $\langle : \bar{\psi}^\dagger(x)\bar{\psi}(x) : \rangle$ given by

$$\langle : \bar{\psi}^\dagger(x)\bar{\psi}(x) : \rangle = \frac{i}{2\pi}\frac{J_\perp^2}{2\pi a}\int_{-\infty}^{0}\frac{d\omega}{2\pi}\left[\frac{\Theta_B(x)}{(\omega-\mu B)-\sum(\omega^+)} - \text{c.c}\right], \quad (5.87)$$

where

$$\Theta_B(x) = [-2\pi i\theta(x)e^{a\omega} + e^{a\omega}\Gamma(0,\omega(ix+a)) - e^{-a\omega}\Gamma(0,\omega(ix-a))] \times \quad (5.88)$$
$$[-2\pi i\theta(-x)e^{a\omega} + e^{a\omega}\Gamma(0,\omega(a-ix)) - e^{-a\omega}\Gamma(0,-\omega(ix+a))],$$

reveals a finite spin-density for distances $x \sim a$.

The numerical expression for the magnetic cloud $X^{\parallel}_{0B}(x)$ is similar to that of (5.56) except for a shift in ω to $\omega - \mu B$:

$$\boxed{X^{\parallel}_{0B}(x) = -2\sqrt{2}\left|\frac{J_\perp}{\sqrt{2\pi a}}\int_{-\infty}^{0}\frac{d\omega}{2\pi}\,e^{i\omega x}\left[\frac{\Theta_R(x)}{(\omega-\mu B)-\sum(\omega^+)} - \frac{\Theta_R(-x)}{(\omega-\mu B)-\sum(\omega^+)^*}\right]\right|^2.} \tag{5.89}$$

To calculate the analytic expression of the magnetic cloud $\tilde{X}^{\parallel}_{0B}(x)$, we note that

$$\langle d^\dagger\bar{\psi}(x)\rangle \simeq \frac{iJ_\perp^2}{4\pi^2\sqrt{2\pi a}}\int_{-\infty}^{0}d\omega\left[\int_{-\infty}^{\infty}dk\frac{e^{ikx}}{(\omega^+-k)[(\omega^+-\mu B)+i\Delta]}\right.$$

$$\left.-\int_{-\infty}^{\infty}dk\frac{e^{ikx}}{(\omega^{+*}-k)[(\omega^{+*}-\mu B)-i\Delta]}\right]. \tag{5.90}$$

From (5.62) and (5.64) it follows that

$$\langle d^\dagger\bar{\psi}(x)\rangle = \frac{J_\perp}{2\pi\sqrt{2\pi a}}\int_{-\infty}^{0}d\omega e^{i\omega x}\left[\frac{\theta(x)}{(\omega-\mu B)+i\Delta}+\frac{\theta(-x)}{(\omega-\mu B)-i\Delta}\right]. \tag{5.91}$$

The above integrals can be expressed in terms of the incomplete Gamma functions defined in (5.39) by setting $\omega - \mu B = ik$ and $t = kx \pm \Delta x$. The first integral of (5.91) comes to

$$\int_{-\infty}^{0}d\omega\frac{e^{i\omega x}}{(\omega-\mu B)+i\Delta} = -e^{(\Delta+i\mu B)x}\Gamma\left(0,(\Delta-i\mu B)x\right), \tag{5.92}$$

while the second reads

$$\int_{-\infty}^{0}d\omega\frac{e^{i\omega x}}{(\omega-\mu B)-i\Delta} = -e^{-(\Delta-i\mu B)x}\Gamma\left(0,-(\Delta+i\mu B)x\right). \tag{5.93}$$

The magnetic cloud $\tilde{X}^{\parallel}_{0B}(x)$ is then given by

$$\tilde{X}^{\parallel}_{0B}(x) = -\,2\sqrt{2}|\langle d^\dagger\bar{\psi}(x)\rangle|^2,$$

$$= -\,\frac{\sqrt{2}}{\pi^2}\frac{J_\perp^2}{4\pi a}\Big|e^{(\Delta+i\mu B)x}\Gamma(0,(\Delta-i\mu B)x)\theta(x)$$

$$+\,e^{-(\Delta-i\mu B)x}\Gamma(0,-(\Delta+i\mu B)x)\theta(-x)\Big|^2,$$

$$= -\,\frac{\sqrt{2}}{\pi^2}\frac{J_\perp^2}{4\pi a}\left|e^{(\Delta+i\mu B)|x|}\Gamma(0,(\Delta+i\mu B)|x|)\right|^2. \tag{5.94}$$

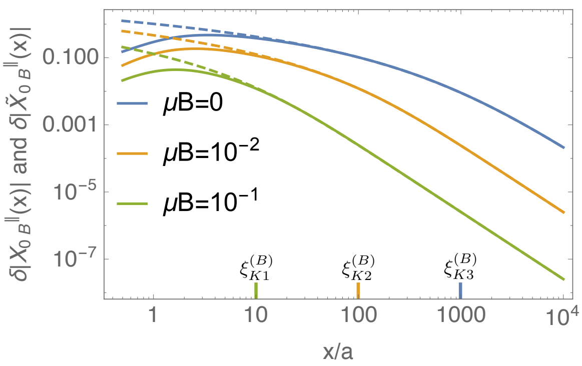

Figure 5.7: Comparison of the numeric $X_{0B}^{\parallel}(x)$ and analytical $\tilde{X}_{0B}^{\parallel}(x)$ forward scattering longitudinal clouds in the presence of a magnetic field. The cloud profiles have been plotted at fixed perpendicular coupling $J_\perp = 0.035\pi$ for three different values of magnetic field. The vertical axis is plotted in units of $1/\delta$, where $\delta = 4\pi^3 a/\sqrt{2}J_\perp^2$, while the horizontal is in units of a.

Defining the function $F(z) = e^{-z}\Gamma(0, -z)$, we find that

$$\boxed{\tilde{X}_{0B}^{\parallel}(x) = -\frac{\sqrt{2}}{\pi^2}\frac{J_\perp^2}{4\pi a}F\left[-\left(\frac{J_\perp^2}{4\pi a} + i\mu B\right)|x|\right]^2.} \tag{5.95}$$

Fig. 5.7 shows the comparison between the numeric and analytic forward scattering longitudinal clouds for three different magnetic field strengths at fixed perpendicular coupling $J_\perp = 0.035\pi$. The exact results have been depicted with solid lines while the approximate results corresponding to (5.95) have been represented with broken lines. Once again, the analytic results agree perfectly for distances sufficiently larger than the ultraviolet length a. The emergent Kondo length for the magnetic case modifies to $\xi_K^{(B)} = 1/\sqrt{\Delta^2 + (\mu B)^2}$, and has been indicated on the horizontal axis for each of the above three curves. This length undergoes a dramatic change when the magnetic field is turned on. As can be seen in Fig. 5.7, slightly increasing the magnetic field from its zero value results in a strong suppression of the cloud.

The asymptotic behavior of the correlator can be deduced by analytically continuing (5.73) and (5.74). The first expression gives

$$\begin{aligned}\tilde{X}_{0B}^{\parallel}(x) = &-\sqrt{2}\Delta e^{2\sqrt{\Delta^2+(\mu B)^2}\cos\left(\tan^{-1}\mu B/\Delta\right)|x|} \\ &\times\left[\left(\gamma + \ln(\sqrt{\Delta^2 + (\mu B)^2}x) + \Delta x + \mathcal{O}(x^2) + \cdots\right)^2\right. \\ &\left.+\left(\tan^{-1}\frac{\mu B}{\Delta} + \mu B x + \mathcal{O}(x^2) + \cdots\right)^2\right]/\pi^2,\end{aligned} \tag{5.96}$$

so that for small x the correlator is given by $\tilde{X}_{0B}^{\parallel}(x) = -\sqrt{2}\Delta\ln(\sqrt{\Delta^2 + (\mu B)^2}x)^2/\pi^2$. On the other hand, using (5.74), the asymptotic behavior of the correlator for large x is

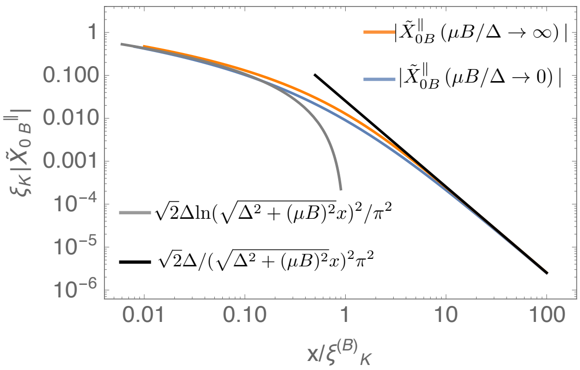

Figure 5.8: Line profiles of correlators for $\mu B/\Delta \to 0$ and $\mu B/\Delta \to \infty$ in units $1/\xi_K$ on the vertical axis and $\xi_K^{(B)}$ on the horizontal axis. The exact logarithmic behavior for small x is shown in gray, while the power law decay for large x is depicted in black.

given by $\tilde{X}^{\parallel}_{0B}(x) = -\sqrt{2}\Delta/(\sqrt{\Delta^2+(\mu B)^2}x)^2\pi^2$. Unlike the case of finite temperature, there is no critical crossover to exponential decay. This means that the long range correlations remain unspoiled in the presence of a magnetic field.

In contrast to the non-magnetic case (5.72), correlators given by (5.95) cannot be collapsed onto a single universal curve. When $x \sim \xi_K^{(B)}$, the sub-leading terms in (5.96) become important and two distinct scales emerge, namely $1/\Delta$ and $1/\mu B$. Because of this, we cannot collapse the clouds for regions near the crossover. However, for distances $x \ll \xi_K^{(B)}$ and $x \gg \xi_K^{(B)}$, there remarkably exists a single scale $1/\sqrt{\Delta^2+(\mu B)^2}$, so that the asymptotic regions of the clouds for large and small x can be collapse onto one another. This scaling behavior is demonstrated in Fig. 5.8, where we have plotted the correlator for $\mu B/\Delta \to 0$ and $\mu B/\Delta \to \infty$ in rescaled units $1/\xi_K$ on the vertical axis and $\xi_K^{(B)}$ on the horizontal axis.

We were able to find a tractable expression for both the magnetic and non-magnetic clouds at the Toulouse point. This makes the Toulouse point unique from a calculational perspective. The question as to whether the physics found at this point persists to other points in the parameter space is open ended. However, we would suggest that the physics at the Toulouse point is not qualitatively different from any other point in the Kondo parameter space. The reason for this is two-fold. Firstly, the profile of the screening cloud at the Toulouse point shares the same decay features common amongst the other points. In particular, the emergent length scale ξ_K acts as a crossover length to $1/x^2$ decay, with the majority of the correlations existing within the universal region. Secondly, it is possible to calculate the cloud profiles at points near the Toulouse point by using the Toulouse ground state as the zeroth order approximation in perturbation theory. This makes the Toulouse point a good representative for points in its proximity, as well as a good candidate for exploring the physics of the rest of the parameter space at a qualitative level.

Conclusion

In this dissertation we have studied the forward scattering longitudinal cloud of the anisotropic spin-1/2 Kondo model. In chapter 2 we derived Anderson's poor man's scaling equations in our own way using a Schrieffer-Wolff transformation. The results showed that both the isotropic and anisotropic model flow to the same strong coupling fixed point. Any information obtained for the anisotropic model therefore remains relevant to Kondo physics in general. The motivation for studying the anisotropic model became clear in chapter 3, where at a particular nontrivial point in parameter space we were able to map the problem to a simple non-interacting resonant level model written in terms of new fermionic degrees of freedom. This model provided the ideal platform for studying the spin-spin correlation function between the impurity spin and the electron spin-density. We discarded the back scattering fast oscillating $2k_F$ contributions of the correlation function and restricted ourselves to the analysis of the forward scattering longitudinal cloud $X_0^{\parallel}(x)$, for which we were able to find a simple analytic expression. This expression accurately represents the cloud for distances $x \gg a$, and remains accurate for distances comparable to the crossover length ξ_K, provided that $\xi_K \gg a$. Clouds for different perpendicular coupling strengths fixed at the Toulouse point can be collapsed onto one another by rescaling the x- and y-axis. This suggests that for this region of the Kondo parameter space, the renormalisation trajectory runs parallel to the $J_\perp$-axis. The results were then generalized for an external time-independent magnetic field. The normal ordered spin-density vanishes on the scale of $x \sim a$, and the correlations are suppressed for increasing magnetic field strengths. Nevertheless, the cloud still exhibits long range correlations with no critical crossover to exponential decay. The extent of the cloud is characterized by the emergent length $\xi_K^{(B)} = 1/\sqrt{\Delta^2 + (\mu B)^2}$. Unlike the non-magnetic case, the cloud exhibits imperfect scaling near the crossover due to the existence of two distinct scales $1/\Delta$ and $1/\mu B$. Remarkably, the asymptotic regions of the cloud for small and large x share the same scale and can be collapsed onto one another. We expect that this is not unique to the Toulouse point, and persist to other points of the parameter space.

Bibliography

[1] K. G. Wilson, Rev. Mod. Phys. **47**, 773 (1975).

[2] N. Andrei, Phys. Rev. Lett. **45**, 379 (1980).

[3] P. B. Wiegmann, J. Phys. C **14**, 1463 (1981).

[4] S. Florens and I. Snyman, Phys. Rev. B **92**, 195106 (2015).

[5] B. Lechtenberg and F. B. Anders, Phys. Rev. B **90**, 045117 (2014).

[6] L. Borda, Phys. Rev. B **75**, 041307 (2007).

[7] T. Posske, C.-X. Liu, J. C. Budich, and B. Trauzettel, Phys. Rev. Lett. **110**, 016602 (2013).

[8] P. S. Cornaglia, H. Ness, and D. R. Grempel, Phys. Rev. Lett. **93**, 147201 (2004).

[9] G. Yoo, J. Park, S.-S. B. Lee, and H.-S. Sim, Phys. Rev. Lett. **113**, 236601 (2014).

[10] I. Snyman and S. Florens, Phys. Rev. B **92**, 085131 (2015).

[11] J. R. Schrieffer and P. A. Wolff, Phys. Rev. **149**, 491 (1966).

[12] A. Altland and B. D. Simons, *Condensed Matter Field Theory*, 2nd ed. (Cambridge University Press, Cambridge, 2010).

[13] A. J. Leggett *et al.*, Rev. Mod. Phys. **59**, 1 (1987).

[14] J. Kondo, Prog. Theor. Phys. **32**, 37 (1964).

[15] P. W. Anderson, J. Phys. C **3**, 2436 (1970).

[16] P. W. Anderson, G. Yuval, and D. Hamann, Phys. Rev. **8**, 1033 (1970).

[17] D. Mattis and E. Lieb, J. Math. Phys. **6**, 304 (1965).

[18] S. Tomonaga, Prog. Theor. Phys. **5**, 544 (1950).

[19] F. D. M. Haldane, J. Phys. C **14**, 2585 (1981).

[20] J. von Delft and H. Schoeller, Ann. Phys. **7**, 225 (1998).

[21] P. Kopietz, J. Hermisson, and K. Schönhammer, Phys. Rev. B **52**, 10877 (1995).

[22] *Mathematica*, version 10.0 ed. (Wolfram Research, Inc., Champaign, Illinois, 2014).

[23] U. Weiss, *Quantum Dissipative Systems*, 1st ed. (World Scientific, London, 1993).

[24] R. Bulla, N.-H. Tong, and M. Vojta, Phys. Rev. Lett. **91**, 1706011 (2003).

[25] M. Stone and P. Goldbart, *Mathematics for Physics, A Guided Tour for Graduate Students* (Cambridge University Press, Cambridge, 2009).

[26] A. C. Hewson, *The Kondo Problem to Heavy Fermions* (Cambridge University Press, Cambridge, 1997).

[27] M. Heyl, Master's thesis, Ludwig Maximilan University, Munchen, 2009.

[28] E. S. S. Doniach, *Green's functions for solid state physics* (Imperial College Press, London, 1998).

[29] Q. Feng, Y.-Z. Zhang, and H. O. Jeschke, Phys. Rev. B **79**, 235112 (2009).

[30] F. W. Olver, D. W. Lozier, R. F. Boisvert, and C. W. Clark, *NIST Handbook of Mathematical Functions*, 1st ed. (Cambridge University Press, New York, 2010).

[31] A. K. Mitchell, M. Becker, and R. Bulla, Phys. Rev. B **84**, 115120 (2011).